

AD-A023 537

PROPAGATION MODELING AND ANALYSIS FOR HIGH ENERGY
LASERS

Science Applications,
Incorporated

Prepared for:

Naval Surface Weapons Center

April 1975

DISTRIBUTED BY:

NTIS

National Technical Information Service
U. S. DEPARTMENT OF COMMERCE

KEEP UP TO DATE

Between the time you ordered this report—which is only one of the hundreds of thousands in the NTIS information collection available to you—and the time you are reading this message, several *new* reports relevant to your interests probably have entered the collection.

Subscribe to the **Weekly Government Abstracts** series that will bring you summaries of new reports as soon as they are received by NTIS from the originators of the research. The WGAs are an NTIS weekly newsletter service covering the most recent research findings in 25 areas of industrial, technological, and sociological interest—invaluable information for executives and professionals who must keep up to date.

The executive and professional information service provided by NTIS in the **Weekly Government Abstracts** newsletters will give you thorough and comprehensive coverage of government-conducted or sponsored re-

search activities. And you'll get this important information within two weeks of the time it's released by originating agencies.

WGA newsletters are computer produced and electronically photocomposed to slash the time gap between the release of a report and its availability. You can learn about technical innovations immediately—and use them in the most meaningful and productive ways possible for your organization. Please request NTIS-PR-205/PCW for more information.

The weekly newsletter series will keep you current. But *learn what you have missed in the past* by ordering a computer **NTISearch** of all the research reports in your area of interest, dating as far back as 1964, if you wish. Please request NTIS-PR-186/PCN for more information.

WRITE: Managing Editor
5285 Port Royal Road
Springfield, VA 22161

Keep Up To Date With SRIM

SRIM (Selected Research in Microfiche) provides you with regular, automatic distribution of the complete texts of NTIS research reports *only* in the subject areas you select. SRIM covers almost all Government research reports by subject area and/or the originating Federal or local government agency. You may subscribe by any category or subcategory of our WGA (**Weekly Government Abstracts**) or **Government Reports Announcements and Index** categories, or to the reports issued by a particular agency such as the Department of Defense, Federal Energy Administration, or Environmental Protection Agency. Other options that will give you greater selectivity are available on request.

The cost of SRIM service is only 45¢ domestic (60¢ foreign) for each complete

microfiched report. Your SRIM service begins as soon as your order is received and processed and you will receive biweekly shipments thereafter. If you wish, your service will be backdated to furnish you microfiche of reports issued earlier.

Because of contractual arrangements with several Special Technology Groups, not all NTIS reports are distributed in the SRIM program. You will receive a notice in your microfiche shipments identifying the exceptionally priced reports not available through SRIM.

A deposit account with NTIS is required before this service can be initiated. If you have specific questions concerning this service, please call (703) 451-1558, or write NTIS, attention SRIM Product Manager.

This information product distributed by

NTIS

U.S. DEPARTMENT OF COMMERCE
National Technical Information Service
5285 Port Royal Road
Springfield, Virginia 22161

UNCLASSIFIED

SECURITY CLASSIFICATION OF THIS REPORT (If different from that of the report)

REPORT DOCUMENTATION PAGE

READ INSTRUCTIONS
BEFORE COMPLETING FORM

1. REPORT NUMBER

2. GOVT. ACCESSION NO.

3. DOCUMENT CATALOG NUMBER

ADA023537

4. TITLE (and Subtitle)

Propagation Modeling and Analysis for High Energy Lasers

5. TYPE OF REPORT & PERIOD COVERED

Final Report
July 1974 - March 1975

6. PERFORMING ORG. REPORT NUMBER

SAI-74-629-WA

8. CONTRACT OR GRANT NUMBER(s)

N60921-75-C-0007

7. AUTHOR(s)

L. N. Peckham
P. R. Carlson

R. T. Liner
C. W. Wilson

9. PERFORMING ORGANIZATION NAME AND ADDRESS

Science Applications, Inc.
1911 North Myer Drive
Arlington, Virginia 22209

10. PROGRAM ELEMENT, PROJECT, TASK AREA & WORK UNIT NUMBERS

11. CONTROLLING OFFICE NAME AND ADDRESS

Naval Surface Weapons Center
White Oak Laboratory
White Oak, Silver Spring, Maryland 20910

12. REPORT DATE

April 1975

13. NUMBER OF PAGES

14. MONITORING AGENCY NAME & ADDRESS (if different from Controlling Office)

15. SECURITY CLASS. (of this report)

Unclassified

15a. DECLASSIFICATION/DOWNGRADING SCHEDULE

16. DISTRIBUTION STATEMENT (of this Report)

Approved for public release; distribution unlimited.

17. DISTRIBUTION STATEMENT (of the Abstract entered in Block 20, if different from Report)

AS SUBJECT TO CHANGE

18. SUPPLEMENTARY NOTES

REPRODUCED BY
NATIONAL TECHNICAL
INFORMATION SERVICE
U. S. DEPARTMENT OF COMMERCE
SPRINGFIELD, VA. 22161

19. KEY WORDS (Continue on reverse side if necessary and identify by block number)

High energy lasers
Laser beams
Propagation codes
Continuous wave

20. ABSTRACT (Continue on reverse side if necessary and identify by block number)

This report analyzes simplified propagation codes and recommends improved models for characterizing the propagation of high energy CW laser beams.

DD FORM 139 3 1973

EDITION OF 1 NOV 65 IS OBSOLETE
(GPO : 1973 : 214-500)

UNCLASSIFIED

DECLASSIFICATION OF THIS PAGE (IF APPLICABLE)

①

PROPAGATION MODELING AND ANALYSIS
FOR HIGH ENERGY LASERS

FINAL REPORT

SAI-74-629-WA

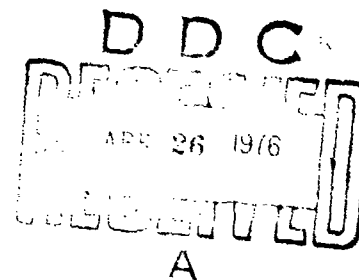
Mr. L.N. Peckham
Mr. P.R. Carlson
Dr. R.T. Liner
Dr. C.W. Wilson

This work was performed under Contract
No. N60921-75-C-0007, July 1974 through
March 1975.

April 1975

SCIENCE APPLICATIONS, INCORPORATED

1911 North Fort Myer Drive, Suite 1200, Arlington, Virginia 22209
(703) 527-7571



DISTRIBUTION STATEMENT A

Approved for public release;
Distribution Unlimited

FOREWORD

This is the final report covering work performed for the Naval Surface Weapons Center under contract N60921-75-C-0007. The purpose of the contract was to analyze simplified propagation codes and recommend improved models for characterizing the propagation of high energy CW laser beams. The work was performed under the direction of Mr. Larry Jobson of NSWC.

This report documents the work performed during the period January-March 1975. It also provides a review of the earlier work (July 1974-January 1975). The earlier work was described in detail in interim reports SAI-74-587-WA (October 1974) and SAI-74-622-WA (January 1975).

The authors wish to express their appreciation to Dr. Tom Tuer of the SAI Ann Arbor office for his development of the multi-line absorption coefficients. We also thank Mrs. T. Peckham for implementing the numerous code modifications.

SEARCHED	INDEXED
SERIALIZED	FILED
APR 1975	
NSWC	
ANN ARBOR	
BY	
DISTRIBUTION	
DISC	
A	

TABLE OF CONTENTS

<u>SECTION</u>		<u>PAGE</u>
1	INTRODUCTION	1-1
2	A SIMPLIFIED OPTICAL TRAIN MODEL	2-1
2.1	MODEL FORMULATION	2-3
2.1.1	Input Beam	2-3
2.1.2	Aerodynamic Window	2-7
2.1.3	Beam Clipper	2-10
2.1.4	High Power Mirrors	2-14
2.1.5	Beam Expander	2-18
2.1.6	Exit Aperture	2-20
2.2	ASSESSMENT OF OVERALL PERFORMANCE	2-24
2.2.1	Transmitted Power	2-24
2.2.2	Beam Quality	2-26
2.2.3	Beam Jitter	2-29
2.2.4	Beam Divergence	2-29
2.3	SAMPLE CALCULATIONS	2-33
3	CREATION OF SAICOM	3-1
3.1	MODIFICATIONS OF COMBO	3-1
3.1.1	Improvements to Computational Speed and Accuracy	3-2
3.1.2	Beam Quality	3-5
3.1.3	The Optical Train Model	3-6
3.1.4	Multi-Line Propagation	3-8
3.1.5	Modification of Turbulence and Jitter to Include Short and Long Term Effects	3-10
3.1.6	Far-Field Intensity Distribution	3-15
3.1.7	Calculation of Optimum Power	3-16
3.1.8	Miscellaneous Modifications	3-17

TABLE OF CONTENTS (CONT'D)

<u>Section</u>	<u>Page</u>
3.1.8.1 Variable Turbulence in Blooming Computations	3-17
3.1.8.2 Extinction Calculations in Blooming Integral	3-18
3.1.8.3 Power Variation	3-18
3.1.8.4 Deletion of Weight and Volume Calculations	3-18
3.1.9 Summary of Equations	3-19
3.2 A USER'S GUIDE TO SAICOM	3-20
3.2.1 OPTRAIN	3-22
3.2.2 ATM	3-25
3.2.3 BB	3-27
3.2.4 Input Data	3-27
4 SUMMARY OF TASKS I-IV	4-1
4.1 REVIEW OF TASK I. CODE COMPARISONS	4-1
4.2 REVIEW OF TASK II. BEAM SHAPE AND DISPLACEMENT	4-4
4.3 REVIEW OF TASK III. BEAM QUALITY	4-5
4.4 REVIEW OF TASK IV. BEAM TRUNCATION AND OBSCURATION	4-6
5 CONCLUSIONS	5-1
APPENDIX A Molecular Absorption of DF Laser Radiation	A-1
APPENDIX B SAICOM	B-1
REFERENCES	R-1

LIST OF FIGURES

<u>FIGURE</u>		<u>PAGE</u>
2.1	Typical Optical Train	2-4
2.2	Comparison of Input Beam Quality Specifications	2-8
2.3	Diffractive Spillover Losses	2-11
2.4	Beam Quality Loss Due to Central Obscuration in Terms of θ and M_t/l_0	2-21
2.5	Effects of Exit Aperture Temperature Fluctuations on Beam Jitter	2-25
2.6	Simplified Optical Train Employed in Defocus Calculations	2-31
2.7	Schematic of Optical Train for Sample Calculations	2-34
2.8	Results of Sample Calculations	2-39
3.1	Variations in Elements of the Blooming Calculations	3-4
3.2	α_1 as a Function of Altitude	3-11
3.3	α_2 as a Function of Altitude	3-12
3.4	α_3 as a Function of Altitude	3-13
3.5	$\alpha_{\text{RESULTANT}}$ as a Function of Altitude	3-14
3.6	SAICOM Flow Diagram	3-21
3.7	OPTRAIN Flow Diagram	3-24
3.8	ATM Flow Diagram	3-25
3.9	BB Flow Diagram	3-28
A-1	Water Concentration Profiles for Five Model Atmospheres and Analytic Fit	A-5
A-2	Demonstration of the Effect of Scaling to Account for Various Atmospheric Water Concentrations - P ₂ (8) DF Laser (a) No Scaling (b) With Scaling	A-6
A-3	Laser Propagation-Altitude Function Type A: Dominated by Water at Low Altitudes but with Underlying Absorption Lines which become Important at High Altitudes	A-8

LIST OF FIGURES

<u>FIGURE</u>		<u>PAGE</u>
A-4	Laser Propagation-Altitude Function Type B: Dominated by Water at Low Altitudes but with Underlying Absorption Lines which become Important at High Altitudes	A-9
A-5	Laser Propagation-Altitude Function Type C: Dominated by Water at Low Altitudes but with Underlying Absorption Lines which become Important at High Altitudes	A-10
A-6	Contributors to the Molecular Absorption of the $P_2(8)$ DF Line (Midlatitude Summer, Sea Level).	A-11
A-7	Contributors to the Molecular Absorption of the $P_2(9)$ DF Line (Midlatitude Summer Sea Level)	A-12
A-8	Contributors to the Molecular Absorption of the $P_3(8)$ DF Line (Midlatitude Summer, Sea Level)	A-13
A-9	Least Squares Fit to Type A Laser Lines	A-15
A-10	Least Squares Fit to Type B Laser Lines	A-16
A-11	Least Squares Fit to Type C Laser Lines	A-17

LIST OF TABLES

<u>TABLE</u>		<u>PAGE</u>
2.1	Summary of Beam Expander Transmissions and Obscuration Calculations	2-19
3.1	Beam Quality Parameters	3-7
3.2	SAICON Subroutines	3-23
3.3	Input Parameters	3-29
3.4	Sample Input Form with Default Values	3-34
3.5	Flags	3-36
A-1	List of DF-BDL Lines	A-2
A-2	Coefficients of Least Square Fit	A-14

Section 1

INTRODUCTION

In support of the Systems Analysis Team of the Naval Surface Weapons Center, Science Applications, Inc. (SAI), performed a series of tasks designed to develop a better understanding of the modeling alternatives available to laser systems analysts and to assist in the continual improvement of the NGL Engagement Code (NOLEC). Emphasis was placed on the resolution of propagation issues of interest to systems analysts. The tasks involved quantitative comparison of simplified HEL propagation codes used by DOD analysts, clarification of the beam quality problem, development of beam distortion and displacement models, development of a simplified optical train model, and expansion and improvement of the AFWL COMBO code.

The work was divided into six tasks. The first four tasks are reviewed in this report (Section 4), but are covered more extensively in interim reports (References 1 and 2):

First Interim Report - July-September 1974,
SAI-74-587-WA, October 1974 (Reference 1)
Task 1. Quantitative Comparison of
Simplified Propagation Codes
Task 3. Beam Quality Modeling.

Second Interim Report - September 1975-
January 1975, SAI-74-622-WA, January 1975
(Reference 2)
Task 2. Beam Shape and Displacement
Due to Thermal Lensing.
Task 4. Effect of Truncation and
Obscuration on the Far-Field Beam Profile.

Task 5 required the development of a simplified optical train model. This work is described in Section 2 of this report. Task 6 involved modification and extension of the AFWL COMBO code and included the incorporation of models developed in the earlier tasks. The new version of the code was named SAICOM. Section 3 describes the modifications and provides a user's guide to SAICOM.

Section 2

A SIMPLIFIED OPTICAL TRAIN MODEL

When performing laser application studies, the system analyst all too frequently assumes that the characteristics of the beam leaving the transmitting optic are the same as the characteristics of the beam leaving the laser device without regard for any changes induced by the optical elements and/or components required to get the beam from the laser device to the transmitting optic, i.e., the optical train. It is known, however, that significant changes to the characteristics of the beam do occur as it propagates through the optical train (see for example References 3 and 4). The finite absorptivity of the high power mirrors, clipping and blockage of a portion of the high power beam, and diffraction effects all reduce the available power in the beam at the transmitting optic. In addition the optical quality of the beam is affected by nearly every component or element through changes in the phase and amplitude distribution of the beam. Therefore, if realistic estimates of the performance of candidate laser systems are to be obtained during these application studies, it is important to include the effect of the optical train on the characteristics of the laser beam.

An accurate assessment of the impact of the optical train is a tedious and difficult calculation requiring a wave optics approach and sophisticated analytical tools for modeling each of the elements in the optical train. Obviously these are not very practical for use in systems analysis

application studies in which a large parameter space must be investigated. Therefore, if the effect of the optical train is to be included in such analyses, the development of simple but reasonably accurate models is required.

One such model has been developed by the AFWL (Reference 5) which is used in their simplified propagation code (COMBO). However, its use is somewhat restrictive in that most of the component effects are left for the user to specify. Prescriptions for scaling these effects in terms of system parameters are not given. In addition, the impact of the optical train on the beam quality is assessed in terms of peak intensity reduction. Based on work under this contract, it is felt that an assessment in terms of the far-field power distribution provides a better characterization of the beam quality (see Reference 1 and Section 4.3 of this report).

We have developed a more comprehensive "simplified" optical train model which can be used to estimate the degradation in system performance caused by the optical components required to direct the beam from the laser device to the transmitting optic (i.e., aerodynamic window, mirrors, beam expander, etc.). The intent of the model is not to provide detailed engineering design data but rather to provide the systems analyst with a rapid assessment capability which will allow him to perform more realistic systems analyses of candidate HEL systems. Hence, emphasis is placed on formulating simple but reasonably accurate models for the various factors influencing the performance of the laser system. The approach is similar to that taken by the AFWL in their simplified model but with new additions and modifications to make the model more flexible. The model has been implemented in a subroutine called OPTRAIN and is included in the SAICOM code as described in Section 3 below.

2.1 MODEL FORMULATION

Conceptually, the optical train may be viewed as a "black box" located between the laser device and the transmitting optic. The input to the box is the output beam from the laser. The model operates on this beam according to the number and type of elements in the train, and its output, in the form of certain performance parameters, provides the input to an atmospheric propagation model. The performance parameters are: (1) the power available at the transmitting optic, (2) beam quality, (3) beam divergence, and (4) beam jitter. In addition, the actual diameter of the beam at the exit aperture is computed for use in the propagation model.

The essential features of the model are illustrated in Figure 2.1. The optical elements and components include (1) an aerodynamic window, (2) a beam clipper, (3) several high power mirrors, (4) a beam expander, (5) an exit aperture, and (6) a focusing element for transmitting the beam to the target plane. In most practical cases the beam expander and focusing element are combined into a single telescope. However, it is convenient for the present analysis to separate them into an ideal beam expander which simply expands the beam and a separate element which applies the curvature to the beam phase front for focusing purposes.

2.1.1 Input Beam

Although it is not an optical element or component, the input beam is necessarily an integral part of the model since it has strong influence on the behavior of the rest of the optical train. In order to simplify the analysis of the components in the optical train, it is assumed that the beam from the laser is circular. However, because of

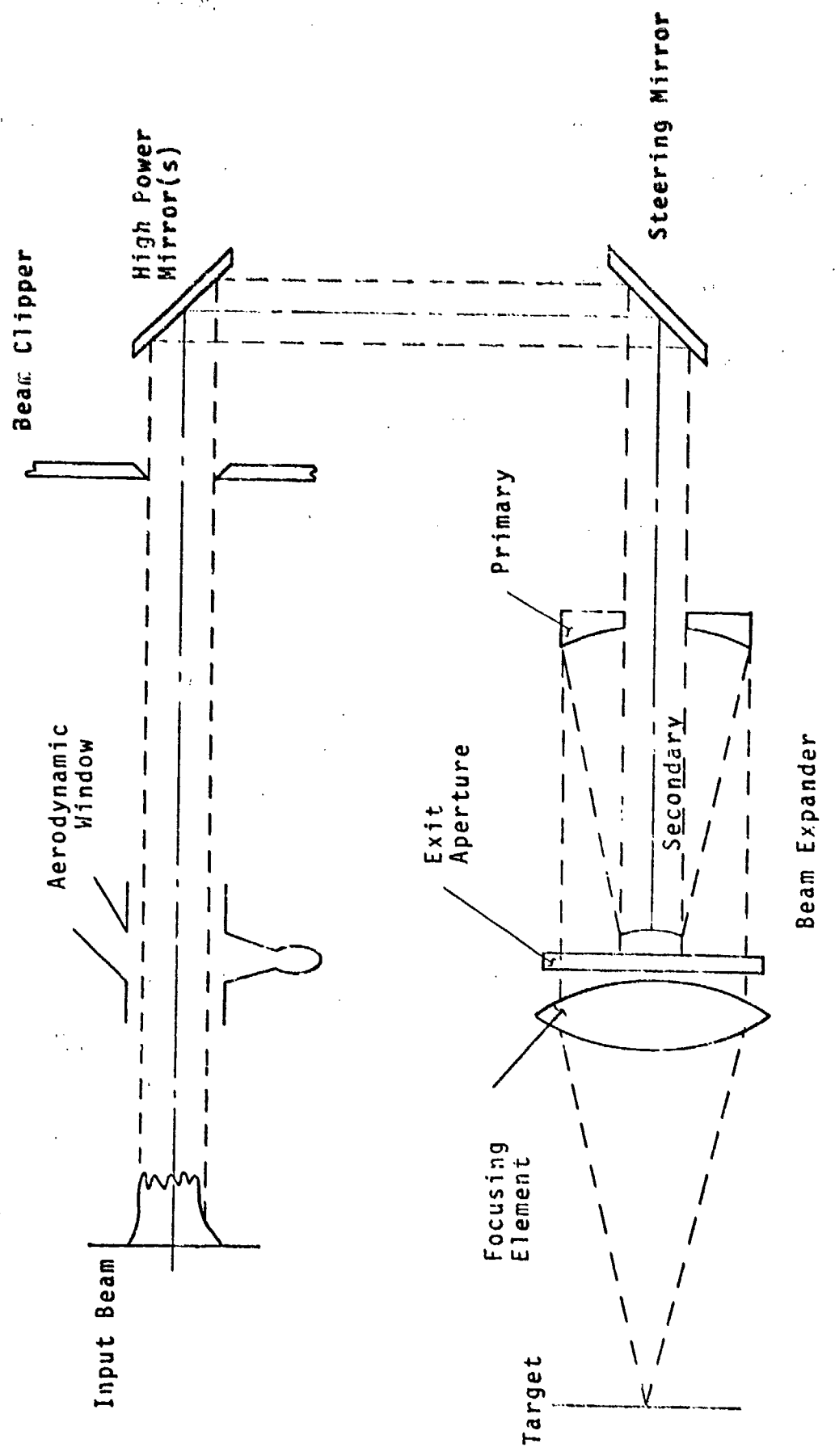


Figure 2.1 Typical Optical Train

the widespread use of unstable resonator configurations to extract power from high power devices, the possibility of a central obscuration in the input beam is incorporated into the model. The inner and outer diameters of the input beam are ϵD_B and D_B respectively. An unobscured input beam profile can be realized by defining $\epsilon = 0$. Other parameters required to specify the input beam are (1) the power in the beam, P_L , (2) the pulse length, Δt , (3) the curvature of the phase front, R_L , and the beam jitter, θ_L .

In order to evaluate the effect the beam has on the high power mirrors in the optical train, it is also necessary to characterize the intensity profile entering the optical train. This is achieved by specifying both the magnitude and scale size of the intensity fluctuations, the magnitude being specified as a fraction of the average intensity ($\Delta I/I_{ave}$) and the scale size as a fraction of the beam diameter (λ_I/D_B). Thus the input beam profile may be visualized as having a uniform intensity I_{ave} with fluctuations ΔI superimposed upon this level.

The optical quality of the input beam is specified by a wavelength scaling factor, n_L . Unfortunately, this definition of beam quality does not allow one to easily incorporate the other beam quality degrading factors induced by the various elements of the optical train. Therefore this parameter is converted by the model into an equivalent root-mean-square phase distortion, σ_L .

Two alternative approaches for this conversion were investigated for use in the model. The first approach is to define the equivalent phase distortion so as to match the reduction in the peak intensity, I_p . According to the analysis presented in Reference 6, the peak intensity reduction is (for a gaussian beam containing small scale random phase variations)

$$I_p/I_g = \exp(-\sigma_L^2)$$

where I_g is the ideal on-axis intensity. According to the wavelength scaling definition of beam quality

$$\frac{I_p}{I_g} = \frac{1}{n_L^2}$$

so that

$$\sigma_L = \sqrt{2 \ln(n_L)} \quad (1)$$

It should be noted that this approach is equivalent to the power scaling definition of beam quality and is also the approach taken by the AFWL in their optical system model (Reference 5).

The second approach investigated was to define the equivalent phase distortion to match the power in the "bucket" ($R\lambda/D = 1$) predicted by wavelength scaling. This is given by (Reference 1):

$$P(R\lambda/D) = P_0 \{1 - \exp(-\pi^2/2n_L^2)\}.$$

Again, following the analysis of Reference 4, the power in the bucket for a non-diffraction-limited gaussian beam is given by

$$P(R\lambda/D) = P_0 \exp(-\sigma_L^2) \{1 - \exp(-\pi^2/2)\}$$

assuming all of the quality degradation can be characterized as a scattering loss. Equating these expressions and solving for σ_L yields,

$$\sigma_L = \left\{ -\ln \left[\frac{1 - \exp(-\pi^2/2n_L)}{1 - \exp(-\pi^2/2)} \right] \right\}^{1/2} \quad (2)$$

Intuitively it would seem that both of these approaches should yield approximately equivalent results. Quantitatively however, substantial differences were found. These are illustrated in Figure 2.2 which compares the phase distortion computed from Equations (1) and (2). The phase distortion based on matching the peak intensity reduction is always considerably higher than that based on matching the power-in-the-bucket, e.g., over a factor of 2.5 for a 1.5 times diffraction-limited input beam. The reasons for these differences are not clear. One possible explanation is the equivalence of wavelength and power scaling methods of defining peak intensity reduction. It was found during previous work under this contract (Reference 1) that power scaling was always more pessimistic in its predictions of the beam quality than wavelength scaling. Therefore, matching the peak intensity based on a method that is equivalent to power scaling might be expected to produce more pessimistic results (i.e., higher σ_L) than matching the power-in-the-bucket based on wavelength scaling.

Whatever the reasons for the differences, we recommend the use of Equation (2) because the power-in-the-bucket is a more meaningful measure of laser performance than peak intensity reduction. The latter suffers from its sensitivity to defocusing errors and difficulty in experimental measurement.

2.1.2 Aerodynamic Window

The first component in the optical train is the aerodynamic window isolating the optical cavity of the laser

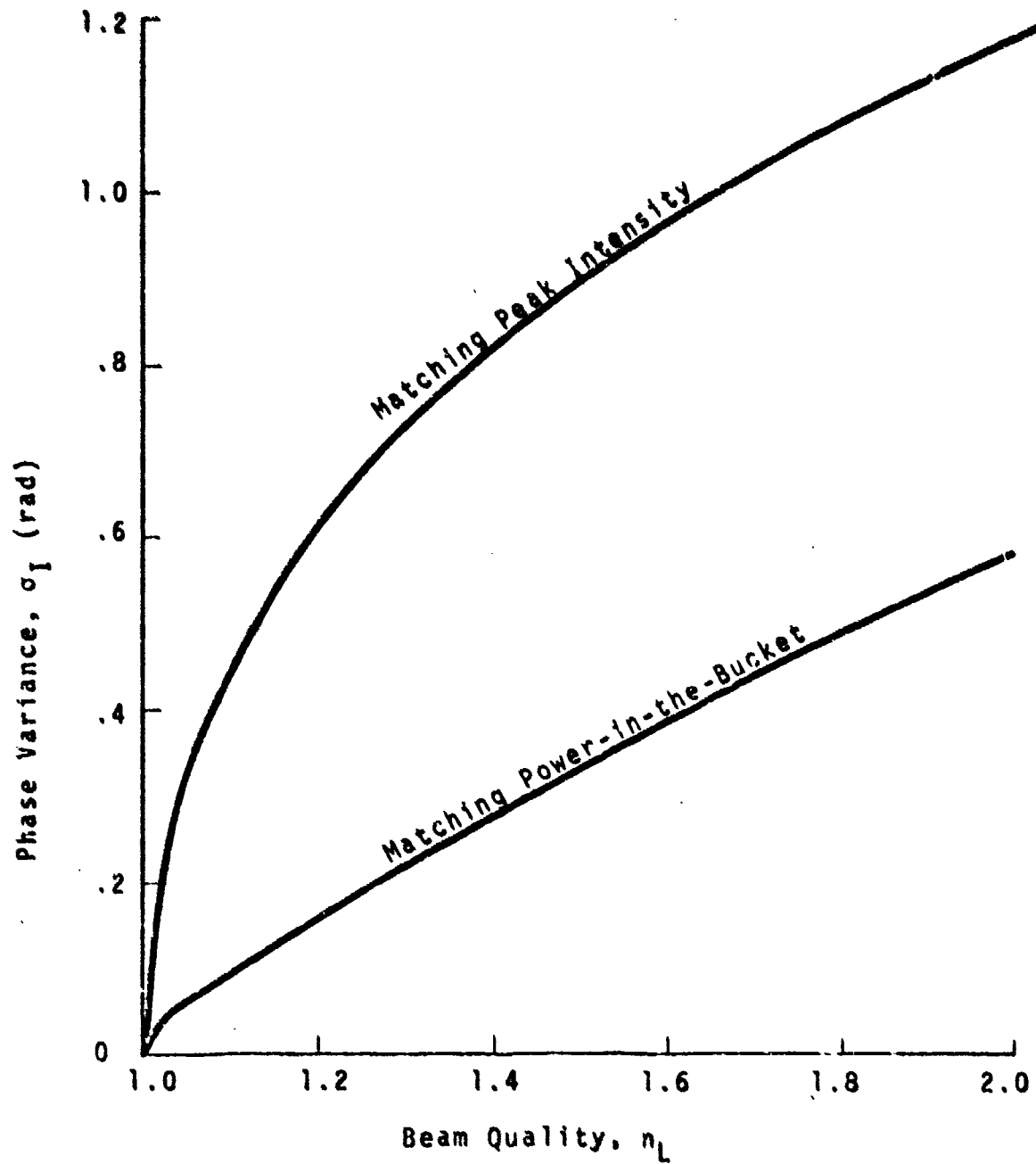


Figure 2.2. Comparison of Input Beam Quality Specifications

from the atmosphere. Basically there are two types of aerodynamic windows currently being considered for HEL applications: (1) focused and (2) unfocused. In both cases, if the window is properly designed, there should be little or no power loss when the beam passes through it. In addition, it is also assumed that no spherical distortion to the phase front will be induced by the aerodynamic window. The shock waves supporting the pressure rise and the turbulence generated by the aerodynamic window will, however, induce a loss in the beam quality. An expression for this loss is given by (Reference 4)

$$\Delta I/I = 2.84 \times 10^{-10} \left(\frac{\Delta \rho}{\rho_s} \frac{D_B}{\lambda} \right)^2$$

where $\Delta \rho$ is density change across the shear layer and ρ_s is a reference density at STP. Again this formulation of beam quality degradation is not convenient for use in the model and is converted into an equivalent phase distortion, σ_{aw}^2 by use of the Strehl formula (Reference 4):

$$\Delta I/I = \sigma_{aw}^2.$$

Solving for the phase distortion yields

$$\sigma_{aw} = 1.69 \times 10^{-5} \left(\frac{D_B}{\lambda} \frac{\Delta \rho}{\rho_s} \right).$$

A typical value of σ_{aw} for a 10 cm beam from a chemical laser ($\lambda = 3.8 \mu\text{m}$), assuming $\Delta \rho/\rho_s = 0.25$ for the density variations, is $\sigma_{aw} = 0.11$ radians. This corresponds to an intensity reduction of $\Delta I/I \approx 1.2\%$.

For the focused aerodynamic window, the beam diameter will typically be very small (<0.1 cm) so that the phase distortion can be neglected, i.e., $\sigma_{AW} \approx 0$.

2.1.3 Beam Clipper

For HEL systems in which the laser device and the pointer/tracker are not closely coupled, a beam clipper or scraper will probably be employed near the pointer/tracker to control the size of the high power beam entering the transmitter. The beam clipper will influence both the power available at the transmitting optic and the beam quality, the latter by limiting the maximum diameter at the transmitting optic.

The loss in power at the beam clipper is due primarily to diffractive spreading of the beam as it propagates between the aerodynamic window and the beam clipper. In general, the diffractive spreading will depend upon the phase and amplitude aberrations in the input beam profile. An accurate assessment of the actual losses requires a detailed calculation involving numerical solutions of the Fresnel diffraction integral or spatial frequency approaches to optical propagation (i.e., Fourier Optics). These techniques are very time consuming and were not considered as viable candidates for the "simplified" model. Instead, an empirical approach based on curve fits of available data in the literature was taken. Unfortunately very little data were available for examination. Only two sources were found (References 4 and 7). The data obtained from these sources are illustrated in Figure 2.3 which shows the variation in power diffracted into the geometric shadow of a uniformly illuminated aperture as a function of the propagation distance from the aperture. The AFWL data were calculated for a one-dimensional beam profile while the HAC (Hughes

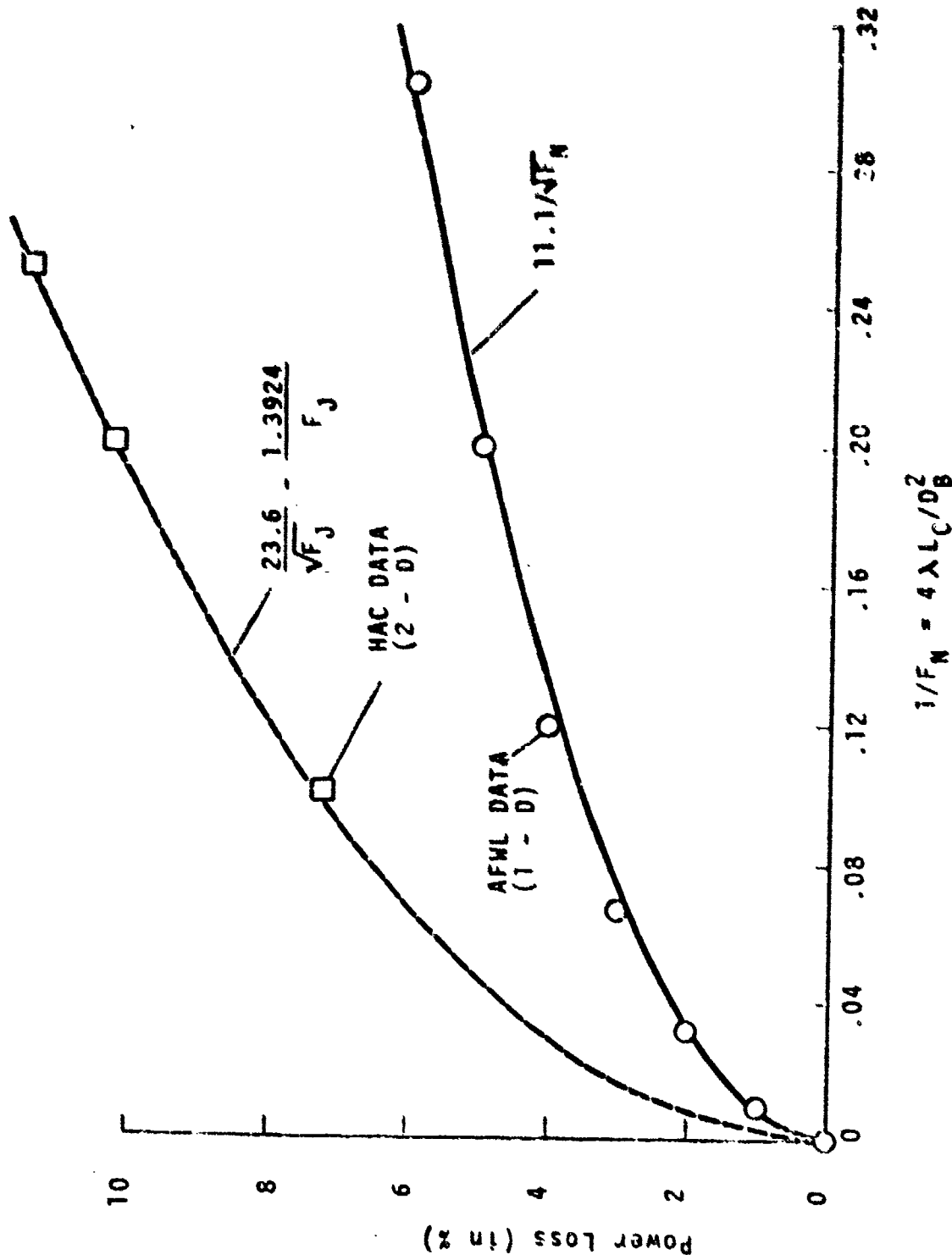


Figure 2.3. Diffractive Spillover Losses

Aircraft Company) calculations were performed for a round beam. Therefore, the data must be adjusted for these differences before a direct comparison can be made.

Intuitively one would expect a factor of two difference between the data based on simple geometrical arguments. For example, a square beam profile would have twice the loss of a one-dimensional profile because of the two additional edges. For a round beam, however, the ratio is not quite as straightforward. Assuming circular symmetry, the fractional power loss is

$$\Delta_{2-0} = \frac{2\pi \int_a^{\infty} I(\sigma) \sigma d\sigma}{\pi a^2 I_0}$$

where a is the radius of the aperture and I_0 is the initial intensity. The major contribution to the integral occurs near the edge of the aperture. Thus over this region the radius can be taken as being approximately constant ($= a$) and removed from the integral without affecting its value, i.e.,

$$\Delta_{2-0} = \frac{2}{a I_0} \int_a^{\infty} I(\sigma) d\sigma.$$

For the one-dimensional beam profile the fractional power loss is given by

$$\Delta_{1-0} = \frac{\int_a^{\infty} I(x) dx (1)}{a I_0 (1)}$$

so that if one further assumes that the intensity profiles at the aperture plane are the same in either case, i.e., $I(r) = I(x)$, then one again gets a factor of two difference between the power losses.

The actual ratio indicated by the data was somewhat higher than a factor of 2 as shown by the corresponding curve fits of the data. Both sets of data correlated very well as a function of the reciprocal of the square root of the Fresnel number. However, the proportionality constant for the HAC data was found to be 23.6 versus 11.1 for the AFNL data.

In order to use these results in the optical train model, the power loss was assumed to be related to an effective increase in the beam diameter at the aperture plane, i.e.,

$$\frac{D_{B_0}}{D_B} = (1 - \text{loss})^{1/2} = 1 - \frac{0.112}{\sqrt{F_N}}$$

where D_{B_0} is the new diameter of the beam at the beam clipper station and $F_N = D_B^2/4\lambda L_C$ is the propagation Fresnel number. It was also assumed, for the case of an obscured beam, that the hole in the beam filled in as much as the diameter of the hole would grow were it a uniformly illuminated aperture (i.e., Babinet's Principle). Thus the inner diameter of the obscured beam, D_{B_i} , is computed by

$$D_{B_i} = \epsilon D_B (1 - 0.112/\epsilon \sqrt{F_N}).$$

If D_c is the diameter of the beam clipper, then the power transmission through the aperture is

$$T_c = \begin{cases} 1.0 & \text{if } D_{B_0} \leq D_c \\ (D_c/D_{B_0}) & \text{if } D_{B_0} > D_c \end{cases}$$

In the latter case, the beam diameter is set equal to the clipper diameter for the remaining calculations in the model.

2.1.4 High Power Mirrors

The mirrors in the optical train will affect all the performance parameters. Although it is not necessary we assume that all of the mirrors are identical in order to reduce the number of inputs.

A mirror alters the amplitude of the beam by absorbing a fraction of the incident radiation. For a series of N mirrors each having a surface reflectivity R , the transmission factor is

$$T_M = R^N.$$

It should be noted that in the present analysis N includes all of the mirrors in the optical train, i.e., relay, steering, secondary and primary.

The beam quality degradation is due to (1) surface roughness and manufacturing errors in the mirror figure, and (2) surface distortions due to absorption of power from the incident beam. The former are independent of the power in the beam while the latter is a function of both the power and the irradiance distribution. In addition, if

cooled mirrors are used, there will also be distortions induced by the pressure variations inside the coolant passages. However, these distortions will depend upon the details of the mirror construction and their characterization is felt to be beyond the scope of this model. Therefore, for this analysis, distortions of this type will be included in (1) above.

The beam quality degradation induced by the mirrors is incorporated into the optical train model through an equivalent phase variance, σ_M where

$$\sigma_M^2 = N\sigma_f^2 + [(N - 1)\sigma_I + \sigma_I/M^2]^2.$$

The first term on the right hand side of the above expression represents the uncorrelated sum of the phase distortion due to fabrication errors such as surface roughness, figure error, coolant passage distortion, etc. The remaining terms represent the correlated sum of the irradiance mapping phase distortion. The distortion of the primary mirror is reduced by the square of the magnification of the beam expander to account for its reduced thermal loading.

In practice, σ_f is not known but is instead specified as a tolerance on the manufacturing process. Therefore, for modeling purposes this parameter was left to the user to specify.

The approach taken to model σ_I was to assume that the distortions scale directly with the irradiance fluctuations. That is,

$$\sigma_I = KI_{rms}$$

where K is a constant which depends upon the physical parameters of the mirror, the cooling scheme, etc. If we assume that the peak to peak intensity fluctuations specified in the input beam description are uniformly distributed and random in character, then

$$I_{rms} = \frac{I_{ave}}{\sqrt{12}} \left(\frac{\Delta I}{I_{ave}} \right)$$

where, for a circular beam,

$$I_{ave} = \frac{4 P_L}{\pi D_B^2}$$

Expressions for the evaluation of K depend upon whether the mirror is water cooled or not, i.e., for cooled optics

$$K(m^2/watt) = 5 \times 10^{-14} (1 - R) (2\pi/\lambda)$$

whereas, for uncooled optics

$$K = 4\pi (1 - R) \alpha \Delta t / \lambda C \rho$$

where

α = the thermal expansion coefficient of the mirror material

C = the specific heat of the mirror material

ρ = density of the mirror material.

The expression for cooled optics is based on the NPT/Chemical Laser Compatibility Study conducted by Hughes Aircraft Company for NSWC (Reference 8) in which similar expressions were employed to compute the phase distortion caused by the NAEL irradiance profile. The expression for uncooled optics is based on a simplified one-dimensional heat transfer analysis (Reference 9).

Local surface distortion is not the only performance degrading factor caused by the finite absorptivity of the mirrors. A bending distortion is also induced by the differential growth of the front and rear mirror surfaces. For properly designed, cooled mirror configurations, this distortion can be kept small. However, for uncooled mirrors, it may be important.

To first order, the bending distortion is primarily a function of the total beam power and not the irradiance distribution. In addition it produces mostly a spherical phase front distortion. Thus in the optical train model, we compute this distortion mode as a beam divergence instead of a quality loss since, in theory, it could be corrected by the focusing optic (if detected).

For an uncooled mirror that was initially flat, the change in the focal length with time can be approximated as (see Reference 9)

$$f = \frac{D_B^2 \ell \cos \theta}{2.44 P_L (1 - R) \alpha} \left(\frac{D \rho K}{\Delta t} \right)^{1/2}$$

where

ℓ is the mirror thickness

θ is the beam angle of incidence on mirror

K is the thermal conductivity of the mirror material

f is the focal length of the distorted mirror.

The mechanism by which the defocusing errors induced by the individual mirrors are accumulated throughout the optical train is explained later.

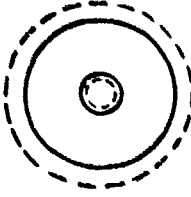
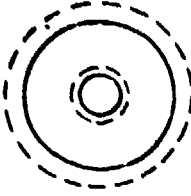
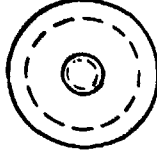
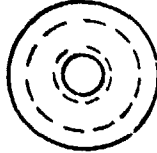
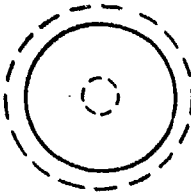
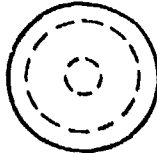
2.1.5 Beam Expander

In the formulation of the beam expander model, we allow for two types: (1) an on-axis or (2) an off-axis system. Either type system affects the available power at the transmitter, the beam quality, beam jitter and beam divergence. A discussion of the methodology for computing the transmission factor and beam quality is given below. The beam jitter and divergence are discussed in a later section.

The power transmission through the beam expander is computed by projecting the exit aperture (defined by the user) onto the plane of the beam clipper station. Simple geometry then allows one to compute the power lost due to a mismatch between the beam diameters and exit aperture diameters. The formulas are illustrated in Table 2.1 for both the on-axis and off-axis cases.

The beam quality is not affected by the off-axis system except to the extent that the limiting diameter is $MD_{B_0} \leq D_t$ for spot size calculations at the target plane. This is also true of the on-axis case. However, the on-axis system also introduces a central obscuration ϵ , which reduces the beam quality. The expressions used in the model to compute the final obscuration of the beam leaving the optical train are also given in Table 2.1.

Table 2.1. Summary of Beam Expander Transmissions and Obscuration Calculations

TYPE	GEOMETRY	TRANSMISSION	OBSCURATION
ON AXIS		$\frac{D_o^2 - D_i^2}{D_{B_o}^2 - D_{B_i}^2}$	D_i/D_o
		$\frac{D_o^2 - D_{B_i}^2}{D_{B_o}^2 - D_{B_i}^2}$	D_{B_i}/D_o
		$\frac{D_{B_o}^2 - D_i^2}{D_{B_o}^2 - D_{B_i}^2}$	D_i/D_{B_o}
		1.0	D_{B_i}/D_{B_o}
OFF AXIS		$(D_o/D_{B_o})^2$	D_{B_i}/D_o
		1.0	D_{B_i}/D_{B_o}

The effect of the obscuration on the beam quality is again computed by relating it to an equivalent phase distortion. This relationship was derived empirically based on the results of the previous work under this contract (Reference 2), and is illustrated graphically in Figure 2.4. Within the computer code, this relationship is represented by a third order polynomial developed from a "least-squares" regression analysis of the data presented in Figure 2.4. Also shown on the figure is the effective scale size of the phase distortion. Its use in the model will be explained below.

2.1.6 Exit Aperture

Provisions were also made in the optical train model for an exit aperture downbeam of the pointer/tracker. It can be either a material window or open port, with an aerodynamic curtain protecting the optics from the environment, based on user specified option parameters.

In either case the loss in power through this exit aperture will be

$$T_E = e^{-\beta L_W} (1 - A_S/A_B)$$

where

β = absorption coefficient of material window

L_W = thickness of material window

A_S = area of struts supporting window or secondary mirror in the case of an on-axis beam expander

A_B = beam area ($\pi M^2 D_{B_0}^2 / 4$).

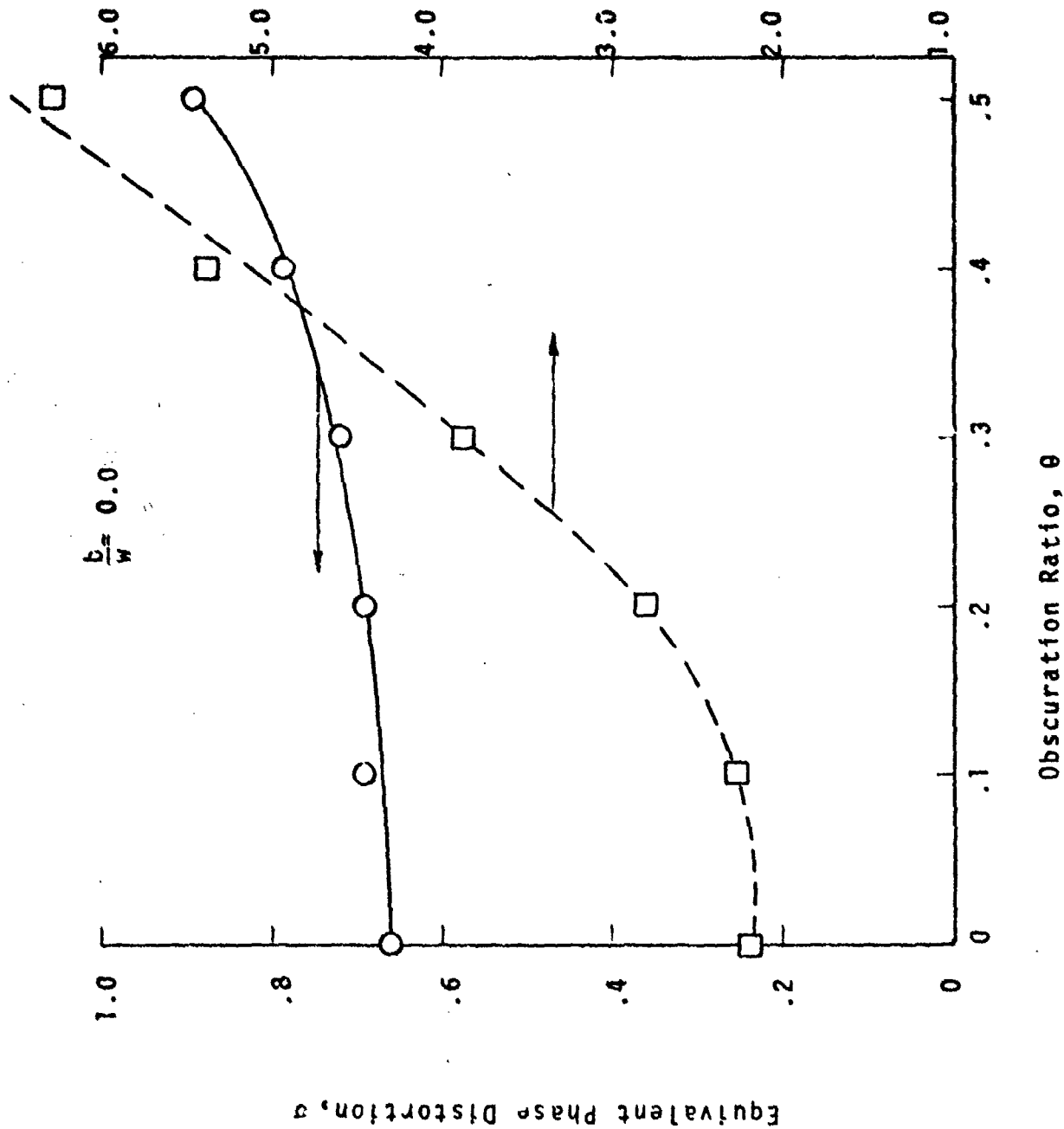


Figure 2.4. Beam Quality Loss Due to Central Obscuration in Terms of θ and $W_t/10$

Note that an open port can be simulated by setting $\beta = 0$.

For simplicity, the phase distortion induced by the material window is assumed to be proportional to the local intensity fluctuations in the beam profile. That is

$$\sigma_w = \left(\frac{2\pi}{\lambda} \right) \frac{\beta \Delta t L_w}{\rho c} \left[(n - 1) \alpha + \frac{\partial n}{\partial T} \right] \frac{I_{rms}}{M^2}$$

where (in addition to those parameters previously defined) n is the refractive index and T is the temperature. The magnification appears because of the assumed location of the window downstream of the beam expander. In order to minimize the number of inputs to the model, the material constants were lumped into a single parameter defined as

$$\gamma = \frac{1}{\rho c} \left[(n - 1) \alpha + \frac{\partial n}{\partial T} \right]$$

which varies between $4 \times 10^{-12} \text{ m}^3/\text{j}$ for the fluoride windows (CaF_2 , MgF_2 , SrF_2) to $15 \times 10^{-12} \text{ m}^3/\text{j}$ for the salt windows (NaCl , KCl). A value of $5 \times 10^{-12} \text{ m}^3/\text{j}$ was hard-wired into the model as being representative of current window technology.

The presence of struts in the beampath will also cause a reduction in the beam quality. To first order, this loss will be directly proportional to the area of the beam blocked by the struts. Consider, for example, the on-axis intensity which, in the context of scalar diffraction theory, is given by the integral of the complex field leaving the transmitting aperture, i.e.,

$$I(0) \sim \left[\iint u(x,y) dx dy \right]^2.$$

Thus, for a constant field aperture strength, the integral is simply the area of the clear aperture. That is

$$I(o) = (A_B - A_S)^2$$

so that the intensity reduction relative to no struts is simply

$$\frac{I(o)}{I_0} = \left(1 - \frac{A_S}{A_B}\right)^2 = T_S (1 - A_S/A_B).$$

For modeling purposes, this intensity reduction was considered to be separable into (1) a power loss due to the transmission of the aperture, T_S , and (2) a beam quality loss characterized by wide angle scattering, $(1 - A_S/A_B)$. The latter can be related to an equivalent phase distortion via the Strehl equation

$$\sigma_S = (A_S/A_B)^{1/4}.$$

The phase distortion induced by an open port is not intensity dependent but instead a function of the turbulence level inside the beam expander and aerodynamic curtain. Because of the presence of turbulence, this effect is treated as an additional source of beam jitter in the model. The magnitude of the jitter is estimated from (Reference 8)

$$\theta_J = 2.14 \times 10^{-7} \left[\frac{L_e^3 \Delta T^6}{\lambda D_t^2} \right]^{1/5}$$

where L_e is the path length through the beam expander and ΔT is the magnitude of the temperature fluctuations within the beam expander. Some representative values of the jitter are illustrated in Figure 2.5 for a 0.7 meter transmitter diameter. For example, a 1°C temperature fluctuation produces approximately $4.5 \mu\text{rad}$ of beam jitter for a $3.8 \mu\text{m}$ wavelength beam.

2.2 ASSESSMENT OF OVERALL PERFORMANCE

The previous discussion was primarily concerned with the influence each of the elements has on the characteristics of the laser beam as it traverses the optical train. In the following section we show how these individual effects are accumulated to arrive at an overall assessment of system performance.

2.2.1 Transmitted Power

The power available at the transmitting optic is simply the input power from the laser device modified to account for all of the power losses that have occurred along the optical train. That is

$$P_t = T P_L$$

where T is an overall transmission factor. Since the power losses are multiplicative, the overall transmission factor is

$$T = (T_C) (T_M) (T_{BE}) (T_E)$$

Diameter = 0.7 m
Length = 2.0 m

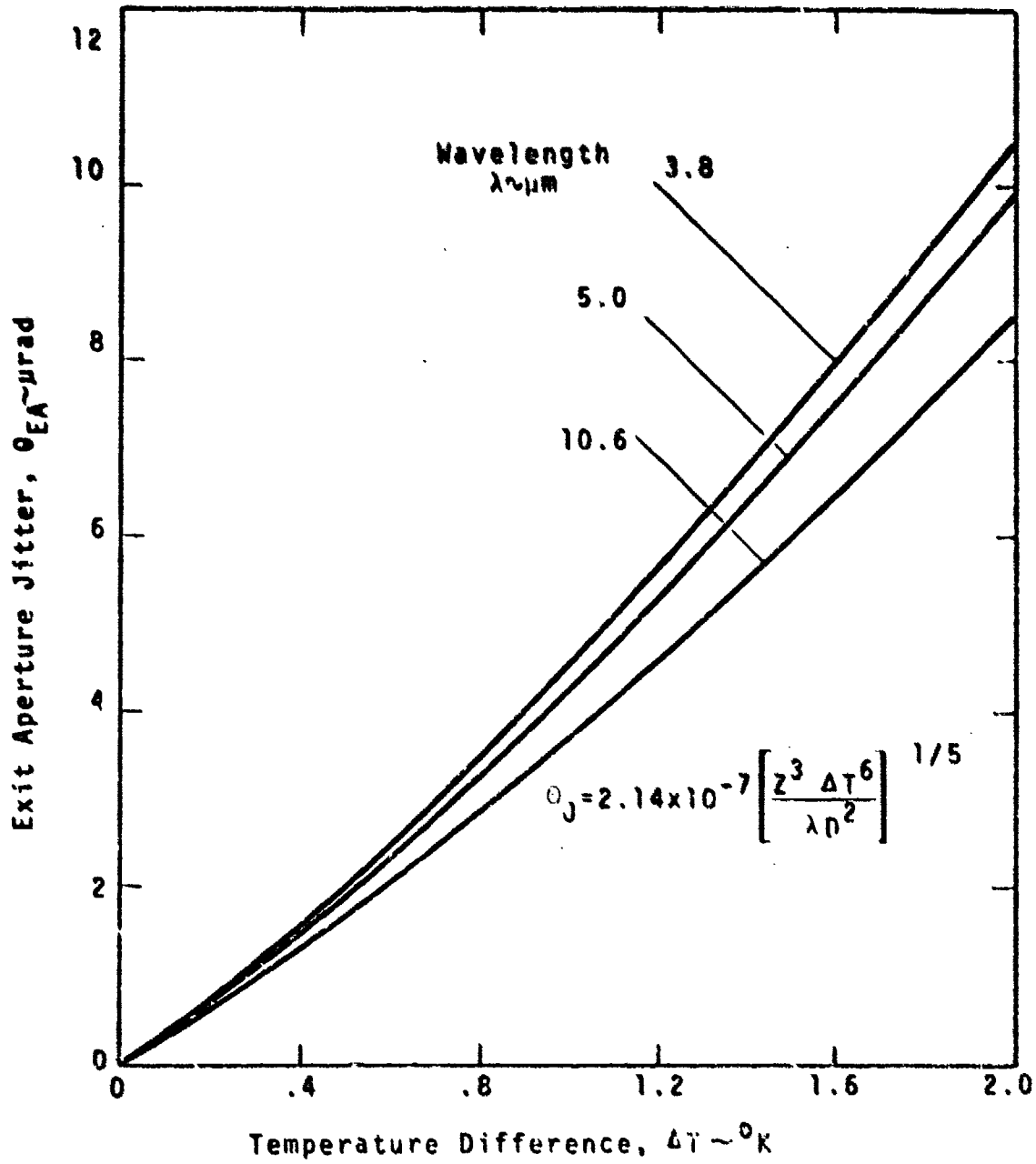


Figure 2.5. Effects of Exit Aperture Temperature Fluctuations on Beam Jitter

where T_c is the transmission factor of the beam clipper, T_M is the transmission factor of all the high power mirrors, T_{BE} is the transmission factor of the beam expander, and T_E is the transmission factor of the exit aperture. Formulas for all of these factors were given previously.

2.2.2 Beam Quality

The quality of the beam at the transmitting optic is characterized by the two beam quality parameters, m_1 and m_2 (see Reference 1 and Section 4.3 of this report). Unfortunately, the calculation of m_1 and m_2 is not simple. The basic problem is to combine the effect of all the quality degrading factors occurring within the optical train. This is somewhat complicated because the phase distortions induced by the individual components do not add up in a straightforward manner but instead depend, in a complicated manner, upon the distribution as well as the magnitude of the phase distortion. For example, a "smooth" distortion behaves differently than a very "rough" distortion even though their magnitudes are the same.

To circumvent this problem, a statistical approach is used within the model to accumulate the phase distortions. This approach is somewhat loosely based on the theoretical investigations of nondiffraction-limited gaussian beams by B. Hogge at the AFWL. Briefly, the approach is to consider the overall beam profile at the focal plane as being composed of two gaussian beam profiles of different relative amplitudes and widths. That is, a certain fraction of the energy in the beam is propagated completely unaffected by the phase distortion, i.e.,

$$I_u(r) = e^{-\sigma^2} \exp\left(-\frac{2r^2}{w_f^2}\right) I_0$$

where w_f is the diffraction limited waist parameter, I_0 is the on-axis intensity and σ^2 is the variance of the phase distortion (assumed to a gaussian random variable). The remaining energy is smeared or spread by the phase distortion into a somewhat larger beam profile, i.e.,

$$I_s(r) = (1 - e^{-\sigma^2}) \left(\frac{w_f^2}{w_f^2 + 2\sigma^2 f^2} \right) \exp \left(\frac{-2r^2}{w_f^2 + 2\sigma^2 f^2} \right) I_0$$

where Θ is the angular spread of the scattered beam.

The problem thus reduces to characterizing the overall phase variance, σ , and beam spread parameters, Θ , that "best" model the summation of all of the phase distortions in the optical train.

A true characterization of σ and Θ is, in reality, not possible. Some theoretical arguments can be made for isolated phase distributions such as the random gaussian noise model investigated by Hogge. In the real world, however, optical systems do not produce such amiable distortions. Nevertheless, using these results as being at least qualitatively correct, we compute the total phase distortion as simply the uncorrected sum of each of the individual distortions, i.e.,

$$\sigma^2 = \sigma_L^2 + \sigma_{AW}^2 + \sigma_M^2 + \sigma_{BE}^2 + \sigma_S^2 + \sigma_W^2.$$

Instead of computing the beam spread, Θ , it is more convenient to compute an effective scale size or correlation length of the overall phase distortion, L . This scale size is related to the beam spread via $\Theta^2 = (\lambda/\pi L)^2$. In the

aforementioned work of Hogge, it was noted that the effective correlation length for a number of sources of phase distortion was found to be an average of the correlation lengths of the individual sources, each weighted by its respective variance. Again, taking the inductive leap, we compute L from

$$L = \frac{1}{\sigma^2} \left[\epsilon_L \sigma_L^2 + \epsilon_{AW} \sigma_{AW}^2 + \epsilon_M \sigma_M^2 + \epsilon_{BE} \sigma_{BE}^2 + \epsilon_S \sigma_S^2 + \epsilon_W \sigma_W^2 \right].$$

In practice very little is known about the magnitude of the scale sizes characterizing the individual components. Therefore, for the present model, we have made some additional assumptions regarding their respective sizes. For example, the irradiance mapping phase distortions such as σ_I and σ_W are assumed to have the same scale size as the intensity fluctuations in the input beam profile. For other components, such as the laser device, the aerodynamic window and the struts, we assume that the scale size is zero. In effect this is assuming that each of these components scatters the energy in the beam beyond a usable radius in the focal plane and therefore is somewhat conservative. The scale size of the beam expander was determined empirically since the effect of obscuration on the near-field beam profile was readily calculated (see Figure 2.4). Within the model this relationship is represented by a third order polynomial.

The computed values of the phase variance and scale size are used to evaluate the power distribution at two radial positions in the far-field, namely $r = w_f$ and $r_2 = 2w_f$. These power points are then used to generate the beam quality parameters m_1 and m_2 . The procedure for doing this is outlined in Reference 1.

2.2.3 Beam Jitter

The beam jitter is accumulated throughout the optical train by assuming that the sources of beam jitter are independent of each other. Thus they may be root-sum-squared to get the total jitter. The primary consideration for the beam jitter calculation is whether or not the source of the jitter is upbeam or downbeam of the beam expander. The beam expander reduces the jitter by a factor of $1/M^2$ where M is the magnification.

The sources of beam jitter considered by the model are

- Tracking jitter, θ_{TR}
- Boresight jitter, θ_{BS}
- Autoalignment system jitter, θ_{AA}
- Servo jitter, θ_S
- Device jitter, θ_L
- Exit aperture induced jitter, θ_E .

The jitter of the input beam and the jitter induced by the beam steering mirror in the autoalignment system are assumed to occur before the beam expander. The remaining jitter sources are assumed to occur after the beam expander. Thus the total jitter leaving the optical train is given by:

$$\sigma_J = \{\theta_{TR}^2 + \theta_{BS}^2 + \theta_S^2 + \theta_E^2 + (\theta_L^2 + \theta_{AA}^2)/M^2\}^{1/2}.$$

2.2.4 Beam Divergence

The beam divergence represents the spherical phase curvature in the beam as it enters the transmitting optic and results in a larger spot size at the target than one

would expect had the beam been collimated when it entered the transmitting optic. As an example, consider a collimated ideal gaussian beam which has been focused to produce a spot size of w_f (actually a radius to the e^{-2} intensity point) at a target. If the beam is instead diverging (or converging) with a radius of curvature $-R_B$ ($+R_B$) as it is reflected from the same transmitting optic, the new spot size w_f' is larger than the original by

$$\left(\frac{w_f'}{w_f}\right)^2 = 1 + \left(\frac{\pi D_B^2}{4\lambda R_B}\right)^2$$

where D_B is the (e^{-2}) diameter of the ideal gaussian beam and λ is the wavelength. For example, 0.1λ spherical phase error will increase the spot size approximately 20% for a 100 cm diameter optic transmitting at $\lambda = 3.8 \mu$. For the present study we assume that any phase curvature in the output beam from the optical train behaves in a similar manner.

The change in the curvature of the phase front of the beam as it propagates through the optical train is computed by employing a simplified geometric optics calculation through the optical elements preceding the beam expander. The usual simplifying assumptions, i.e., paraxial rays, thick lenses, etc., are made in order to make the calculation tractable.

Following the ray matrix approach of Reference 10 we first obtain the equivalent ray matrix of the optical train illustrated in Figure 2.6 by multiplying together the individual ray matrices of the individual elements, i.e.,

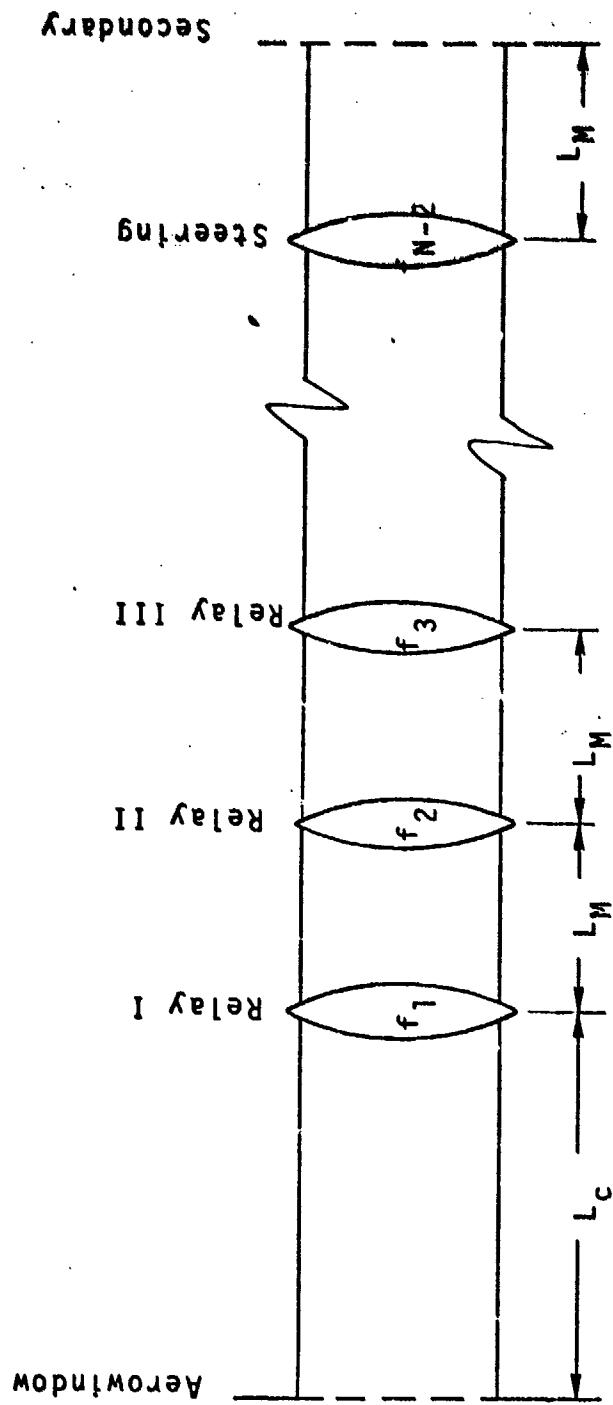


Figure 2.6. Simplified Optical Train Employed in Defocus Calculations

$$\begin{bmatrix} A & B \\ C & D \end{bmatrix} = \begin{bmatrix} 1 & L_M \\ 0 & 1 \end{bmatrix} \begin{bmatrix} 1 & 0 \\ -1/f_{N-2} & 1 \end{bmatrix} \cdots \begin{bmatrix} 1 & 0 \\ -1/f_2 & 1 \end{bmatrix} \begin{bmatrix} 1 & L_M \\ 0 & 1 \end{bmatrix} \begin{bmatrix} 1 & 0 \\ -1/f_1 & 1 \end{bmatrix} \begin{bmatrix} 1 & L_C \\ 0 & 1 \end{bmatrix}$$

where (going from right to left) the first matrix represents the propagation distance between the aerodynamic window and the beam clipper, the second matrix represents the reflection of the beam from the first relay mirror in the optical train, the third matrix represents the propagation distance between the first relay mirror and the second relay mirror, the fourth matrix represents the reflection of the beam from the second relay mirror, and so on until the beam is incident upon the secondary mirror. At this point we assume that the beam expander simply expands the beam by the specified magnification. The curvature of the phase front at this point, R_B , is related to the phase front curvature of the input beam, R_L , by

$$R_B = M \left(\frac{AR_L + B}{CR_L + D} \right).$$

The computed value of R_B is then used to compute the new spot size of the focused beam. In order to transfer this information to the propagation model, the beam quality parameter, m_2 , which characterizes the spread of the beam profile in the absence of other effects, such as thermal blooming, turbulence and beam jitter, is internally adjusted by the model to reflect the increased beam spread, i.e.,

$$(m_2)_{\text{final}} = \sqrt{1 + \left(\frac{\pi D_B^2}{4\lambda R_B} \right)^2} (m_2).$$

2.3 SAMPLE CALCULATIONS

As an illustration of how the optical train influences the performance of a laser system, we present below a sample calculation for the optical train schematically illustrated in Figure 2.7.

The laser device is assumed to be operating in an unstable confocal resonator mode with the power coupled out of the device via a scraper mirror located in front of the convex optic of the resonator. Accordingly, the output beam contains a central obscuration. The parameters assumed for this beam are:

Beam Diameter = 0.1 meters
Power = 400 kw
Wavelength = 3.8 microns
Obscuration = 0.5

In addition, it is assumed that the beam is essentially collimated ($R_L = \infty$) and contains peak-to-peak intensity fluctuations that are 50 percent of the average intensity ($\Delta I/I_{ave} = 0.5$). The scale size of these fluctuations is taken to be 1 cm or $\lambda_1/D_B = 0.1$. We also assume that the quality of the beam leaving the device is characterized as being 1.2 times diffraction-limited ($n_L = 1.2$). This corresponds to an equivalent rms phase distortion in the beam of $\sigma_L = 0.16$ radians or about $\lambda/40$ (see Figure 2.2).

The output beam from the laser device is focused through an aerodynamic window to a collimating mirror. Since the beam size is very small (typically < 0.1 cm) at the aerodynamic window, we neglect any phase distortion induced by the aerodynamic window (i.e., $\sigma_{aw} = 0$).

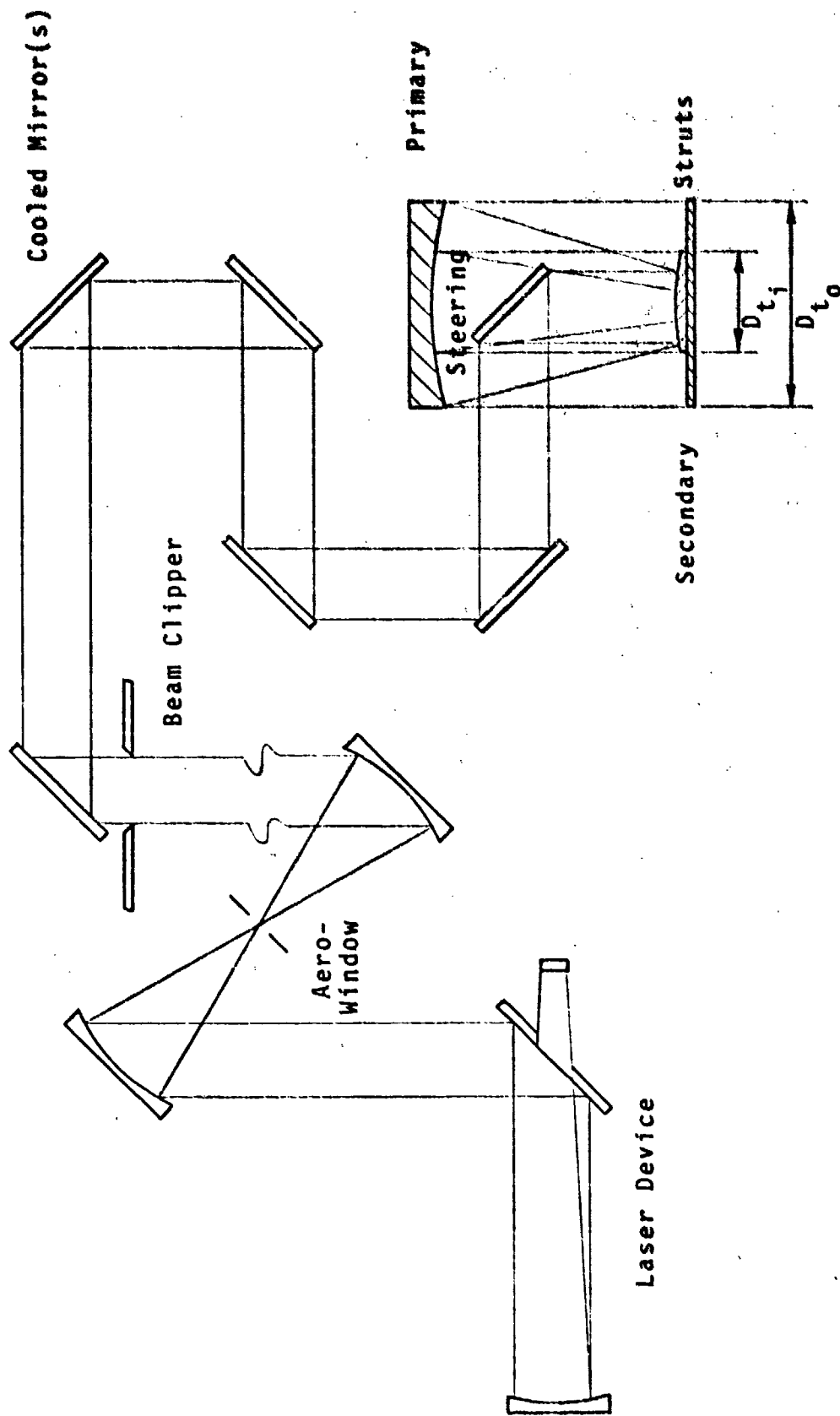


Figure 2.7. Schematic of Optical Train for Sample Calculations

For the example, we assume that the beam expander is located 50 meters from the aerodynamic window. Over this distance, diffraction effects cause the beam to expand somewhat. The Fresnel number for this propagation distance is

$$F_N = \frac{4D_B^2}{\lambda L_c} = 13.16$$

so that the beam diameters at the entrance to the beam expander are

$$D_{B_0} = \frac{D_B}{1 - 0.112\sqrt{F_N}} = 0.103 \text{ m}$$

and

$$D_{B_i} = \left(\epsilon - \frac{0.112}{\sqrt{F_N}} \right) D_B = 0.047 \text{ m.}$$

In this example, we have assumed that the diameter of the beam clipper is 16 cm so that no power loss due to clipping occurs, i.e., $T_c = 1.0$.

The nine (9) mirrors employed in the optical train are assumed to be water cooled with a reflectivity of $R_i = 0.986$. We also take the fabrication error as being $\lambda_v/8$ where λ_v is 0.564 microns. Accordingly, the power lost to the beam due to the finite absorptivity of the mirrors is

$$T_M = (0.986)^9 = 0.88.$$

The phase distortion induced by each mirror depends upon the rms intensity fluctuations, which for the case being considered are

$$I_{rms} = \frac{4P_L}{\pi D_H^2} \frac{\Delta I / I_{ave}}{12} = 7.35 \times 10^6 \text{ w}/\pi^2$$

so that

$$\sigma_I = 5 \times 10^{-14} (1 - R)(2\pi/\lambda) I_{rms} = 0.0085 \text{ radians.}$$

Combining this with the fabrication error yields (for all of the mirrors in the optical train)

$$\sigma_M = 9\sigma_f^2 + [8\sigma_I + \sigma_I/M^2]^2 = 0.3454 \text{ radians.}$$

The beam expander is an on-axis system of magnification. $M = 4.375$. The inner and outer diameters of the clear output aperture are $D_{t_0} = 0.7$ and $D_{t_i} = 0.252$ meters respectively. Since the beam entering the expander is not perfectly matched to the reduced clear aperture dimensions (i.e., $D_{t_0} = 0.16$ and $D_{t_i} = 0.576$), there is a power loss induced by the beam expander. From the geometry of the case being considered, this loss is computed to be approximately 13 percent or $T_{BE} \approx 0.87$. In addition, the beam expander has altered the obscuration of the input beam because of clipping. The final obscuration of the beam leaving the beam expander is $\epsilon = 0.0576/10.3 = 0.558$. Note that the final obscuration is not the observation of the

telescope ($D_{t_1}/D_{t_0} = 0.36$) because the input beam was not large enough to fill the transmitting optic. The effective phase distortion of the actual beam is therefore much larger than one would compute based on the obscuration of the telescope. For the example being considered, this equivalent phase distortion is $\sigma_{BE} = 0.72$ radians.

The exit aperture was assumed to be an open port so that the only power loss is that due to blockage by the struts required to support the secondary mirror of the beam expander. Thus, $T_E = 0.95$. The quality loss due to the struts is

$$\sigma_S = (A_S/A_B)^{1/2} = 0.2236 \text{ radians.}$$

Within the model, the open port would also induce jitter into the beam. However, for the purposes of this example, we have ignored any performance loss caused by beam jitter.

Combining the above losses, we get for the overall transmission factor

$$T = T_C \cdot T_{BE} \cdot T_E = 0.727.$$

Thus, the power from the device that is available for propagation to the target is

$$P_t = 0.727 P_L = 290 \text{ kw.}$$

The total distortion is

$$\sigma = \left(\sigma_m^2 + \sigma_{BE}^2 + \sigma_S^2 + 0.433 \right)^{1/2} = 1.06 \text{ rads.}$$

This phase distortion is characterized by a scale size

$$\frac{\lambda}{D_B} = \frac{1}{\sigma^2} \left\{ \frac{k_{BE}}{D_B} \sigma_{BE}^2 + \frac{k_1}{D_B} \left[(N-1)\sigma_1 + \frac{\sigma}{M^2} \right]^2 + 0.196 \right\} = 0.114$$

in terms of the two parameter descriptions of the beam quality employed by the model $m_1 = 0.3536$ and $m_2 = 1.1076$. For this example, there were no defocusing errors induced by any of the components in the optical train so that no adjustment was made to the beam spread parameter m_2 . Note that the constraints in the last two equations (0.433 and 0.196) are needed to ensure the proper conversion of σ and $\frac{k}{D_B}$ to m_1 and m_2 .

In order to quantify the impact of the optical train, we evaluate the power delivered to a particular spot in the focal plane, namely $r^* = f\lambda/D_{t_0}$. In the absence of atmospheric effects and beam jitter, this power is simply

$$P(r^*) = P_t m_1 \left\{ 1 - \exp \left[- \frac{\pi^2}{m_2} \left(\frac{D_B}{D_{t_0}} \right)^2 \right] \right\}$$

where D_B is the actual diameter of the beam on the transmitting optic, i.e., $D_B = M D_{B_0} \leq D_{t_0}$.

The results of this calculation for the example being considered is shown in Figure 2.8 along with some additional calculations made for various input beam diameters. For the conditions described above, only 83 kw of the initial 400 kw are delivered to the target. Note, however, that by expanding the input beam a significant increase in power can be achieved. The initial beam size of 10 cm was too small to effectively use the entire diameter of the transmitting optic. Hence, the beam profile at the target was

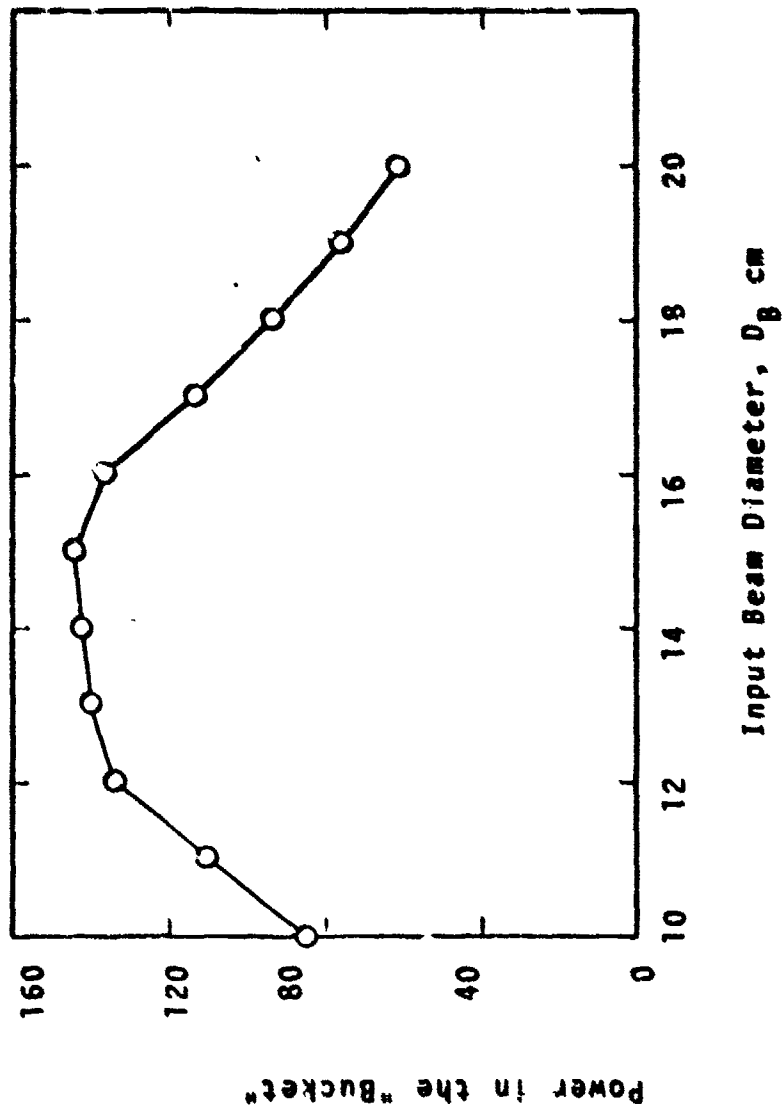


Figure 2.8. Results of Sample Calculations

larger than it should have been. In addition, because of the mismatch of device output beam and beam expander clear aperture, a significant power loss occurred. As the beam diameter is allowed to increase, both of these effects are reduced. Of course, at the point where the beam begins to spill-over onto the beam clipper, the near-field power is again reduced resulting in the performance fall-off shown in the figure.

It is recognized that a true performance evaluation cannot be made without including the propagation effects between the transmitter and target plane. However, the example does point out the necessity of including the effects of the optical train in any application study, since it indeed has a substantial impact on the near-field characteristics of the beam. In addition, the model also should provide some insight into the problems of integrating lasers and pointer/tracker systems. It is interesting to note that a detailed study of a similar system using a wave optics code resulted in an additional beam expander ($M = 1.3$) being placed in the optical train.

The simplified optical train model has been developed using state-of-the-art knowledge of the contribution of each element (windows, mirrors, etc.). It should be noted, however, that the model has not been verified using the more detailed wave optics codes. Such comparisons would be useful to not only verify, but also to improve, these simplified models.

Section 3

CREATION OF SAICOM

One of the High Energy Laser (HEL) propagation codes commonly used by the laser systems analysts is the COMBO (or ATM) code developed by the Air Force Weapons Laboratory (Reference 11). ATM is the propagation model documented in Reference 11. COMBO is a code which combines ATM with the Air Force HEL weight and volume projections (Reference 12). COMBO also includes some additional features such as the ability to perform reverse calculations in which the user specifies a desired intensity and the code determines the range at which the intensity can be delivered (given the power) or the power required (given the range). The primary asset of COMBO (or ATM) is its ability to make variable altitude calculations, including propagation paths extending to or from space.

One of the tasks performed under the present contract was devoted to modifying COMBO. The objectives were to reduce execution time, improve computational accuracy and to incorporate several of the newer developments resulting from the other tasks of this contract. A number of other minor additions, corrections and deletions were also made.

All of the primary modifications are discussed in Section 3.1. Collectively, they are sufficient to warrant a new code name -- SAICOM. A brief user's guide to SAICOM is provided by Section 3.2.

3.1 MODIFICATIONS OF COMBO

The primary modifications are dealt with in individual subsections below. The basic structure and organization

of the code remain essentially the same as in the original version (Reference 11). A summary of the more important equations is given in Section 3.1.9.

3.1.1 Improvements to Computational Speed and Accuracy

A substantial part of the COMBO modification effort was devoted to improving the speed of the calculations. Several modifications simply involved improvements in coding techniques. These included: (1) reducing the number of calls to MEGAIR (the subroutine which provides altitude dependent parameters such as temperature, pressure, etc.); (2) lumping several blooming parameters (viz., n , $\partial n/\partial T$, and C_p) into a single curvefit (GALTIN); (3) using a better search algorithm in the reverse calculations; and (4) reducing the subroutine calls.

Most of the improvement in both speed and accuracy was obtained by developing a completely new algorithm for performing the double integration required to compute the blooming parameter, NI. The expression for NI is of the form

$$NI = C \int_0^L \frac{1}{r(z')} \int_0^{z'} G(z'') dz'' dz'$$

where C is fixed for a given set of conditions (Reference 13). The integration paths are along the beam. In the original code, the double integral was evaluated by assuming the integrals to be constant between uniformly spaced points along the beam. The evaluation was successively repeated with reduced spacing until the results for consecutive evaluations agreed with 10 percent. This procedure

was found to be inefficient and often inaccurate. This should be readily apparent from Figure 3.1, which shows the important elements of the integral for a particular case of a highly focused beam. Note that the value of NI is dominated by the conditions within the last few percent of the range.

The new algorithm examines the local behavior of the integrand and chooses an efficient scheme and mesh spacing dynamically. It selects either a locally quadratic or locally exponential representation of the integrand. If neither is satisfactory, it reduces the mesh spacing and tries again. On the other hand, if the local convergence exceeds the accuracy requirements, it increases the mesh size to increase speed. Both integrations as well as a third implicit in G are performed in a single loop.

When the new algorithm was used for the severe example illustrated in Figure 3.1, the calculation required 1.49 seconds; the original COMBO exceeded a time limit of 200 seconds without completing the calculation!

As mentioned earlier, an additional improvement in computation time was obtained by modifying the convergence algorithm used in the reverse propagation calculation where the range is successively adjusted to obtain a desired target plane intensity. The range R' for one iteration is determined by modifying the previous range, R, viz.,

$$R' = KR \sqrt{I/OI}$$

where OI and I are the desired and computed intensities, respectively. In the original COMBO, the constant K was always 1.0, whereas in SAICOM, it varies between 0.7 and 1.0 to accelerate convergence. In addition, the convergence criterion was relaxed from 1% to 5%.

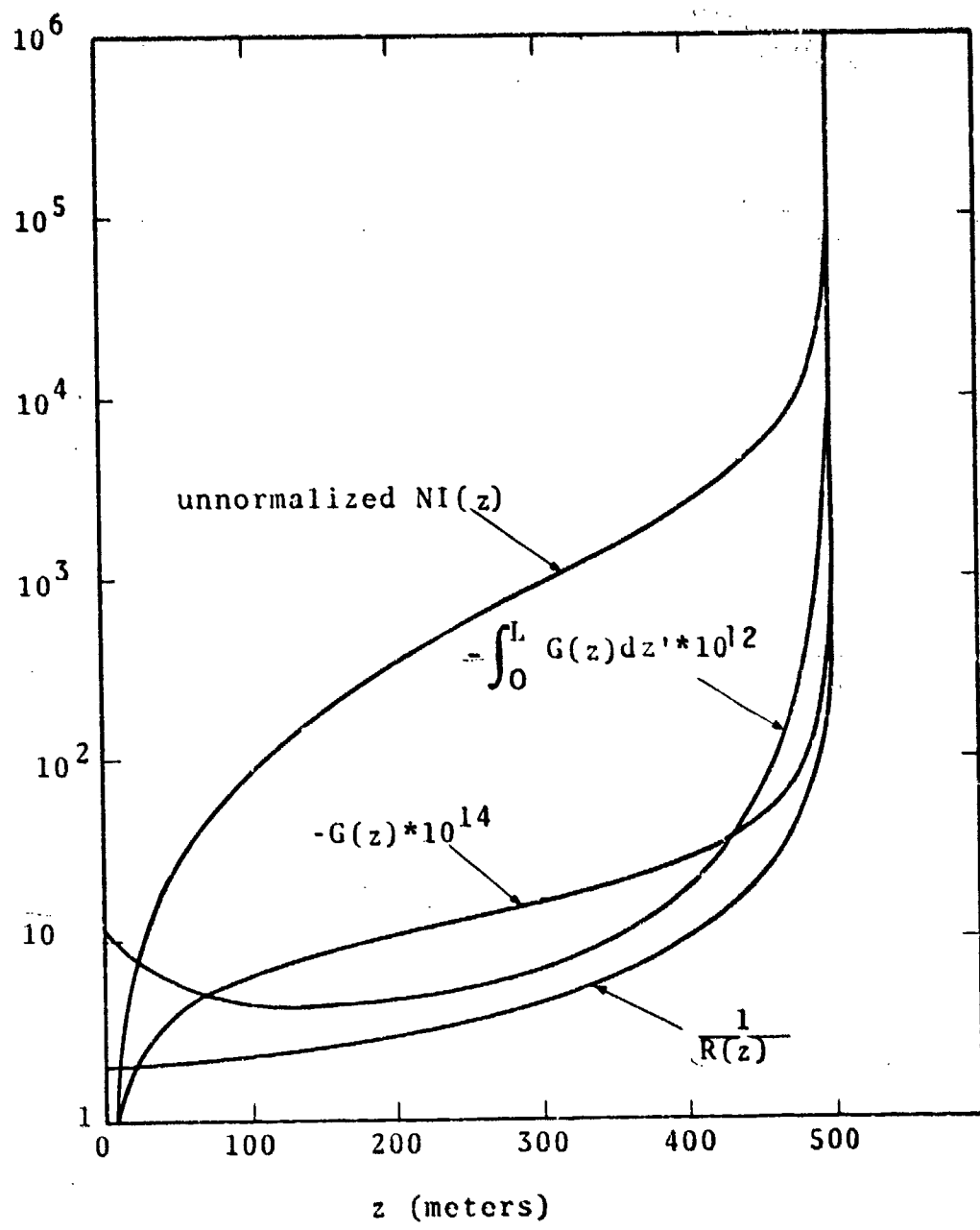


Figure 3.1 Variations in Elements of the Blooming Calculation

3.1.2 Beam Quality

The SAICOM code includes a significant innovation in the treatment of beam quality. It essentially replaces the usual one parameter concept of an "m x diffraction limited" beam by a two parameter representation. The two parameters, designated m_1 and m_2 , are used to specify a gaussian representation of the focal plane intensity profile so as to approximate the actual integrated power distribution. The two parameter model is inherently capable of including effects leading both to beam spreading (m_2) and to power loss due to wide angle scattering (m_1).

The origin and interpretation of m_1 and m_2 are discussed in some detail in Reference 1 and in Section 4.3 of this report. Their use in characterizing the effects of beam truncation and obscuration is discussed in Reference 2. In general, they are calculated in the new optical train model which is an integral part of SAICOM (see Section 2).

SAICOM incorporates the two parameter approach even though the user is only required to stipulate a single parameter, m . If the device power (P_D) and beam quality (m) are stipulated, the optical train portion of the code converts them to the appropriate aperture or transmitted power (P_T) and beam quality (m_1 , and m_2). If the optical train calculations are bypassed because the user specifies P_T , the specified beam quality is assumed to be pure beamspread.

The SAICOM intensity expression for a focused beam is of the form

$$I = \frac{[1 - (1 - 0.865 m_1 z/L)] P_T e^{-\alpha z}}{\pi r^2(z)}$$

where

$$r^2(z) = \frac{D}{4L^2} |L - z|^2 + 4z^2 \left[\left(\frac{0.3183 m_2 \lambda}{D} \right)^2 + \sigma_T^2 + \sigma_J^2 \right]$$

The term in the numerator that decreases as z increases represents the power losses that may be thought of as wide angle scattering. The 0.865 factor is present because the basic propagation equation used in the code is based on the $1/e^2$ radiance of an infinite Gaussian beam. Since m_1 and m_2 are used to account for the effect of different beam profiles as well as phase perturbation, these terms may be not the unity even for perfect beams. This situation is clarified in Table 3.1. In this table the $M1$ and $M2$ terms are the parameters computed in the optical train subroutine while m is the user specified beam quality for the total system. Note that if the optical train is bypassed (the user specifies P_T) and $m=1$, m_1 and m_2 are 0.89 and 1.29 respectively for a uniform beam and not unity because the basic propagation equation is based on an infinite gaussian model. But if the optical train is not bypassed, $m_1 = M1=0.89$ and $m_2 = M2=1.29$ because the basic profile used in the optical train subroutine is uniform.

3.1.3 The Optical Train Model

The development of an improved optical train model was the prime objective of Task 5 and is discussed in detail in Section 2 of this report. The model has been incorporated into SAICOM as subroutine OPTRAIN. It computes power losses, jitter, and beam quality degradation associated with transmission of the beam from the laser through

Table 3.1 Beam Quality Parameters

Aperture	Intensity Profile	Infinite Gaussian	$1/e^2$ Gaussian	Uniform
OPTRAIN	m_1	1	1	0.89
BYPASSED	m_2	1	1.41 m	1.29 m
OPTRAIN	m_1	0.89 M1	0.89 M1	M1
USED	m_2	0.775M2	1.092M2	M2

the final transmitting optic. It accepts a quite general specification of the optical train through a list of input parameters. OPTRAIN accounts for beam truncation and obscuration and for various contributions to phase perturbations. The output includes the two beam quality parameters m_1 and m_2 described above.

OPTRAIN can be bypassed simply by specifying the transmitted power, P_T , rather than the device power in the input. In this case, beam quality is based on wavelength scaling as usual.

3.1.4 Multi-Line Propagation

Since many of the lasers of interest for high energy applications emit several lines simultaneously, it is desirable to include these multi-line characteristics in the simplified propagation codes.

The approach used in SAICOM is to compute the amount of energy absorbed by the air on a line-by-line basis. This means that $\exp\left\{-\int_0^R \alpha(z''') dz'''\right\}$

$$\sum_i \frac{P_i}{P_T} \exp\left\{-\int_0^R \alpha_i(z''') dz'''\right\}$$

and $\alpha(z'') \exp\left\{-\int_0^{z''} \alpha(z''') dz'''\right\}$ in the integrand of the

expression for the blooming parameter becomes

$$\sum_i \frac{P_i}{P_T} \alpha_{ai}(z'') \exp\left\{-\int_0^{z''} \alpha_{ei}(z''') dz'''\right\}$$

where

α_{ai} = absorption coefficient of the i^{th} line
 α_{ei} = extinction coefficient of the i^{th} line.

In SAICOM, the 3.8 μm DF propagation has been extended to include three distinct families of lines. These encompass ten lines of the DF laser, and represent 80% of the output of the BDL device. With the basic modification having now been made, it is straightforward to include multi-line HF or CO propagation.

The derivation of the DF absorption coefficients is given in Appendix A and is based on the BDL spectral data. The resulting SAICOM equations are

$$\alpha_i = A_0 e^{-A_1 + h(-A_2 + A_3 h)}$$

$$\text{where } A_0 = 1 + (0.9446 RH - 1)e^{-h(6.738 \times 10^{-5} + 9.61 \times 10^{-9} h)},$$

for groups 1 and 2

= 1, for group 3

A_1 = 10.047, 10.082, and 9.948 for group 1, 2 and 3, respectively

A_2 = 6.388×10^{-4} , 6.952×10^{-4} , and 2.199×10^{-4}

A_3 = 2.25×10^{-8} , 1.55×10^{-8} , and -1.96×10^{-8}

h = altitude in meters.

These equations imply that at sea level α varies between 0 and 0.0409 km^{-1} as relative humidity varies between 0 and 100%, α_2 between 0 and 0.0395 km^{-1} , and α_3 is a constant 0.0478 km^{-1} .

The above equations are only valid to around h=13 km; for the higher altitude the original COMBO coefficients are used. Unfortunately, a discontinuity existed at the 13 km altitude; so transition equations were created to connect the multi-line data below 13 km with the single-line data above that point. Figures 3.2, 3.3, 3.4, and 3.5 plot the α_1 , α_2 , α_3 , and $\alpha_{\text{resultant}}$ equations where

$$\alpha_{\text{resultant}} = \frac{\alpha_1 + \alpha_2 + \alpha_3}{3}$$

The scattering equations are the same as those used in the original COMBO (Reference 11).

3.1.5 Modification of Turbulence and Jitter to Include Short and Long Term Effects

During the code comparison work in Task 1 of this contract, it was noted that one of the useful features of ESP was the flexibility of including beam jitter in the blooming calculation if the frequency were high enough and excluding it otherwise (References 1 and 14). This feature has been included in SAICOM. The output jitter factors in SAICOM are high-frequency jitter (σ_{JHF}) and low-frequency jitter (σ_{JLF}). The former is used in the calculation of the blooming parameter and both are combined to give the total beamspread due to jitter. Similarly, the turbulence calculations are expanded to include the total, long-term turbulence (σ_{TLT}) and the high-frequency, short-term turbulence (σ_{TST}). The turbulence equations in SAICOM are based on work of Yura (References 15 and 16) whereas the COMBO code was based on Fried's work (Reference 17), but the results differ only slightly in the regions of interest. The equations used are

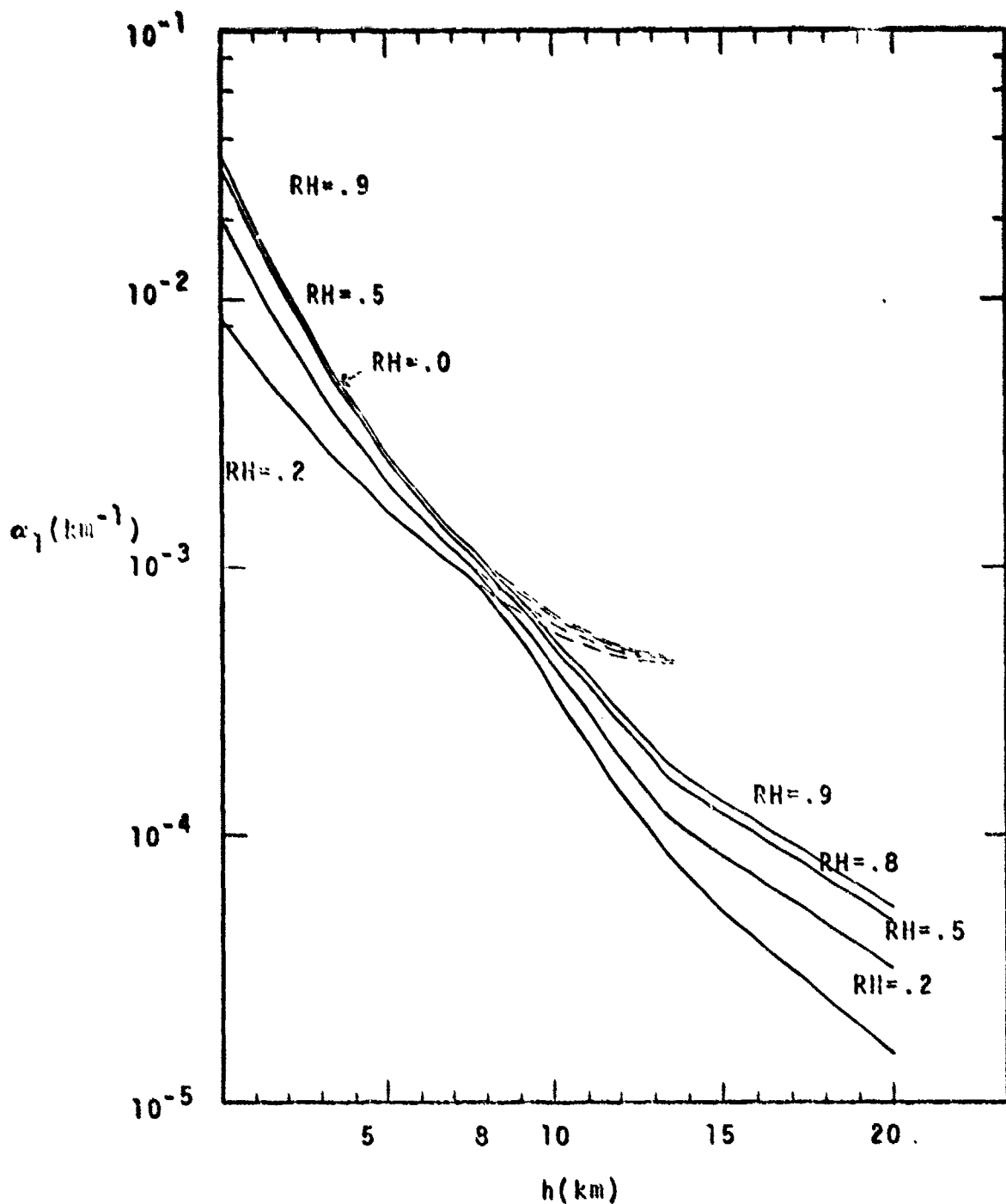


Figure 3.2. α_1 as a Function of Altitude

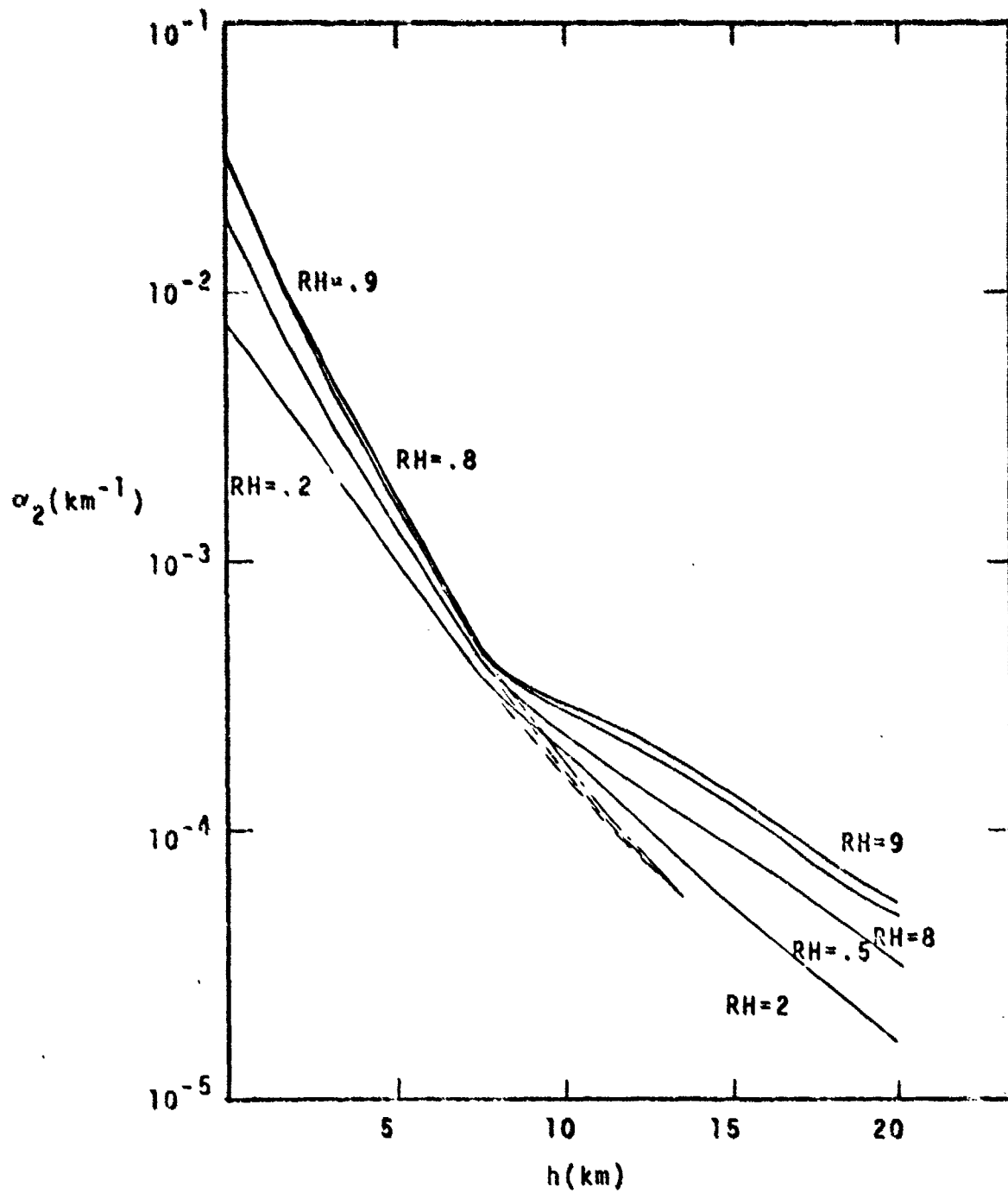


Figure 3.3. α_2 as a Function of Altitude

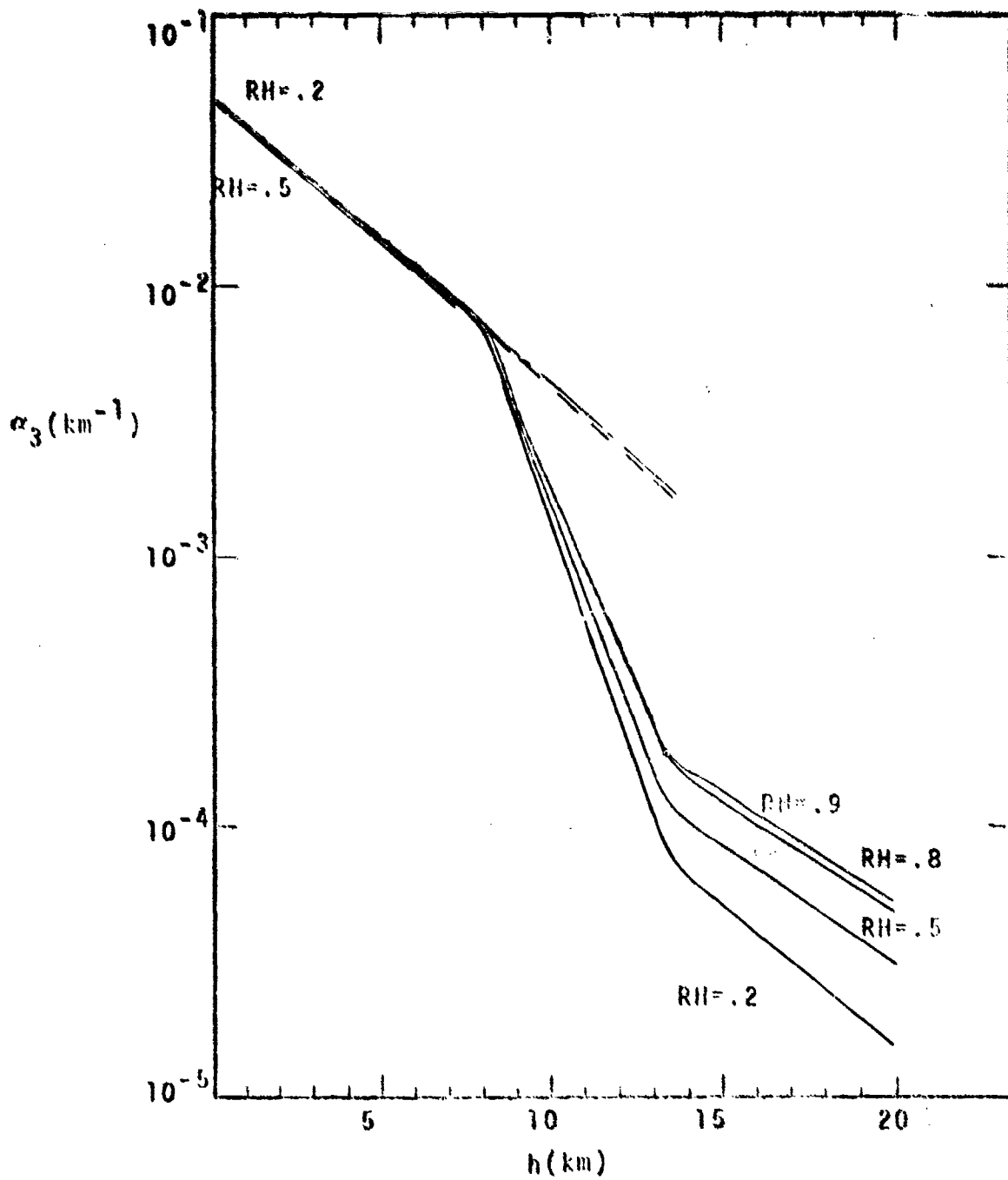


Figure 3.4. α_3 as a Function of Altitude

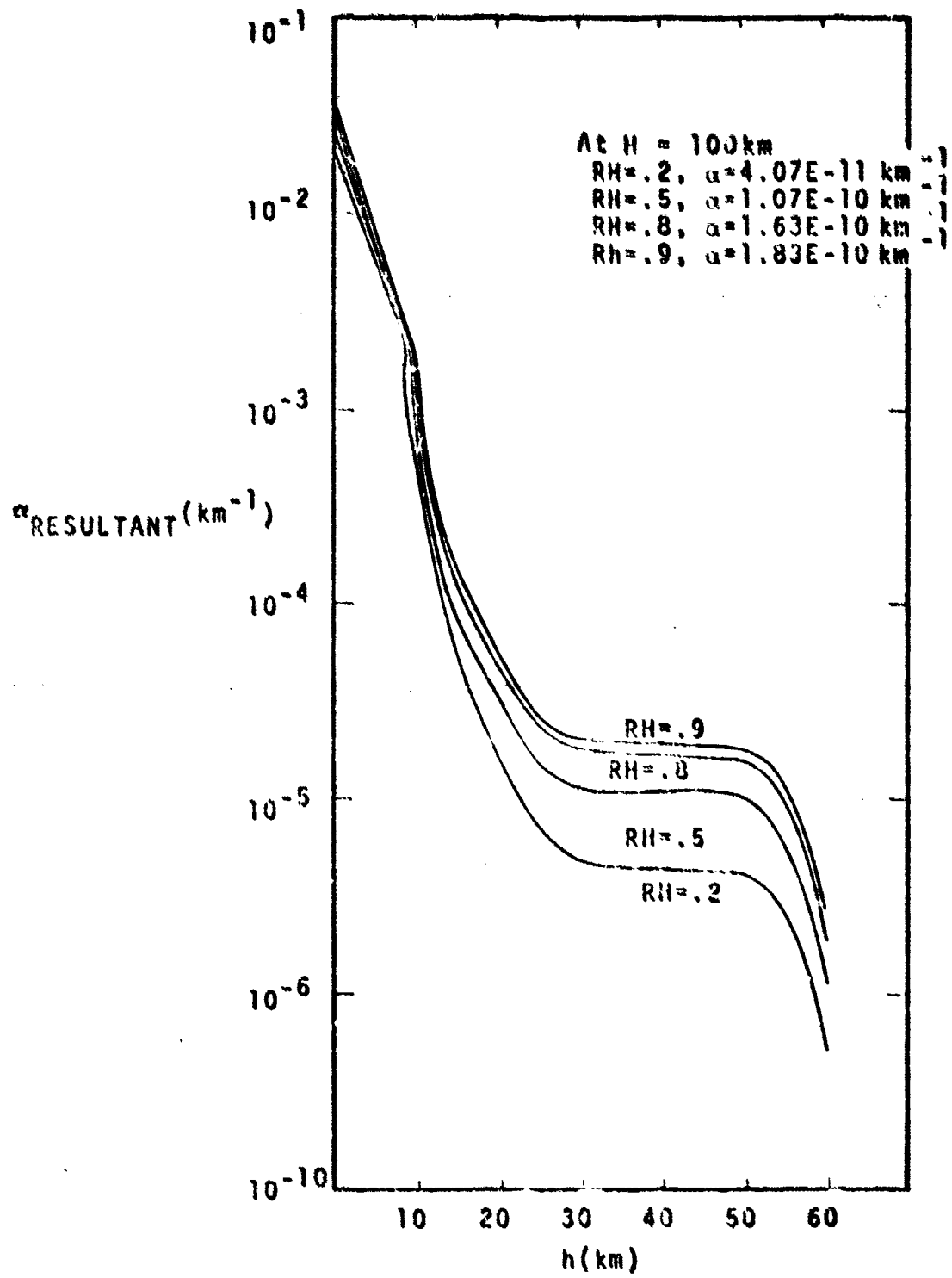


Figure 3.5. $\alpha_{\text{RESULTANT}}$ as a Function of Altitude

$$\sigma_{\text{TLT}} = \frac{2.549}{\lambda^{1/5}} \left[\int_0^L C_N^2(z) \left(\frac{L-z}{L}\right)^{5/3} dz \right]^{3/5}$$

and $\sigma_{\text{TST}} = \left[1 - 0.37 \left(\frac{\rho_0}{D}\right)^{1/3} \right] \sigma_{\text{TLT}}$

where $\rho_0 = \frac{1.439}{k^{1.2}} \left[\int_0^L C_N^2(z) dz \right]^{3/5}$

$$k = 2\pi/\lambda$$

D = diameter of the exit aperture.

These equations are generalizations of the co-altitude expression developed in Reference 16. In the blooming calculation σ_{TST} is used instead of the long-term expression, but it should be noted that some research indicates that no turbulence should be included in the beamspread before the blooming calculation (Reference 18).

3.1.6 Far-Field Intensity Distribution

In COMBO the standard calculation of the average intensity is based on the $1/e^2$ intensity radius in the far-field with a few other radii available for user specification (e.g., $1/e$ and $1/2$ intensity points). Since SAICOM is based on a gaussian approximation to the actual far-field distribution, it is a simple matter to use the $1/e^2$ results to describe the complete far-field profile. In addition to $I(1/e^2)$, the peak intensity $I_p = 2.312 \times I(1/e^2)$, is printed along with contour data. These contour data assume a

bivariant normal profile of the beam due to blooming distortion as developed in Reference 2. For each 10% contour ($I = \gamma I_p$, $\gamma = 0.9, 0.8, \dots, 0.1$) the area within that contour,

$$A(I > \gamma I_p) = \frac{\pi r^2 \ln(1/\gamma)}{2 KIP}$$

the total power within that area,

$$P(I > I_p) = P(1 - \gamma)$$

and the corresponding average intensity are printed. In addition, the beam displacement due to non-linear bending into the wind and the eccentricity of the resulting elliptical profile are computed and printed.

3.1.7 Calculation of Optimum Power

One of the more useful bits of information that comes from laser effectiveness studies is specification of optimum power based on maximizing energy on the target (Reference 19). Using the Gebhardt and Smith curve-fit for the intensity reduction due to blooming (Reference 20), the far-field intensity is related to transmitted power, P_T , by

$$I = a P_T I_{REL}(N)$$

where $N = b P_T$ and a and b are constants (independent of power). Setting $\partial I / \partial P_T = 0$ leads to

$$\partial \ln(I_{REL}) = -\partial \ln N$$

as the optimum condition. For the Gebhardt and Smith curve,

this condition is satisfied when $N=5.54$. Therefore, the optimum power is given by

$$P_{\text{optimum}} = \frac{5.5^4 P_T}{N}$$

where N is the value of the blooming parameter corresponding to the power P_T . The corresponding maximum intensity is

$$I_{\text{optimum}} = \frac{1.205 I}{N \text{ KIP}}$$

(KIP is the computer variable representing I_{REL}). It should be noted that the optimization does not include the possible effects associated with the optical train, i.e., it does not involve an iterative recall of OPTRAIN.

SAICOM prints the optimum power as derived above unless the corresponding intensity exceeds the air breakdown threshold. In that case, it prints the power at which breakdown would occur as the optimum power. The breakdown power level is estimated on the basis of peak intensity without blooming.

3.1.8 Miscellaneous Modifications

Several relatively minor additions, deletions and corrections are described below.

3.1.8.1 Variable Turbulence in Blooming Computations

In COMBO the turbulence is not varied as the blooming along the beampath is computed; instead only the final value is used. In SAICOM the distributive nature of turbulence is included in the integral calculation of the blooming parameter.

3.1.8.2 Extinction Calculations in Blooming Integral

In COMBO the linear power losses due to absorption and scattering are computed using $\exp[-\alpha_e(h)z]$ in the integrand whereas the expression should have been

$$\exp\left[-\int_0^z \alpha_e(h)dz\right].$$

This error causes an over-estimate of the extinction losses when firing downward and an under-estimate when firing upward. The appropriate correction has been made in SAICOM.

3.1.1.3 Power Variation

The reverse calculation option in COMBO involving calculation of the required power to deliver a desired intensity at a given range has been replaced in SAICOM. Now, whenever the intensity is calculated in a normal propagation run, the power is automatically varied between one-tenth the specified value and twice the original power. The output then lists the average intensity within the $1/e^2$ intensity area, the area over which the intensity is above a specified minimum value, and the total power available within that area. The equations used in these computations were discussed in Section 3.1.6. The user is allowed to stipulate the minimum intensity of interest through the input parameter OI. If the user does not specify the desired minimum intensity contour, the program automatically selects 10 kw/cm^2 .

3.1.8.4 Deletion of Weight and Volume Calculations

The technology projection portion of COMBO is an interesting but seldom used facet of the code. Therefore, it has been eliminated.

3.1.9 Summary of Equations

The basic equations used in SAICOM are as follows:
Average intensity in the $1/e^2$ intensity radius

$$I(Z) = \frac{\left[1 - (1 - 0.865 m_1 \frac{Z}{L})\right] P_T k_B e^{-\sum_i \int_0^Z \alpha_{ci}(Z') dZ'}}{\pi r^2(Z)}$$

where k_B = intensity reduction due to blooming
(sometimes written as KIP)
= $f(N)$

$$r^2(Z) = k_2 r_0^2 + k_3 \frac{r_0^2}{L^2} \left[|L-Z|^2 + 4Z^2 \left[\left(\frac{0.3183 m_2 \lambda}{D} \right)^2 + \sigma_{TLT}^2 + \sigma_J^2 \right] \right]$$

$$\sigma_J^2 = \sigma_{JHF}^2 + \sigma_{JLF}^2$$

$$\sigma_{TLT}^2 = \frac{2.549}{\lambda^{1/5}} \left[\int_0^L C_H^2(Z) \left(\frac{L-Z}{L} \right)^{5/3} dZ \right]^{3/5}$$

The blooming parameter, N , is computed by

$$N = \frac{6.54}{\pi} \int_0^L \frac{1}{r(Z')} \int_0^{Z'} \frac{\left[1 - (1.865 m_1 \frac{Z}{L})\right] F(Z'') G(Z'') dZ'' dZ}{v(Z'') r^2(Z'')}$$

where

$$F(Z'') = P_T \sum_1 \frac{P_1}{P_T} \alpha_{A1}(Z'') e^{-\int_0^{Z''} \alpha_{ei}(Z'') dz''}$$

$$r^2(Z'') = k_2 r_0^2 + k_3 \frac{r_0^2}{L^2} |L-Z|'^2 + 4Z^2 \left[\left(\frac{0.318 m_2 \lambda}{D} \right)^2 + \sigma_{TST}^2 + \sigma_{JHF}^2 \right]$$

$$\sigma_{TST} = \left[1 - 0.37 \left(\frac{l_0}{D} \right)^{1/3} \right] \sigma_{TLT}$$

$$l_0 = \frac{1.439}{k^{1.2}} \left[\int_0^L C_N^2(z) dz \right]^{3/5}$$

$$k = 2\pi/\lambda$$

$$G(Z'') = \frac{\frac{\partial n}{\partial T}(Z'')}{n(Z'') \rho(Z'') c_p(Z'')}$$

3.2 A USER'S GUIDE TO SAICOM

A brief description of the key features of the SAICOM code is given along with a discussion of how to operate the code. Users familiar with COMBO (Reference 11) should have little trouble with SAICOM since many of the subroutines are unchanged and the same modular format has

been retained. The basic structure of the executive routine (SAICOM) is shown in Figure 3.6. A substantial portion of this routine is devoted to initializing the input variables. As with COMBO, most of the input parameters are defined through a default namelist which requires the user to specify only those parameters which will differ from the default values. However, it should be noted that even if the propagation and optical train namelists are not used, namelist cards are required which read \$INPUT \$ and \$CASES \$, respectively. The optical train is called if the user specified PD; if PT is given, this subroutine is bypassed. A subtle point worthy of note is that when PD is given, SIGMF is assumed to refer to the device jitter only, and this term is combined with the four 1 σ jitters (THIR, THES, THAA, and THSV) given in namelist CASE to determine the high-frequency jitter of the total system.

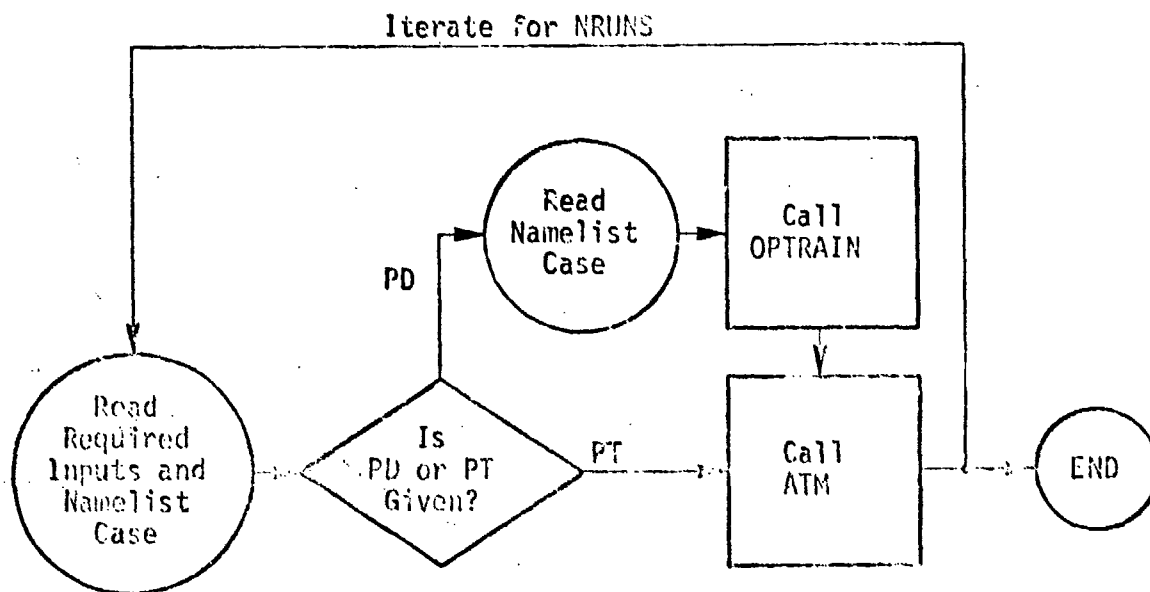


Figure 3.6 SAICOM Flow Diagram

Following these initialization activities, control is transferred to ATM, which handles the propagation calculations; control returns to SAICOM only after the calculations are completed and the results printed. Then SAICOM cycles through the same process until all of the specified cases have been completed.

In Table 3.2 a complete list of the SAICOM subroutines is given along with brief descriptions of their functions. Three of the subroutines, OPTRAIN, ATM, and BB, are discussed in further detail since they are the more important and complex portions of the program.

3.2.1 OPTRAIN

The calculation procedure within the Optical Train Model (OPTRAIN) is schematically shown in Figure 3.7. All inputs to the subroutine are passed through a labeled COMMON/OPTIN/statement and must be defined by the user prior to calling the subroutine. Following some initial calculations characterizing the input beam, the effect that each component within the optical train has on the transmitted power and beam quality is evaluated in a step by step manner. Although the specific elements within the optical train are fixed, i.e., aerodynamic window, beam clipper, mirrors, beam expander, and exit aperture, the user is allowed to specify, through the input parameters, different types of individual components such as cooled or uncooled mirrors, on-axis or off-axis beam expanders, and open port or material window exit apertures.

The output from the model is returned to the calling program via the labeled COMMON/OPTOUT/ and consists of (1) the diameter of the laser beam at the exit aperture, (2) the power in the beam, (3) the total beam jitter and (4)

Table 3.2 SAICOM Subroutines

<u>NAME</u>	<u>DESCRIPTION</u>
OPTRAIN	Calculation of Power Loss and Beam Degradations in the Optical Train.
ATM	Initialization of Propagation Parameters and Iteration of Reverse Calculations.
AA	Calculations for Laser and Target Above 100 km.
AB	Calculation for Laser Above 100 km and Target Below 100 km.
BA	Calculation for Laser Below 100 km and Target Above 100 km.
BB	Calculations for Laser and Target Below 100 km.
ALFSET	Sets Power Ratios for Multi-Line Propagation.
ALFFAC	Calculations of $\alpha_A e^{-\alpha_e z}$ and $e^{-\alpha_e z}$.
ALFAAB	Single Line Absorption Coefficients.
ALFAEX	Single Line Scattering Calculation.
CNSQ	Atmospheric Structure Constant.
KI	Computer Reduction in Intensity Due to Blooming.
GALTIN	Altitude Dependent Parameters Used in Blooming Integral.
MEGAIR	Pressure, Density and Temperature as a Function of Altitude.
VX	Calculation of Total Crosswind.

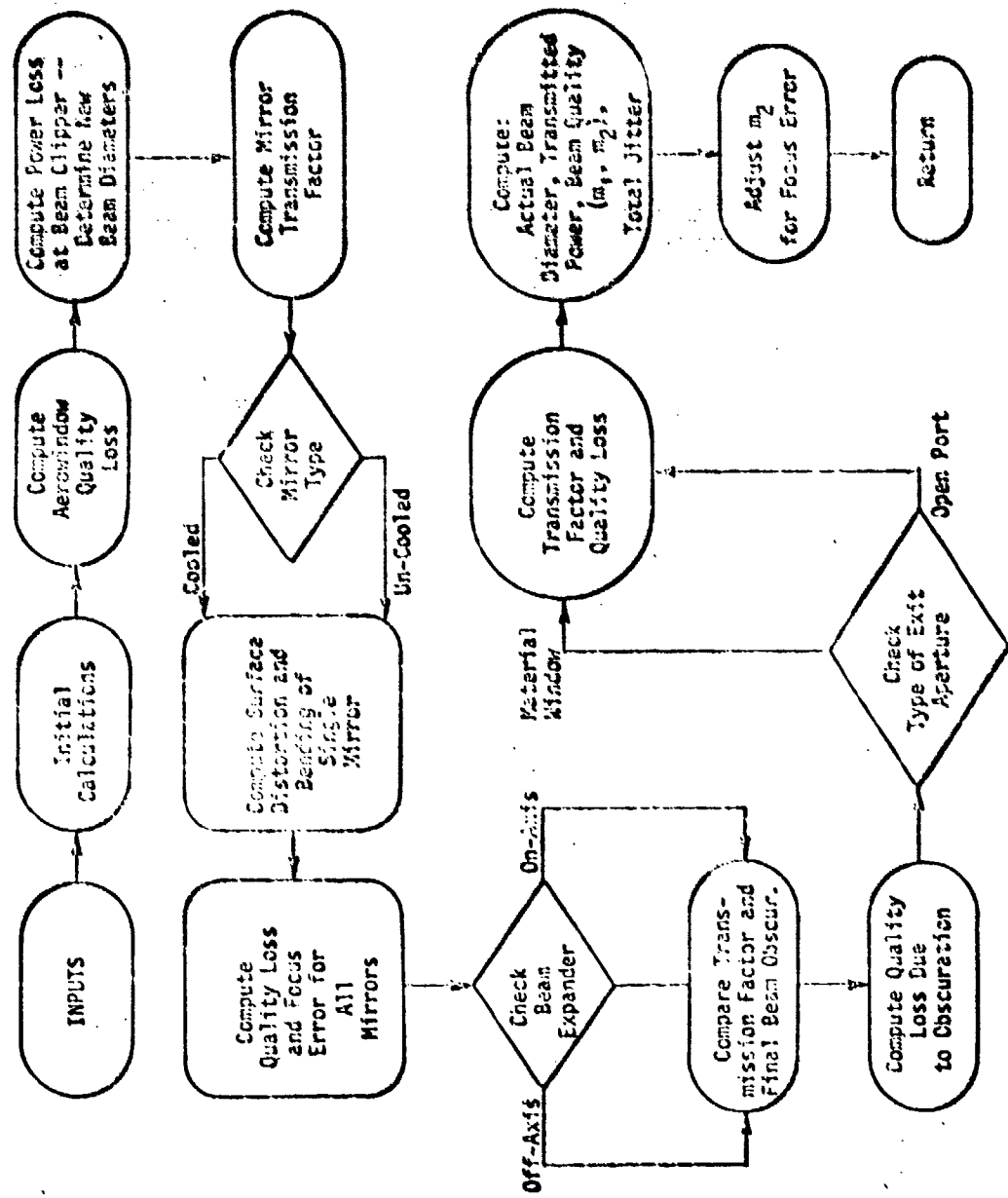


Figure 3.7 OPTRAIN Flow Diagram

two parameters (m_1 and m_2) characterizing the optical quality of the beam. The beam quality parameter m_2 is internally adjusted to account for any defocusing error induced by the high power mirrors in the optical train.

3.2.2 ATM

Part of the initialization process in ATM is to determine if the user has specified a negative wavelength (e.g., $-1.06E-5$ or $-3.8E-6$) which means the user is specifying his own single line absorption and scattering coefficients

$$\alpha_A = ABL * EXP (-ABE * R)$$

$$\alpha_S = SCL * EXP (-SCE * R)$$

or his own power ratios for the multi-line $3.8 \mu\text{m}$ propagation (see Figure 3.8). Note that single-line $3.8 \mu\text{m}$ propagation is available only if the user specifies his own coefficients. Also note that if one wishes to alter the power ratio, $PLINE(I)$, $I = 1, 2, 3$ without altering the built-in multi-line coefficients, simply set $LAMDA$ equal to $-3.8E-6$ and leave the absorption and scattering coefficients off namelist $USPEC$. The three power ratios need not total unity since the program is self-normalizing. The heart of ATM is the call to AA , AB , BA , or BB where the intensities for the pathlengths of interest are calculated. If AB or BA are called, they in turn call BB for those portions of the propagation path that lie below 100 km. Following the return to ATM, the beam displacement, eccentricity, contour data, breakdown power, optimum power, and effects of power variations are determined for straight propagation unless the propagation path is totally exo-atmospheric (AA), or the blooming parameter NI is less

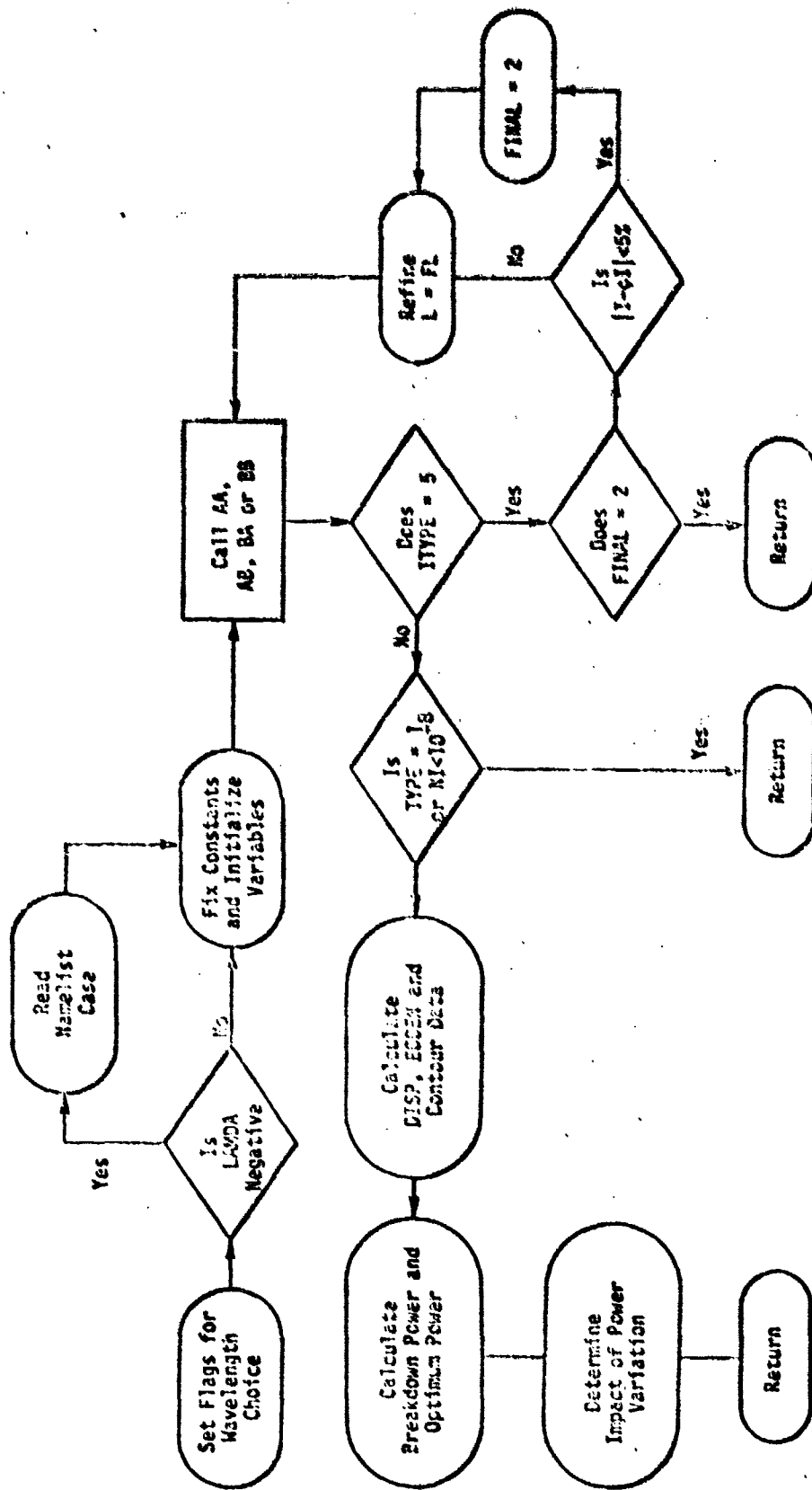


Figure 3.8 ATM Flow Diagram

than 10^{-8} . It should be noted that when the power is varied to compute the impact of propagating a beam that is more or less powerful than the specified level, the beam quality is not altered; this gives some error to the results since beam quality is affected by the total power transmitted through the optical train.

If the reverse propagation option (ITYPE = 5) has been chosen, the calculations are repeated using different target ranges (= focal ranges for ITYPE = 5) until the calculated intensity is within 5% of the desired value. If convergence is not achieved within 20 iterations, the program returns control to SAICOM and goes to the next case.

3.2.3 BB

In Figure 3.9, the logic flow for the BB subroutine is shown. All cases except AA use this subroutine to compute the atmospheric effects on the high-power beam propagation. The subroutine performs calculations at discrete points along the beampath. For calculations of the linear propagation effects, the pathlength intervals are fixed (NSTEP = 30 is the default value) while in the blooming loop the intervals are increased or decreased as required to minimize time and increase accuracy of the calculation. A series of linear or exponential extrapolations for the i^{th} interval based on the $i^{\text{th}} - 1$ interval are made and compared with the actual calculation for the i^{th} interval. If the comparison is unfavorable, the interval is decreased. If the comparison is favorable, the contribution from the interval is incorporated into the integral, if the comparison is unnecessarily good, the interval is increased. This procedure replaces the time-consuming multiple iterations used in CONBO.

3.2.4 Input Data

In Table 3.3 a list of the input parameters and their functions is given. This reference list does not

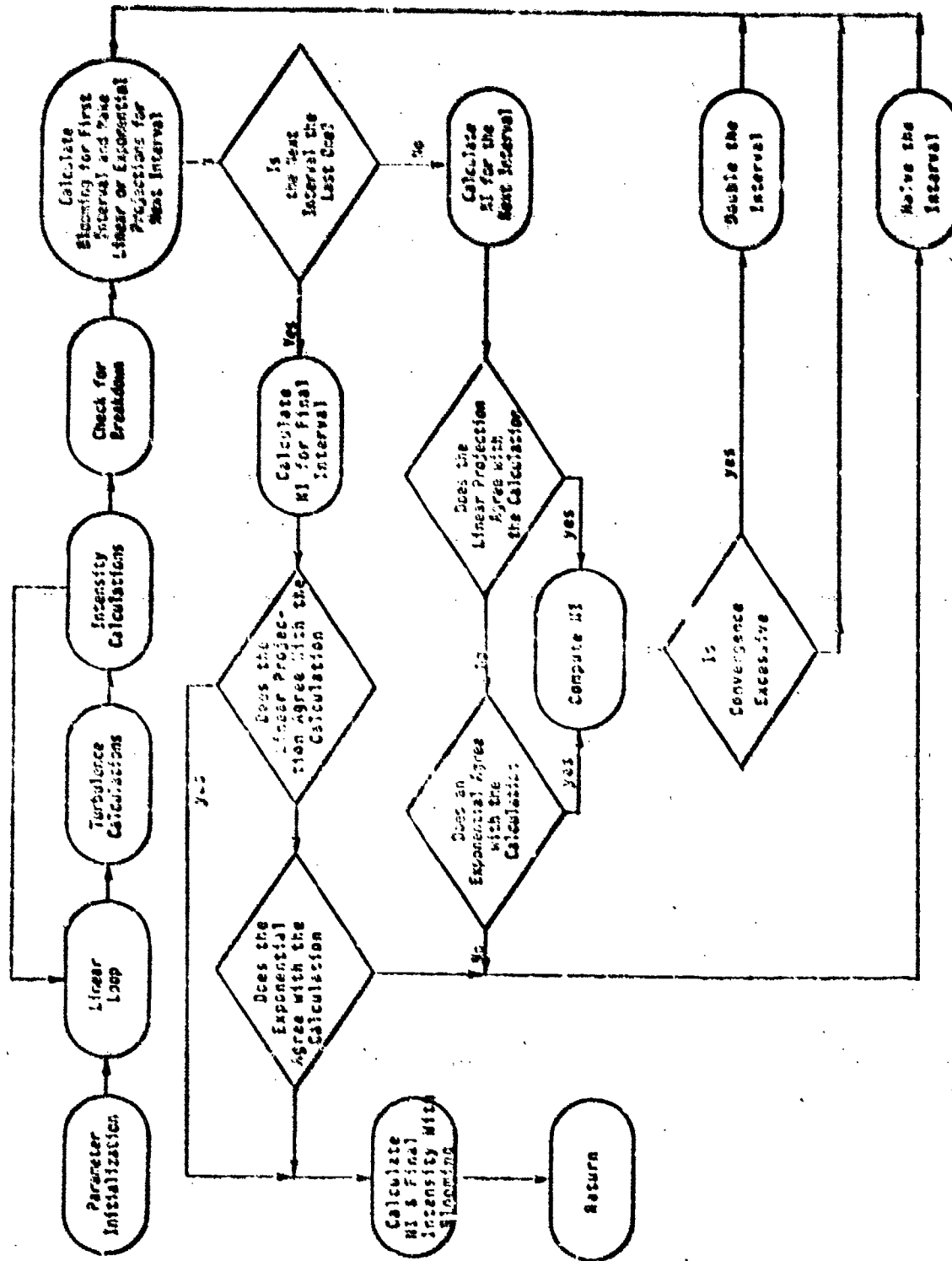


Figure 3.9. BB Flow Diagram

Table 3.3 Input Parameters

REQUIRED

ITYPE	If ITYPE = 5 reverse calculation is called with OI and PD or PT specific. All other entries will result in straight propagation.
PD or PT	User may stipulate either device power or telescope power; if IT is specified (PT=0) is bypassed.
OI	Desired intensity of ITYPE = 5; otherwise it is the minimum intensity contour in the variable power calculation.
L	Range from laser to the target if ITYPE \neq 5; if ITYPE = 5, L is a first guess for the range.

OPTIONAL - NAMELIST/INPUT/

Beam	0 \Rightarrow Collimated, 1 \Rightarrow Focused.
CHI	Horizontal projection of beampath with respect to the direction of platform movement.
DEPUG	1 \Rightarrow no extra diagnostic statement, 2 \Rightarrow extra diagnostic statement.
FL	Focal length.
GL	Ground level.
HTM	Target altitude.
HOM	Laser altitude.

Table 3.3 (Continued)

OPTIONAL - NAMELIST/ INPUT/ (Continued)

LANDA	Wavelength 3.8×10^{-6} , 5.0×10^{-6} , and 1.06×10^{-5} are the acceptable values. A negative sign in front is a flag that the user will specify the multi-line power ratios or the single line absorption and scattering coefficients.
M	Beam quality.
NSTEP	Beampath intervals in the linear calculation.
OMEGA	Slowing rate.
OUT	1 \Rightarrow standard output, 2 \Rightarrow extra output.
PHI	Firing angle with respect to zenith. If PHI is specified HIM should not be given and vice versa.
PROP	1 \Rightarrow $1/e^2$ 2 \Rightarrow plane wave, truncated Gaussian 3 \Rightarrow infinite Gaussian.
RH	Relative humidity.
RI	Radius of obscuration.
RO	Outer radius of exit aperture.
SIGHF	High-frequency turbulence.
VP	Platform velocity.
VXB	Total crosswind across beam. If it is specified VP, OMEGA and natural wind are inoperative.
WTHR	-1 \Rightarrow high turbulence, low natural wind 0 \Rightarrow nominal turbulence and natural wind 1 \Rightarrow low turbulence, high natural wind.

Table 3.3 (Continued)

OPTIONAL - NAMELIST/CASE/

DB	Beam diameter coming from the laser.
EPS	Obscuration ratio.
DL	Pulse length.
XRI	Phase front curvature.
DIOVI	Peak-to-peak intensity fluctuation.
DLI	Scale size of fluctuation wrt beam size.
DELTAR	Aerowindow.
RREF	Aerowindow density divided by ambient density.
XLC	Distance from laser exit to beam clipper.
DC	Clipper diameter.
N	Number of mirrors in optical train.
REFL	Reflectivity of each mirror.
SFAB	Mirror fabrication error.
ITYPE:	Mirror type: 1 ⇒ cooled, 2 ⇒ uncooled.
XMLIR	Distance between mirrors.
XMAG	Telescope magnification.
ITYPEB	Telescope type: 1 ⇒ on-axis, 2 ⇒ off-axis.
XLEA	Exit aperture width.
BETA	Exit aperture absorption coefficient.
ASAB	Strut area/beam area.
ITYPEA	Type of exit aperture: 1 ⇒ material window, 2 ⇒ open port.

Table 3.3 (Continued)

OPTIONAL - NAMELIST/CASE/ (Continued)

THTR	Tracker jitter (1σ).
THBS	Boresight jitter (1σ).
THAA	Autoalignment jitter (1σ).
THSV	Servo jitter (1σ).

OPTIONAL - NAMELIST/USPEC/

PLINE (1)	Percent (or actual) power in line 1.
PLINE (2)	Percent (or actual) power in line 2.
PLINE (3)	Percent (or actual) power in line 3.
ABL	User specified linear absorption coefficient.
ABE	User specified exponential absorption coefficient.
SCL	User specified linear scattering coefficient.
SCE	User specified exponential scattering coefficient.

include the first two cards which must precede each set of runs. The first uses I2 format in columns 1 and 2 to state the number of cases (NRUN) which will be run, the second uses free-field format to allow the user to title each of the runs. The first card appears only once while the title card must precede each new case. Hence, the data stream is as follows:

```

NRUN CARD
Title
Required Inputs
Namelist INPUT
Namelist CASE
Namelist USPEC (if required)
} Case 1

Title
Required Inputs
Namelist INPUT
Namelist CASE
Namelist USPEC (if required)
} Case 2

```

Table 3.4 provides a convenient work sheet format that may be used to specify each case. It includes a list of the default values and units. Those familiar with COMBO will recognize a change in some of the default values; the default statements now reflect sea level applications. Note that either PHI or HTM may be specified, but that PHI should always be given as a positive angle (measured from the zenith). A negative PHI is a flag that HTM was specified.

For additional convenience, Table 3.5 lists several of the important program flags which may be of interest to the user. A complete program listing and sample run is supplied along with a sample problem output in Appendix B.

Table 3.4 Sample Input Form with Default Values

Required	Type	Position	Units	Case 1	Case 2	Case 3
I _{TYPE} ✓	(3,5)	12				
PD ² or PT	(3,5) (3,5)	11-20 21-30	w w			
O _I ⁵ L	(3,5) (3)	31-40 41-50	w/m ² m			
Header	Header		Header	Header	Header	Header
Header	Header	Header	Header	Header	Header	Header
Header	Header		Header	Header	Header	Header
BEAM ✓	1 (focused)					
CHI	0.52		rad			
FL	L		m			
GL	0.		m			
HOM	50.		m			
HTN	10.		m			
LAMDA	3.2E-6		m			
M	1.5					
NSTEP ✓	30					
OMEGA	0.		rad/sec			
OUT ✓	1 (short)					
PHI ³	-1.E-6		rad			
PROP ✓	1 (Gaussian)					
RH	0.5					
RI	.08		m			
RO	.35		n			
SIGHF	5.E-6					
SIGLF	5.E-6					
VP	15.		m/sec			
VXB	0.		m/sec			
WTHR ✓	0 (normal)					

Table 3.4 (Continued)

Namelist "CASE" Optional	Default	Units	Case 1	Case 2	Case 3
ASAB	0.05				
BETA	0.01	m ⁻¹			
DD	.16	m			
DC	0.166	m			
DELT	1.0	°K			
DELTAR	0.1				
DIOVI	0.5				
DLI	0.1	L/WT			
DI	2.0	seconds			
EPS	.35				
ITYPAW ✓	1 (focused)				
ITYPEA ✓	2 (open)				
ITYPEB ✓	1 (on-axis)				
ITYPEM ✓	1 (cooled)				
N	5				
REFL	0.985				
R1	1.170	m			
RRI1	2.5				
SIAB	1./8.	vis lambda			
THAA	5.E-6	rad			
THBS	5.E-6	rad			
THSV	5.E-6	rad			
THTR	5.E-6	rad			
XLC	50.	m			
XLEA	0.05	m			
XMLIR	.15	m			
XNAC	4.375				
Namelist "USPEC" Optional	Default	Units	Case 1	Case 2	Case 3
Pline (1)	.338				
Pline (2)	.32				
Pline (3)	.342				
ADE	0.	m ⁻¹			
ABL	0.	m ⁻¹			
SCE	0.	m ⁻¹			
SCL	0.	m ⁻¹			

NOTES:

1. Check mark (✓) indicates "I" format is required.
2. User may specify either power exiting the device or telescope.
3. PHI need not be specified if HIM is given.
4. Although data on \$INPUT\$ card are optional, the card must be present even when all default values are to be used. The same applies to data card \$CASE\$. The namelist card \$USPEC\$ is only read when a negative lambda has been inserted on data card \$INPUT\$ as a flag.
5. If ITYPE = 5, OI is the desired intensity for the reverse calculation; otherwise it is the minimum useful intensity for the variable power tabulation (default value of 10⁷ w/m²).

Table 3.5 Flags

<u>FORM</u>	<u>MEANING</u>
<u>Inputs</u>	
Negative LAMDA	The users will specify the multi-line power ratios or the single-line absorption and scattering coefficients.
Negative PHI	HTM is specified (Default).
<u>Internal</u>	
CNVRGD	TRUE => the last blooming interval passed over the end point.
ENDED	TRUE => this is the last blooming interval.
ERR	TRUE => the reverse calculations have not converged in 20 iterations.
FINAL	= 1, the reverse calculations have not converged yet; = 2, last pass through the propagation calculation.
FRACT	Tells the fraction of the last blooming interval that is within L.
LAM	= 1, 10.6 μm = 2, 3.8 μm (multi-line) = 3, 5 μm (single-line at present) = 4, user will specify single-line absorption and scattering coefficients.
OK	TRUE => save previous values for multi-line absorption and scattering calculations.

Table 3.5 (Continued)

<u>FORM</u>	<u>MEANING</u>
<u>Internal (Continued)</u>	
TYPE	= 1, AA = 2, BB = 3, AB = 4, BA.
UNIFORM	TRUE => last two blooming intervals were the same.

Section 4

SUMMARY OF TASKS I-IV

The purpose of this section is to briefly review the objectives and results of the original four tasks. Specific details may be found in the first and second interim reports (References 1 and 2). The primary objective here is to highlight some of the issues which arose during the course of the work and to indicate some of their implications as they relate to propagation modeling in general.

4.1 REVIEW OF TASK I. CODE COMPARISONS

The objective of Task I was to quantitatively compare the results obtained from three propagation codes over a parameter space representative of realistic engagement conditions. The codes were: NOLEC (Naval Surface Weapons Center); COMBO (Air Force Weapons Laboratory); ESP-I (United Aircraft Research Laboratories). The comparisons were presented at the First DOD Conference on High Energy Laser Technology on 3 October 1974 in San Diego (Reference 14). An unclassified version of this paper is included as an appendix in the first interim report (Reference 1). The major conclusions from these comparisons were that all three codes give comparable results for situations in which thermal blooming is not severe, but that ESP-I gives intensities up to an order of magnitude or more higher than the other two codes when blooming is significant. NOLEC and COMBO agree reasonably well under most conditions.

A secondary objective of Task I was to ascertain the reasons for major discrepancies between the codes. The effort was concentrated on COMBO and ESP-I since there is considerable disparity in their results even though they both use essentially the same approach for calculating thermal blooming. NOLEC uses an entirely different approach. In reviewing the theoretical basis of the codes, several issues were raised whose significance goes beyond the immediate objectives of the present work.

The blooming subroutines in both COMBO and ESP-I are based on the theoretical and experimental work of Gebhardt and Smith (Reference 20). The essence of the basic approach is the representation of the ratio of the bloomed and unbloomed focal plane peak intensities, I_{REL} , as a function of a single "blooming parameter," N . N is a theoretically derived, dimensionless, similarity parameter. However, the relationship between I_{REL} and N was obtained experimentally. Both COMBO and ESP-I use the same empirical relationship for $I_{REL}(N)$. They yield different results in blooming calculations because they compute N differently. The differences in the recipes for calculating N were identified explicitly in the First Interim Report (Reference 1). The question as to which method is more "correct" could not be resolved on theoretical grounds for several reasons.

1. An approximation to the theoretically derived expression for N was used in correlating the experimental data. The approximation was not generally valid even for the conditions of the experiments. It is even more questionable for realistic engagement-scale conditions such as those for which the simplified propagation codes are used.

2. COMBO uses the theoretical expression for N except for a relatively minor ad hoc correction. In principle, this has some important advantages, such as an inherent capability to treat non-coalitude engagements. Unfortunately, it is not consistent with the empirical relationship used to correlate the experimental data.

3. ESP-I uses the same expression for N as was used for the empirical correlation. In that sense, it is at least consistent. However, it does not engender much confidence in the extrapolation from small scale laboratory experiments to realistic engagement conditions.

To summarize the situation, both COMBO and ESP-I use a semi-empirical blooming model which is flawed by a basic inconsistency between its theoretical and empirical components. The First Interim Report implies a preference for COMBO simply because it was in closer agreement with NOLEC. It should be emphasized, however, that this may be, at least to some extent, fortuitous. Furthermore, there does not exist sufficient data to provide convincing validation of any of the codes.

Evaluation of the codes on theoretical grounds in any kind of absolute sense was beyond the scope of the study, but two observations are in order. First, the consistency problem with the Gebhardt and Smith blooming model does not necessarily reflect adversely on its basic approach; the deficiencies are primarily associated with its implementation. Secondly, there are no clear and obvious theoretical reasons why either of the basic approaches should be superior in accuracy to the other. All of the codes incorporate numerous simplifying assumptions and approximations, both explicit and implied, and rely to some extent on heuristic arguments.

4.2 REVIEW OF TASK II. BEAM SHAPE AND DISPLACEMENT

The objective of this task was to develop empirical models for predicting beam shape distortion and displacement in the focal plane due to thermal lensing. Results from the NRL non-linear propagation code were used as the data base for the analysis.

Since beam distortion and displacement both are closely related to thermal blooming, I_{REL} (the reduction in peak intensity due to blooming) was used as the primary correlation parameter. This automatically accounts for much of the dependence on the independent parameters and has the further advantage of being readily computed from the NRL scaling law.

The beam displacement model is represented by

$$\left(\frac{d}{a_f}\right)^{\eta, 29} = \frac{-0.519 + \sqrt{(0.519)^2 + 1.500 \ln(1/I_{REL})}}{0.750}$$

where d is the displacement of the peak intensity into the wind, a_f is the e^{-1} beam radius (without blooming) in the focal plane, a_i is the e^{-1} beam radius in the source plane, and $\eta = a_f / a_i$.

The beam shape model represents the constant intensity contours as ellipses and the intensity distribution as

$$I(x,y) = I_{PEAK} \exp \left\{ -SD \left[\left(\frac{x}{a_f}\right)^2 + \left(\frac{y-d}{Da_f}\right)^2 \right] \right\}$$

where

$$D = 0.3 + 0.7 I_{REL}$$

$$S = I_{REL}$$

$$I_{PEAK} = \frac{P e^{-\alpha R} I_{REL}}{\pi a^2 f^2}$$

This model automatically gives the correct peak intensity and conserves total power. It also provides an excellent representation of the data in terms of the area within a given constant intensity contour and the eccentricity of the constant intensity contours.

These models, of course, are subject to the same limitations as the data from which they were derived. For example, they do not apply (unless suitably modified) in the presence of jitter or turbulence or when slewing is not in the same plane as the wind. Actually, the most significant result of this task is that both distortion and deflection are probably too minor to have a significant impact on system effectiveness.

4.3 REVIEW OF TASK III. BEAM QUALITY

The objective of this task was to develop an approach to modeling the effect of phase and amplitude aberrations in the aperture plane on the far-field beam profile. In more general terms, it was desired to obtain a rational approach to representing beam quality.

The recommended approach involves approximating the far-field intensity profile (neglecting blooming) as a Gaussian distribution of the form

$$I(R) = \frac{m_1 P_T e^{-\alpha eR} \exp \left\{ -\frac{r^2}{2R^2 \left(\frac{m_2^2 \sigma_{DL}^2}{I_{REL}} + \sigma_J^2 + \sigma_T^2 \right)} \right\}}{2\pi R^2 \left(\frac{m_2^2 \sigma_{DL}^2}{m_1 I_{REL}} + \sigma_J^2 + \sigma_T^2 \right)}$$

The parameters m_1 and m_2 are the proposed beam quality parameters and are determined so that the integrated power distribution corresponding to the above expression matches the actual distribution at two specified points, e.g., $r = w_f$ and $r = 2w_f$, where w_f is the beam waist.

This two parameter representation of beam quality is a significant advance over the usual "m x diffraction limited" concept. It can account both for power loss due to wide angle scattering and for beam spreading. It should be fully adequate to represent all situations in which the far-field beam profile is dominated by a central lobe. Furthermore, the general approach is sufficiently flexible that it can include effects associated with beam truncation and obscuration (see following section) as well as with other amplitude perturbations and with phase aberrations. For example, the simplified optical train model (OPTRAIN) described in Section 2 provides a method of estimating m_1 and m_2 for a wide range of system parameters.

4.4 REVIEW OF TASK IV. BEAM TRUNCATION AND OBSCURATION

The effect of truncation and obscuration were investigated both analytically and within the empirical framework of the beam quality model developed in Task III,

i.e., the results were presented in terms of the parameters m_1 and m_2 . Detailed results of the analysis are presented in Reference 2. Since the degree of truncation and obscuration is determined by the optical train, the model itself has been incorporated into the optical train model (Section 2).

Section 5

CONCLUSIONS

In any high technology program, like the DOD laser program, it is important that technologists and analysts work together to resolve the issues and support the efforts of the other group. During the early phases of a new program the technologists severely bound the problem under study to facilitate modeling of complicated processes. On the other hand, the analysts use extremely simplistic models for the elements of the system under study because they must address every aspect of the problem albeit in a naive manner. As time passes these two groups move closer together with the theoreticians studying ever increasing segments of the problem and the systems analysts improving their models and studying the issues in greater depth.

The atmospheric propagation coding studied under this contract is really second generation modeling. Improving the speed and accuracy of a program, adding multi-line propagation, and studying beam shape are exemplary of the movement of HEL system analysts toward increasingly complex modeling. One of the other areas investigated -- the optical train analysis -- is less well developed. The detailed tools for modeling the beam propagation through the optical train have been operational only recently. Hence, the simplified codings developed under this contract are first generation models. The authors hope that both of these modeling tasks will contribute to the continuing convergence of laser technology and systems analysis.

APPENDIX A

Molecular Absorption of DF Laser Radiation

A.1 INTRODUCTION

This appendix was written by Dr. T. Tuer of the Ann Arbor SAI office. This work was undertaken to provide better values for the molecular absorption coefficients used in the thermal blooming code. These coefficients are required as a function of both altitude and of atmospheric water vapor content for several "typical" DF laser line groups. Here, "typical" means a characteristic laser propagation-altitude function (this will be clarified in Section A.3). For convenience in the thermal blooming code, the coefficients are given as a simple analytical function of altitude and water content, with different sets of coefficients (i.e., one for each typical group).

A.2 APPROACH

Due to time constraints, it was decided to use McClatchey's DF absorption coefficients (Reference A.1) rather than re-calculating them with our own line-by-line codes. The ten BDL laser lines that McClatchey considered were selected for this study (see Table A-1). However, since McClatchey did not include the water continuum absorption in his calculations, it was necessary to add this component. A simple computer program DAFT (DF Altitude Fitting Code), was written to: (1) evaluate this continuum component for the frequencies, altitudes and model atmospheres desired, (2) add this to McClatchey's

results, and (3) plot the total absorption coefficient as a function of altitude.

Table A-1. List of DF-BDL Lines

DF Laser Line	Frequency (cm ⁻¹)	Relative Power	Considered by McClatchey and Here
P ₃ (8)	2546.37	10.7	yes
P ₃ (7)	2570.51	10.2	yes
P ₂ (10)	2580.16	6.2	yes
P ₃ (6)	2594.23	7.7	yes
P ₂ (9)	2605.87	9.7	yes
P ₃ (5)	2617.41	1.8	yes
P ₂ (8)	2631.09	12.9	yes
P ₂ (7)	2655.97	10.0	yes
P ₁ (10)	2665.20	3.9	yes
P ₂ (6)	2680.28	6.2	yes
P ₁ (9)	2691.41	9.1	no
P ₁ (8)	2717.54	6.6	no
P ₁ (7)	2743.03	3.5	no
P ₁ (6)	2767.91	2.0	no

The water continuum absorption coefficient is given by (Reference A.2).

$$n = c_S^0 \cdot p_w^* + c_N^0 \cdot p^*$$

where p_w is the partial pressure of water vapor, P is the total pressure and the * indicates the density-equivalent-

pressures¹. This reference also gives measured values of $c_{S,W}^0$ as a function of frequency at 294° K², and recommends value of $c_{N,W}^0 = 0.12 c_{S,W}$. The absorption coefficient n differs from the usual coefficient k by:

$$k = nU/L$$

where U is the absorber thickness and L is the path length. Values for p^* , P^* and U were calculated as a function of altitude using data given by the Handbook of Geophysics and Space Environment (Reference A.3).

The attenuation of most of the DF laser lines is dominated by atmospheric water absorption (i.e., H₂O or HDO line absorption, or H₂O continuum absorption). In order to account for different atmospheric water content, the calculated absorption coefficient was normalized by:

$$k^* = k/\rho^*$$

Here ρ^* is a normalized water density-altitude profile which varies between a value of ρ_0^* at sea level, to unity as $h \rightarrow \infty$. The quantity ρ_0^* is the sea level density of the model atmosphere under consideration, normalized to that of the midlatitude summer model atmosphere. The form of ρ^* was arbitrarily taken to be:

$$\rho^* = 1 + (\rho_0^* - 1)10^{R/2}$$

1. Since the pressures are generally less than one atmosphere, we used the usual pressure in place of the density-equivalent-pressure.
2. Since the temperature dependency of this quantity is uncertain, its value at 294°K was used throughout.

where R is the normalized water density profile based on the data in Reference A.3 (see Figure A-1). An example of the effect of this scaling is shown in Figure A-2, where the absorption coefficient profiles for the five different model atmospheres are seen to collapse nicely into a narrow band.

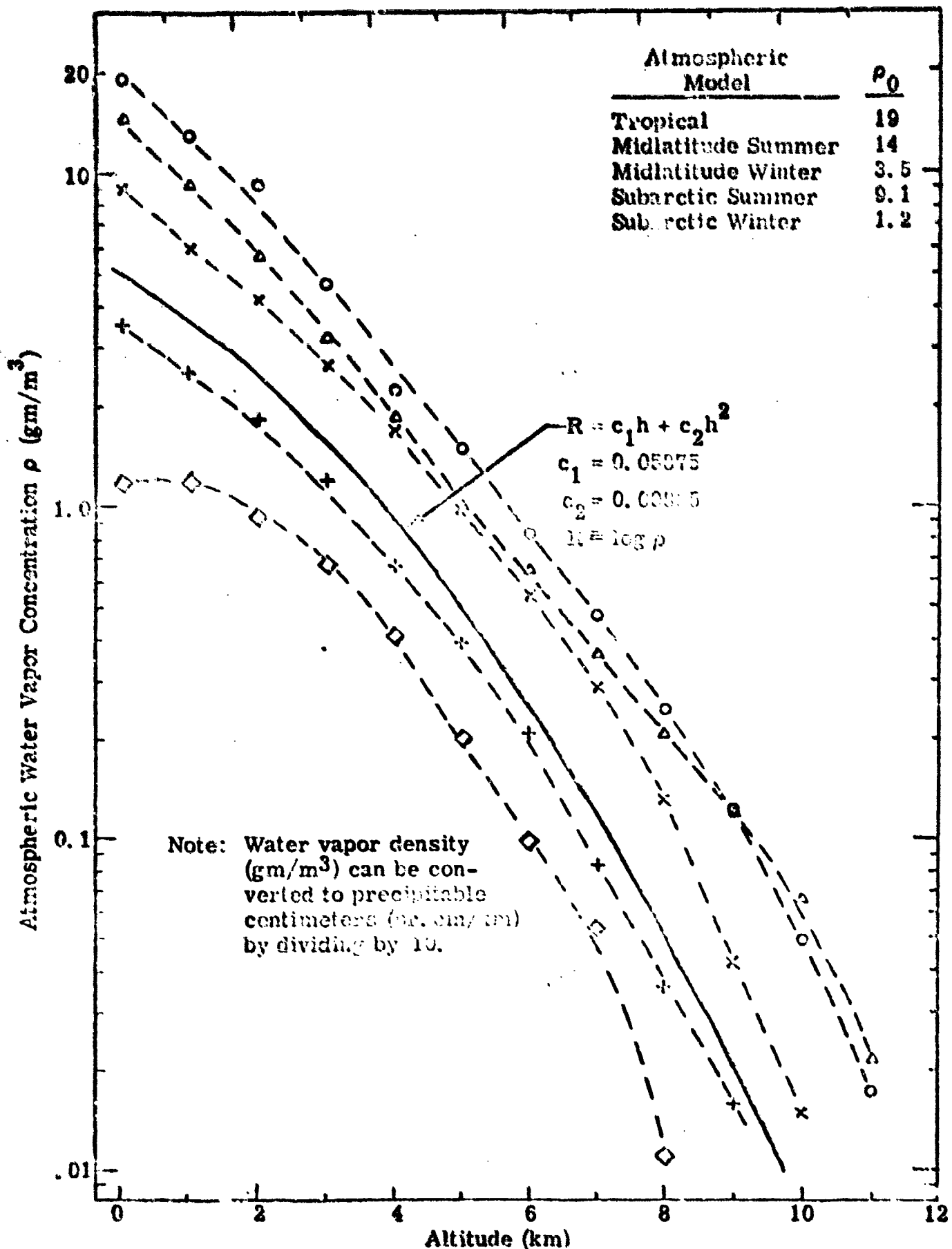


Figure A-1. Water Concentration Profiles for Five Model Atmospheres and Analytic Fit.

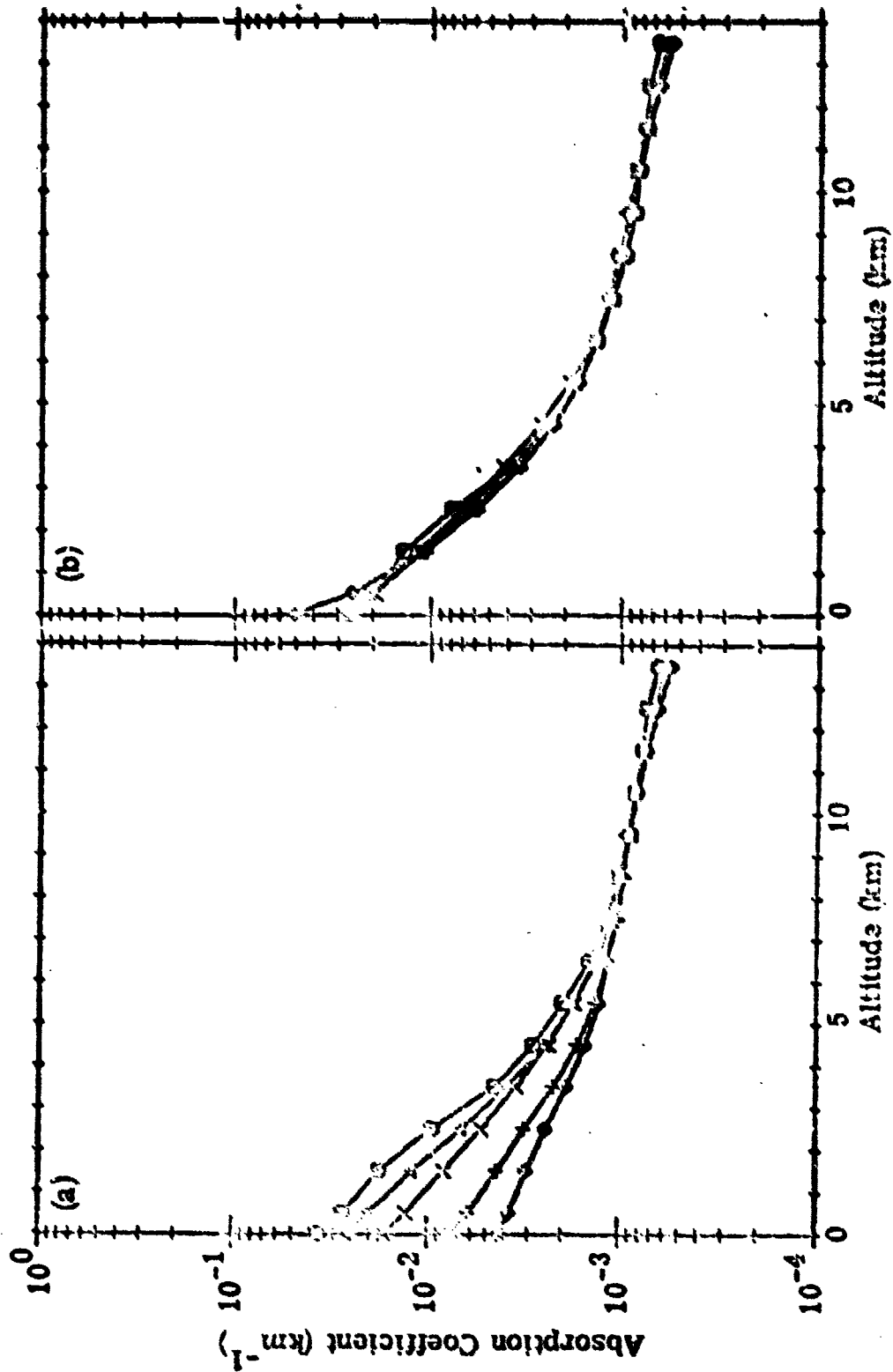


Figure A-2. Demonstration of the Effect of Scaling to Account for Various Atmospheric Water Concentrations - P₂(8) DF Laser.
 (a) No Scaling
 (b) With Scaling

A.3 DETERMINING TYPICAL GROUPS

Normalized profiles for all the water dominated laser lines were plotted on a common scale. Of course the lines which are dominated by other species (e.g., N_2O line absorption), were not normalized in this fashion but simply plotted. These plots tend to collect in three general groups. Those laser lines which are dominated by water at low altitudes, but happen to fall on underlying absorption lines (Type A), have a knee in their profile (see Figure A-3). Those that do not have underlying lines (Type B), do not have a pronounced knee but continue to decrease with altitude, at least for the altitude range considered here (see Figure A-4). Lines which are not dominated by water (Type C), have no knee but fall off less rapidly with altitude (see Figure A-5).

The mechanism for each type can be elucidated by examining the details of the absorbing lines and continuum. Figure A-6 shows components of the absorption coefficient of a Type A laser line at sea level. Notice the underlying CH_4 absorption line (M2), which will become important at higher altitude as the absorption by water diminishes. Figure A-7 shows a Type B laser line where there is no important underlying absorption lines. Finally, a Type C laser line is shown in Figure A-8, which is dominated by N_2O absorption even at sea level, and is affected little by water.

A.4 RESULTS

A least squares fit was applied to each group of laser lines (i.e., Types A, B and C). The analytic form used was:

$$\ln k^* = A_0 + A_1 h + A_2 h^2$$

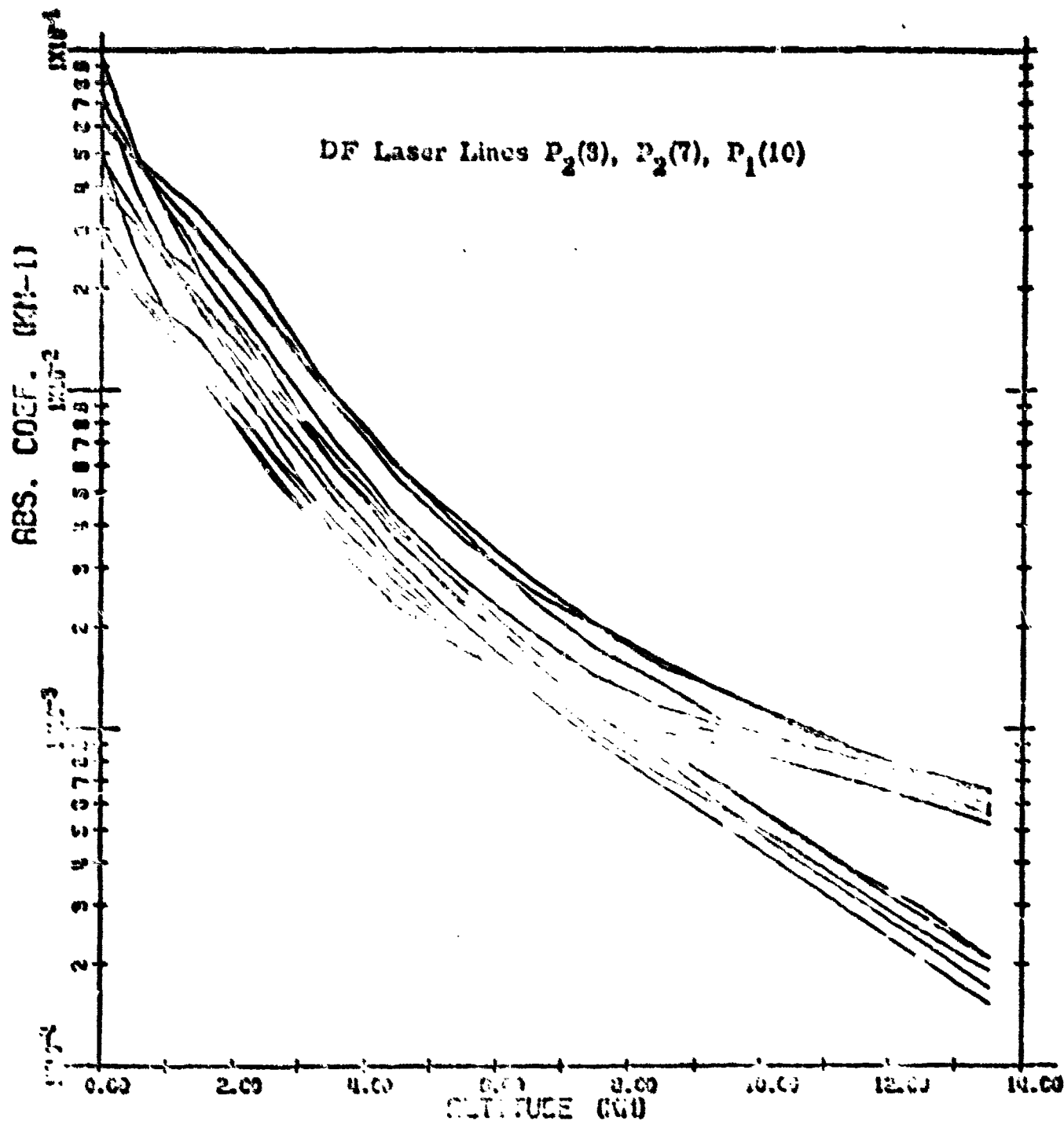


Figure A-3. Laser Propagation-Altitude Function Type A: Dominated by Water at Low Altitudes but with Underlying Absorption Lines which become Important at High Altitudes.

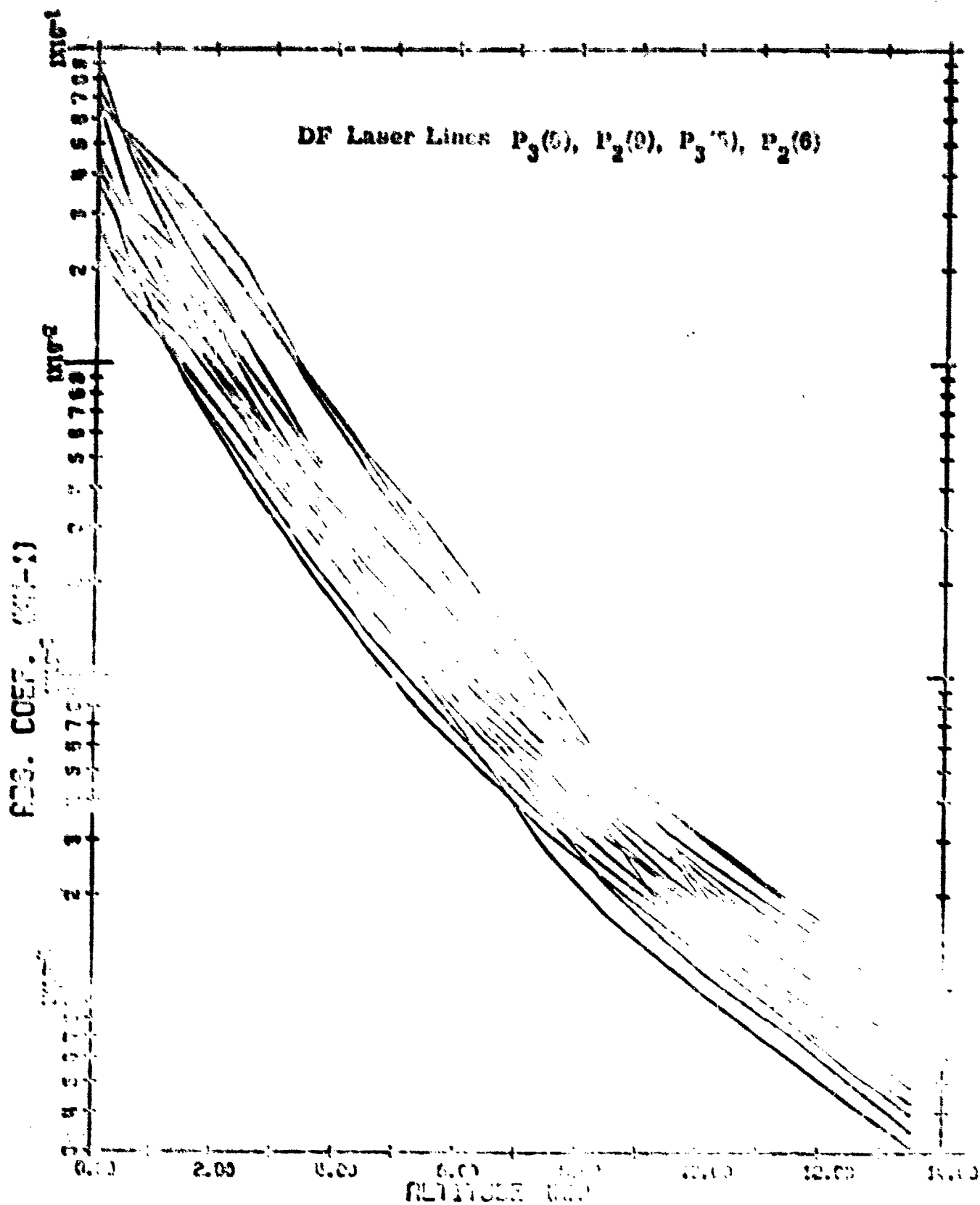


Figure A-4. Laser Propagation-Altitude Function Type B: Dominated by Water at Low Altitudes but with Underlying Absorption Lines which become Important at High Altitudes.

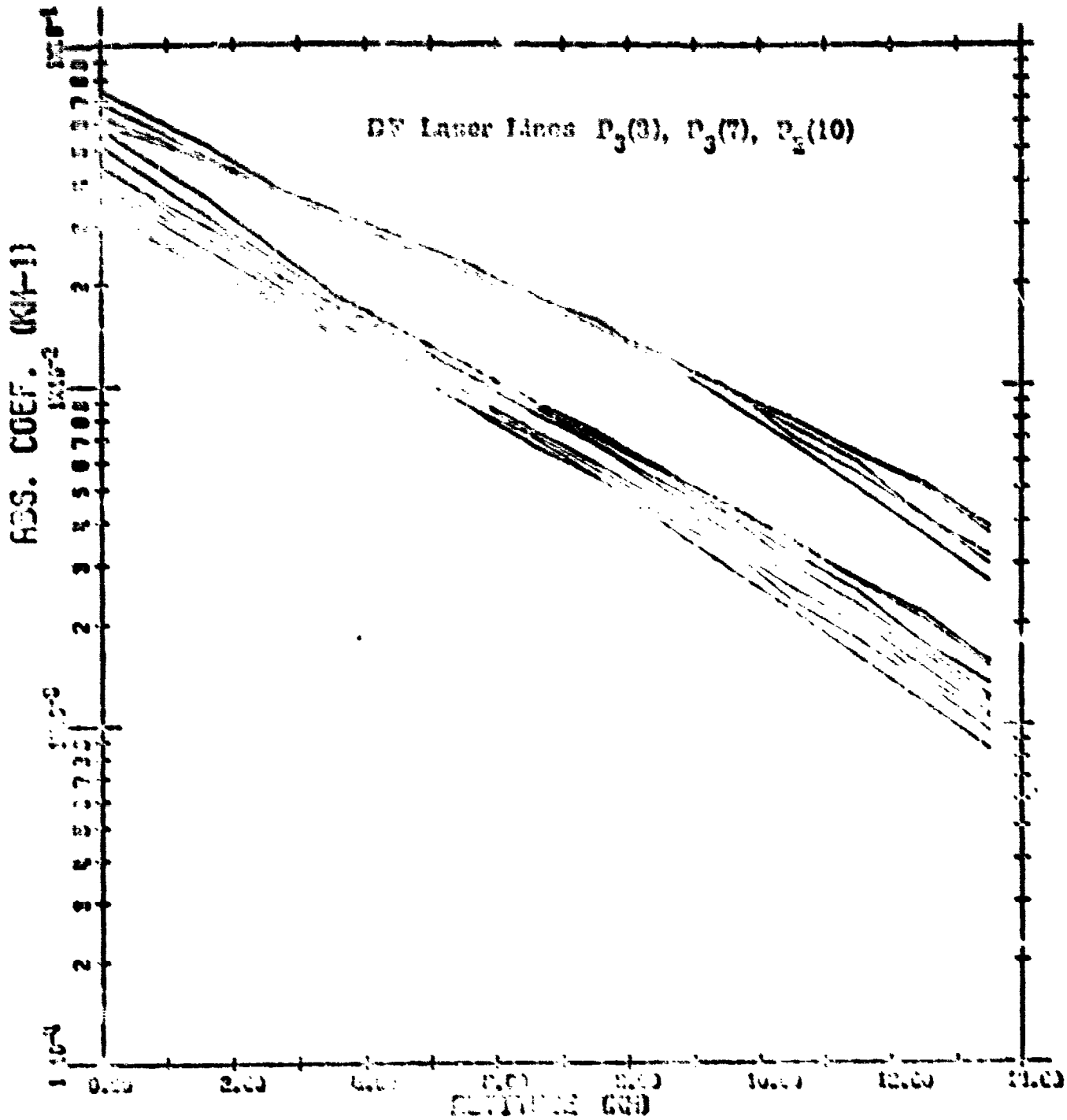


Figure A-5. Laser Propagation-Altitude Function Type C: Dominated by Water at Low Altitudes but with Underlying Absorption Lines which become important at High Altitudes.

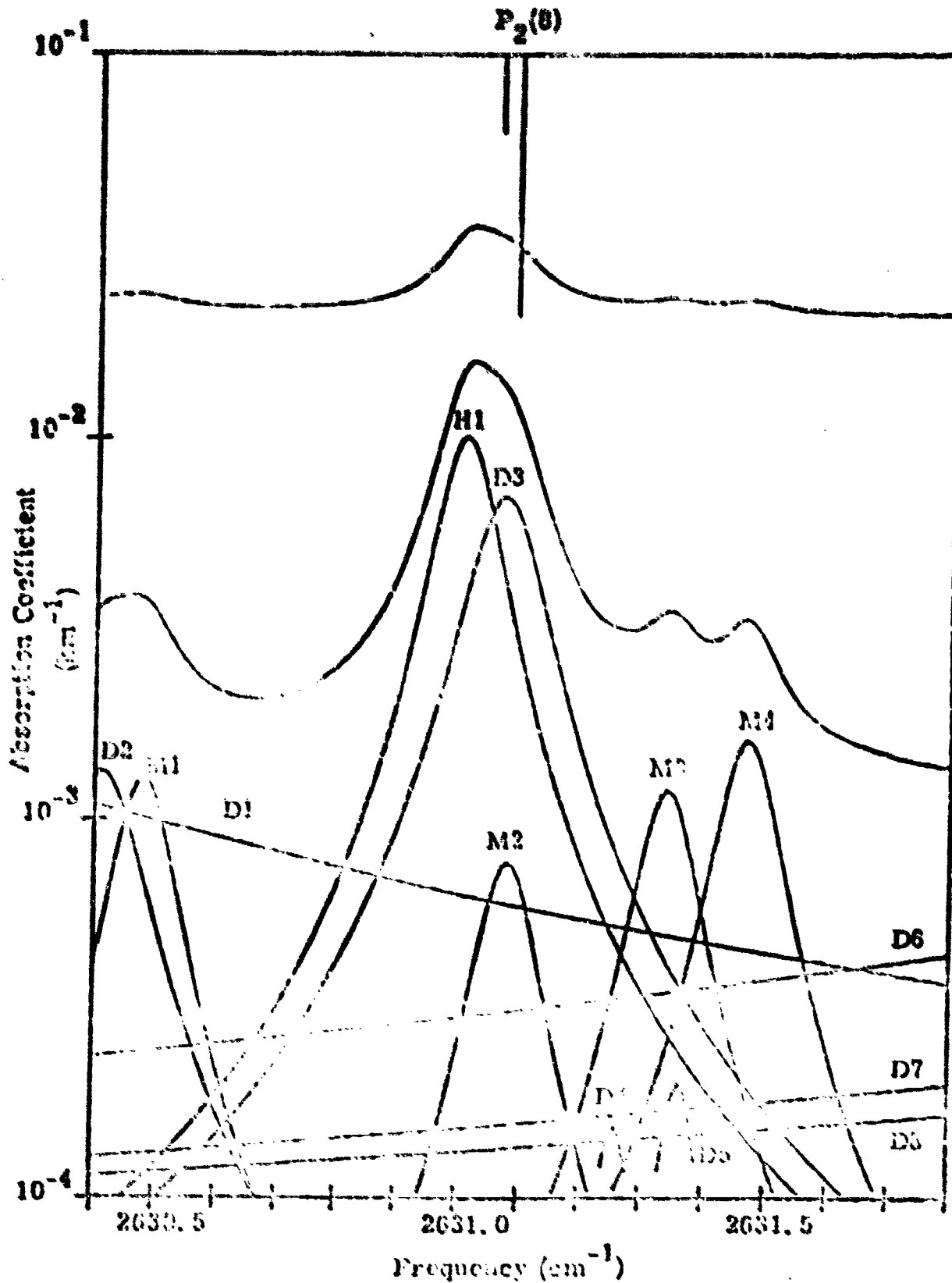


Figure A-6. Contributors to the Molecular Absorption of the P₂(S) DF Line (Midlatitude Summer, Sea Level).

Example of Type A Absorption, Extracted from Ref. A.4.

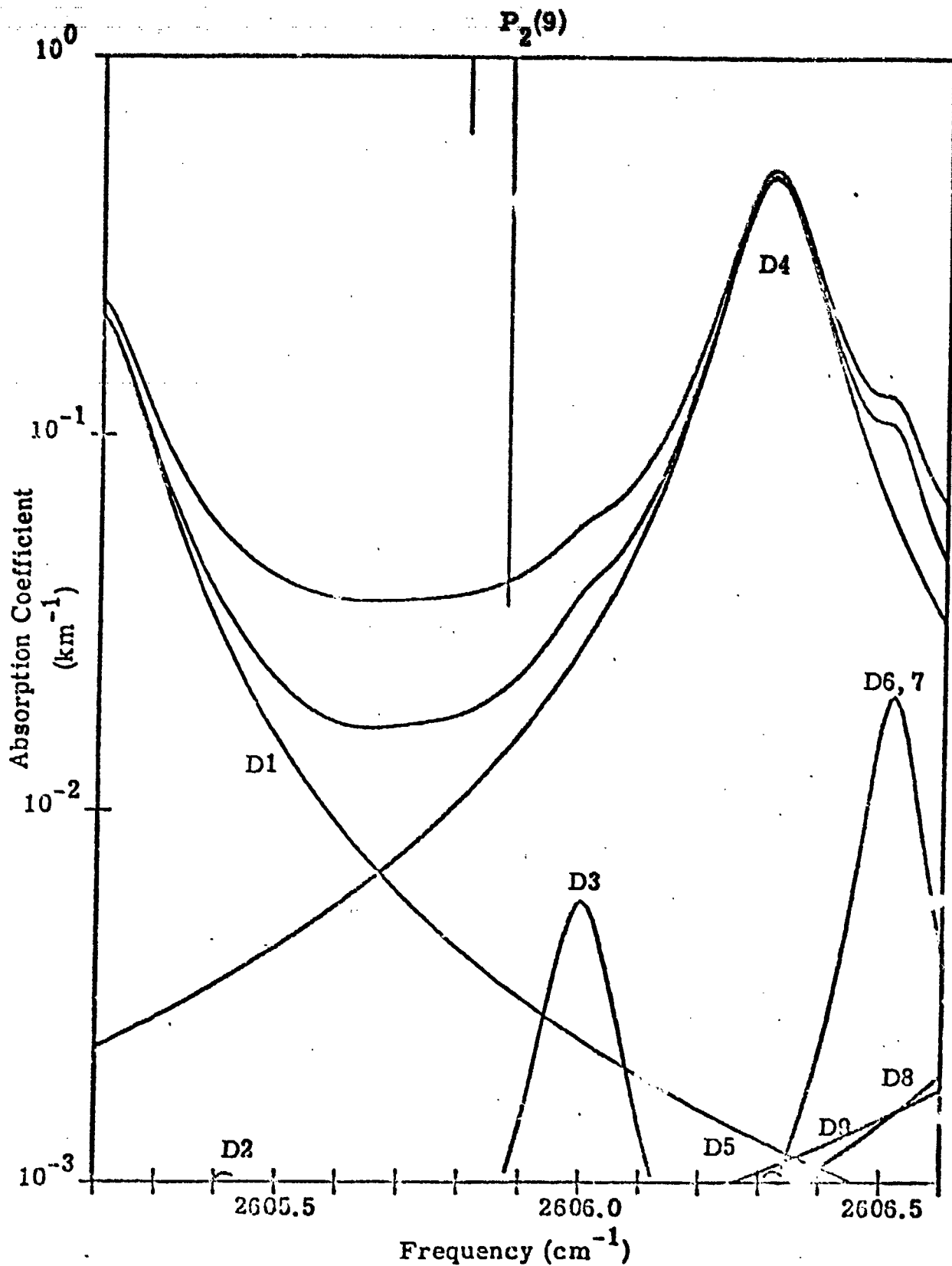


Figure A-7. Contributors to the Molecular Absorption of the $P_2(9)$ DF Line (Midlatitude Summer, Sea Level).

Example of Type B Absorption, Extracted from Ref. A.4

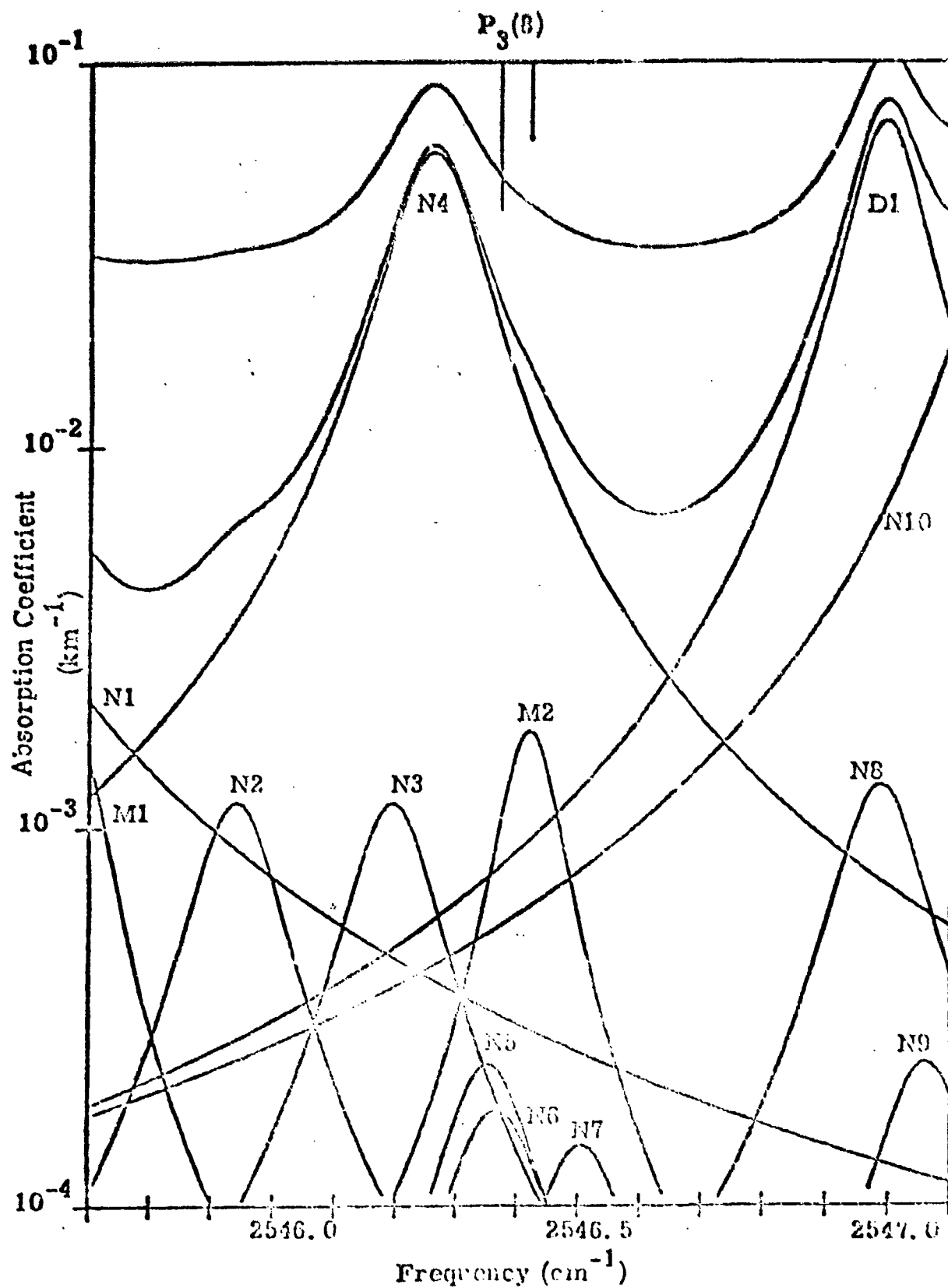


Figure A-8. Contributors to the Molecular Absorption of the $P_3(8)$ DF Line (Midlatitude Summer, Sea Level).

Example of Type C Absorption, Extracted from Ref. A.4

where k^* is the normalized absorption coefficient (km^{-1}) and h is the altitude (km). The results of this fit for each group are shown in Figures A-9 through A-11, and the determined coefficients (i.e., A_0 , A_1 , A_2) given in Table A-2.

Table A-2. Coefficients of Least Squares Fit

Type	DF Laser Lines	A_0	A_1	A_2
A	$P_2(8)$, $P_2(7)$, $P_1(10)$	-3.138	-0.6388	0.0225
B	$P_3(6)$, $P_2(9)$, $P_3(5)$, $P_2(6)$	-3.173	-0.6952	0.0155
C	$P_3(8)$, $P_3(7)$, $P_2(10)$	-3.039	-0.2199	-0.00196

For Type C laser lines this normalized coefficient k^* is identical to the un-normalized coefficient k (since water absorption is insignificant):

$$k = k^* \quad (\text{for Type C})$$

Type A and B lines must be un-normalized by:

$$k = \rho^* k^* \quad (\text{for Types A \& B})$$

where $\rho^* = 1 + (\rho_0^* - 1) 10^{R/2}$ and: $\rho_0^* = 1 + (\rho_0^* - 1) 10^{R/2}$ and:

$$R = C_1 h + C_2 h^2$$

with $C_1 = 0.05875$ and $C_2 = 0.00835$.

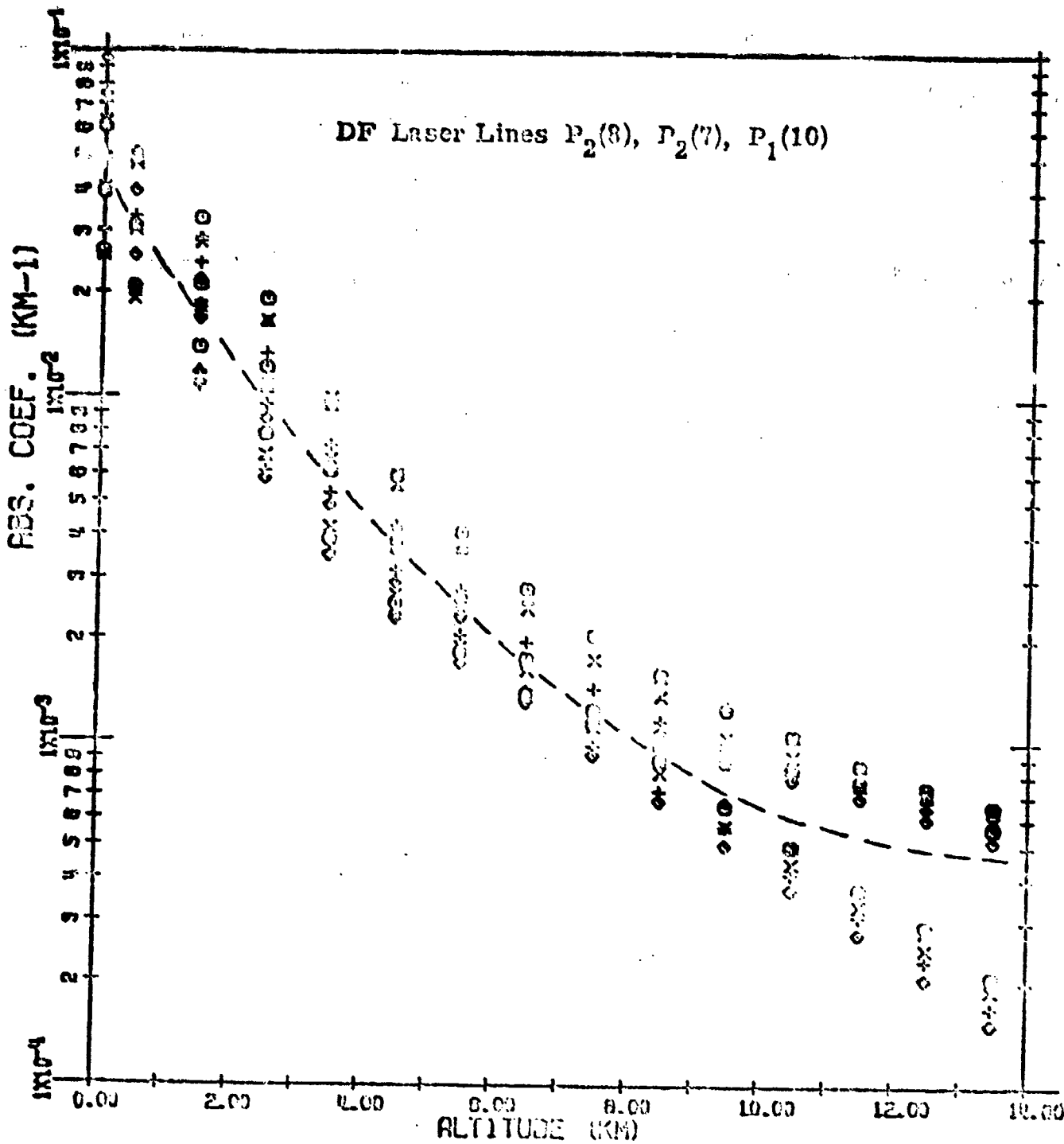


Figure A-9. Least Squares Fit to Type A Laser Lines

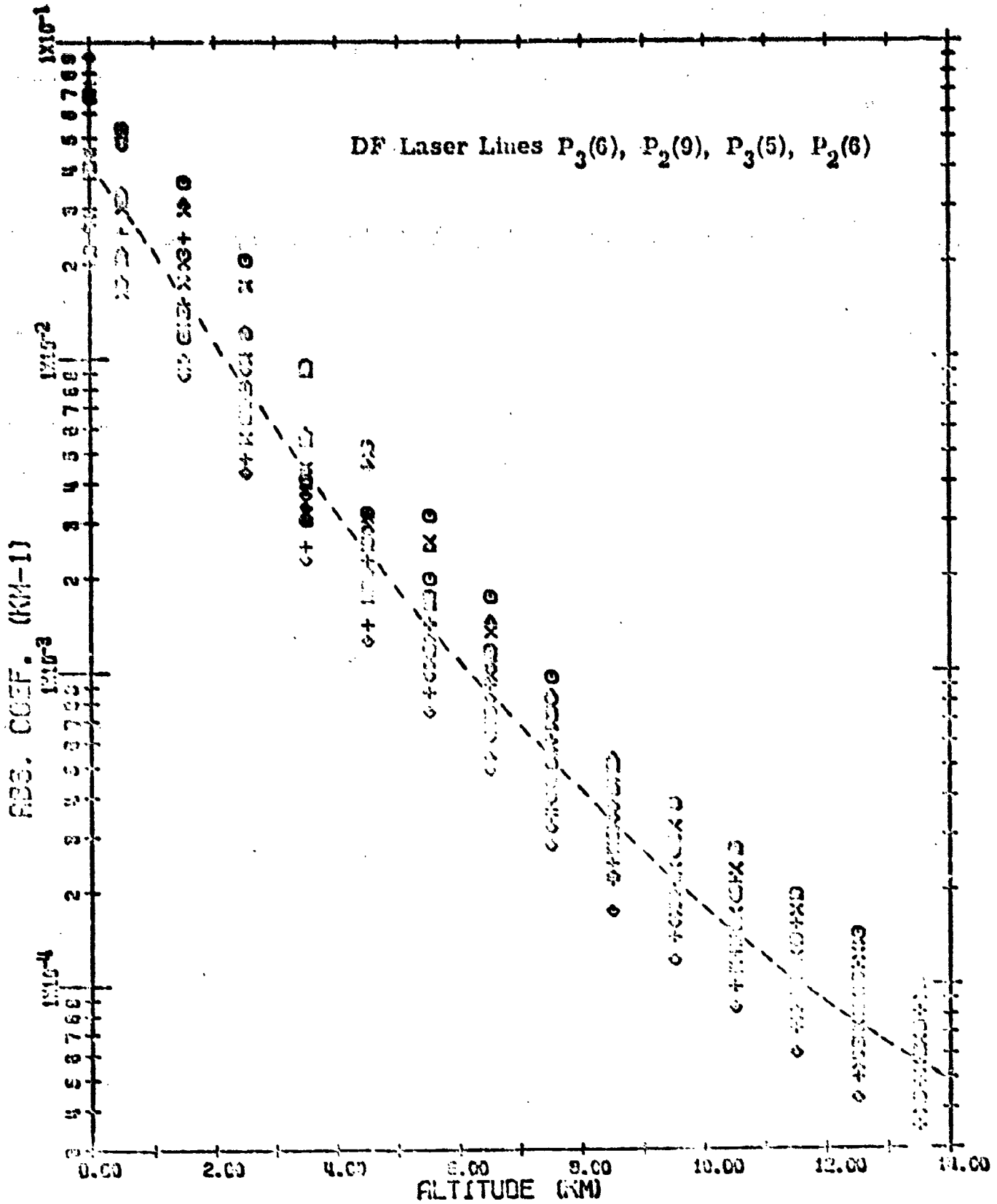


Figure A-10. Least Squares Fit to Type B Laser Lines

Reproduced from
best available copy.

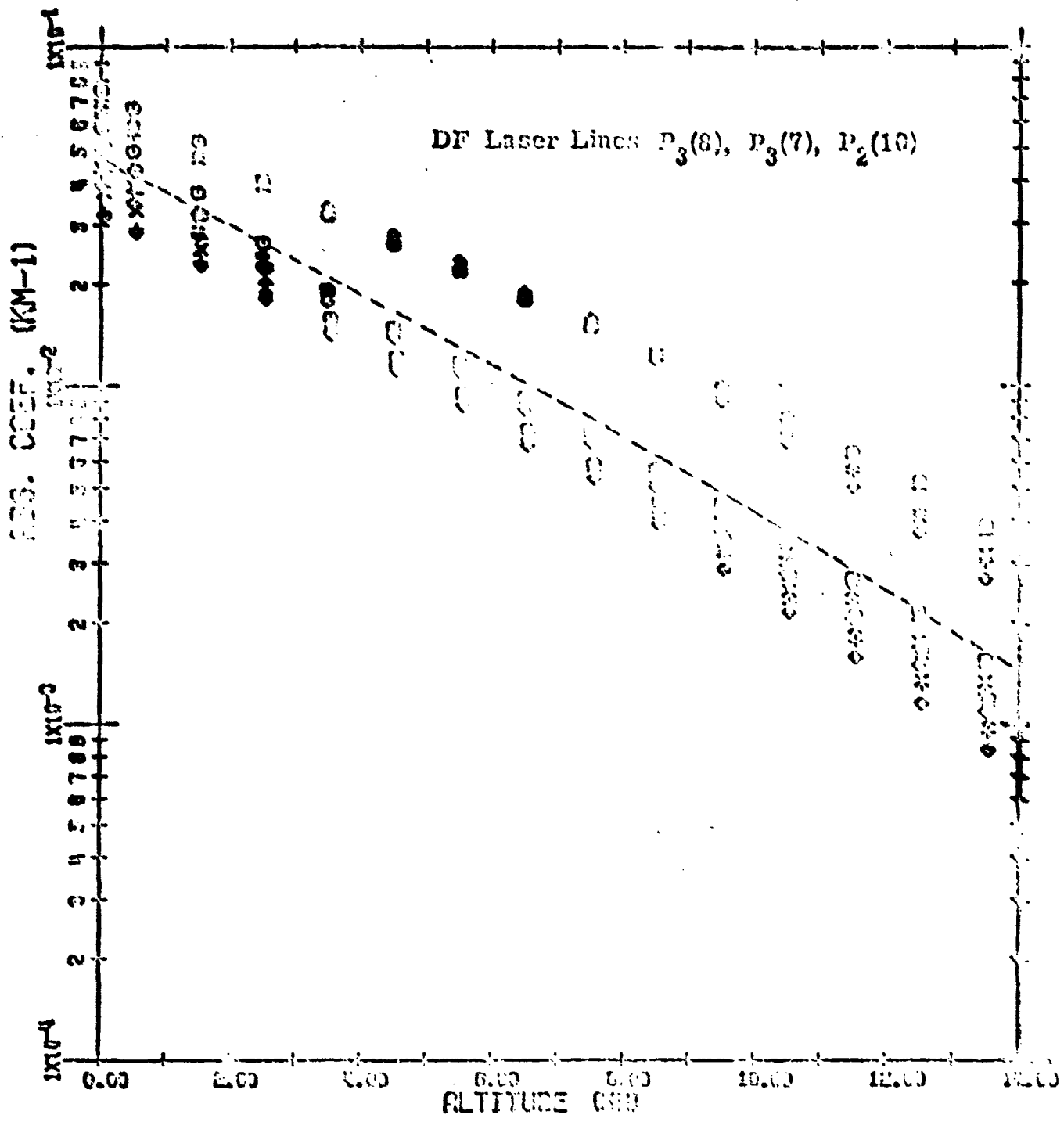


Figure A-11. Least Squares Fit to Type C Laser Lines

APPENDIX B

1
2
3
4
5
6
7

```

5          PROGRAM SAICOM(INPUT,OUTPUT,TAPES=INPUT,TAPE6=OUTPUT)          SIC
C          SAICOM IS THE EXECUTIVE ROUTINE WHICH READS THE INPUTS AND DEFINES THE CONDITIONS AT EXIT OF THE TELESCOPE.          SIC
C          LOGICAL ERR          SIC
C          EQUIVALENCE (RO,RO)          SIC
C          EQUIVALENCE (MOM,MOM)          SIC
10         INTEGER BEAM,BEAN,DERUG,OUT,PROP,SPOT,TITLE(7),WTMR          SIC
          REAL IND,L,LAMDA,M,M1,M2          SIC
          COMMON /ERROR/ ERR          SIC
          COMMON /ATIN/ M,OI,PROP,SIGLF,SIGMF,WTMR,M1,M2          SIC
          COMMON /ATMS/ BEAM,FL,GL,MTM,IRD,L,LAMDA,NSTEP,PHI          SIC
          COMMON /IN/ COEF,MOM,R1          SIC
          COMMON /INS/ DEHUG,ITYPE,OUT,PT,R0          SIC
          COMMON /INT/ PI          SIC
          COMMON /ALFA/ LAM,RH          SIC
          COMMON /OPTIN/ DR,PIN,WL,EPS,XNL,DT,XRI,TMI,DIOVI,DLI,DELTA,RREF,          SIC
          XLC,DC,N,REFL,SFAR,ITYPEM,XLM,K,XMAG,DIR,ITYPE,XLEA,BETA,ASAB,ITY          SIC
          ZPEA,TMTR,THRS,TMAA,TMSV,DT,DEL,ITYPAN          TICP
          COMMON /OPTOUT/ DR,P,XM1,XM2,TH          SIC
          COMMON /X/ CHI,OMEGA,VP,VP5C,V5A          SIC
          DIMENSION IBEAM(2), IDERUG(2), II(3), IJTYPE(4), IOU(2), IPROPI          SIC
          1)          SIC
          NAMELIST /INPUT/ BEAM,CHI,DERUG,FL,GL,MTM,MCM,IRD,LAMDA,M,NSTEP,OM          SIC
          IEGA,OUT,PHI,PROP,RH,R1,R0,SIGMF,SIGLF,VP,V5C,VTMR          SIC
          NAMELIST /CASE/ DR,EPS,DT,XRI,TMI,DIOVI,DLI,DELTA,RREF,XLC,DC,M,R          SIC
          IEFL,SFAR,ITYPEM,XLMIR,XMAG,TMRE,ITYPEB,XLEA,BETA,ASAB,ITYPEA,TMTR,          SIC
          ZTHRS,TMAA,TMSV,DEL,ITYPAN          TICP
          DATA IBEAM/I0MCOLLIMATED,I0MFOCUSED /          SIC
          DATA IDERUG/I0HOUT DEBUG,I0H DEHUG /          SIC
          DATA II/I0MILD,I0NORMAL,I0HSEVERE /          SIC
          DATA IOU/I0SHORT,5H LONG/          SIC
          DATA IPROP/I0NGAUSSIAN,I0MPLANE WAVE,I0MHP GAUSS /          SIC
          READ (5,7) NRUNS          SIC
          DO 6 IRUNS=1,NRUNS          SIC
          READ REQUIRED INPUTS          SIC
          READ (5,8) TITLE          SIC
          HEAD (5,9) ITYPE,PD,PT,OI,L          SIC
          SET DEFAULT VALUES OF OPTIONAL PROPAGATION INPUTS          SIC
          IF (OI.EQ.0.) OI=1.E7          SIC
          BEAM=1          SIC
          CHI=.52          SIC
          DEHUG=1          SIC
          FL=L          SIC
          GL=0.          SIC
          MTM=10.          SIC
          MOM=50.          SIC
          IND=1E12          SIC
          LAMDA=.3.EE-6          SIC

```

```

60 M=1.5
   NSTEP=30
   OMEGA=0.
   OUT=1
   PHI=-1.E-6
   PROP=1
   RM=.5
   KI=.08
   RO=.35
   SIGMF=5.E-6
   SIGLF=5.E-6
   VAM=0.
   VP=.15.
   WTM=0
70
   C READ (5,INPUT)
75
   BEAM=BEAM+1
   IM=IMR+2
   ERR=.FALSE.
   IF (VAR.NE.0.) VP=0.0
80
   IF (PD.EQ.0.) GO TO 1
   C
   C SET DEFAULT VALUES FOR OPTICAL TRAIN
   C
85 TMSORT(SIGMF+SIGLF+SIGLF+SIGLF)
   WLSAHS(LAMDA)
   PIN=PC
   KVL=K
   OIY=2.*RI
   OIY=2.*RO
   DMS=.15
   EPS=.36
   OY=2.0
   XPI=1.E70
   OIOW=0.5
   OLI=0.1
   DELTAR=0.1
   PDEF=2.5
   ALC=50.
   DC=.166
   N=7
100 REF=.996
   SFAP=1./8.
   IYPM=1
   XLMIP=.15
   XLAG=4.375
   IYPM=1
   IYPM=1
   XLEA=.05
   RETA=.01
   ASAD=.05
105 TMS=5.E-6
   TMS=5.E-6
   TMS=5.E-6
   TMS=5.E-6
110

```

```

SIC 59
SIC 60
SIC 61
SIC 62
SIC 63
SIC 64
SIC 65
SIC 65
SIC 67
SIC 68
SIC 69
SIC 70
SIC 71
SIC 72
SIC 73
SIC 74
SIC 75
SIC 76
SIC 77
SIC 78
SIC 79
SIC 80
SIC 81
SIC 82
SIC 83
SIC 84
SIC 85
SIC 86
SIC 87
SIC 88
SIC 89
SIC 90
SIC 91
SIC 92
SIC 93
SIC 94
SIC 95
SIC 96
SIC 97
SIC 98
SIC 99
SIC 100
SIC 101
SIC 102
SIC 103
SIC 104
SIC 105
SIC 106
SIC 107
SIC 108
SIC 109
SIC 110
SIC 111
SIC 112
SIC 113
SIC 114
SIC 115

```

```

115 DELT = 1.0
      ITPAN = 1
      C
116 READ (5,CASE)
      C
117 WRITE INPUTS
      C
118 IF (PHI.NE.-1.E-6) MTM=0.0
      C
119 MCF=3.2E10*OH
      C
120 MTF=3.2E10*MTM
      C
121 WRITE (6,10) T, TLE
      C
122 IF (ITYPE.EQ.5) GO TO 2
      C
123 WRITE (6,11) IOUT(OUT), IOENUG(DEBUG), L, S, FL, PT
      C
124 GO TO 3
      C
125 WRITE (6,12) IOUT(OUT), IOENUG(DEBUG), OI, PD, FL, PT
      C
126 WRITE (6,13) CALAND, HON, SIGMF, MCF, SIGLF, MTM, JMEGA, MTF, RO, PHI, RI
      C
127 WRITE (6,14) CHI, IPROP, PROP, VP, IHEAK(MEAN), VXS, H, IIM(IM), NSTEP, RM
      C
128 OPTICAL TRAIN CALCULATIONS
      C
129 IF (PD.CO.0.) GO TO 4
      C
130 CALL OPTIMAIN
      C
131 RC=RY/2.
      C
132 PTEP
      C
133 M1=X1
      C
134 M2=X2
      C
135 SIGMF=TH
      C
136 SIGLF=X0.
      C
137 IF (PROP.EQ.1) GO TO 5
      C
138 M1=X1/.89
      C
139 IF (PROP.EQ.1) M2=X2*.892*RM2
      C
140 IF (PROP.EQ.3) M2=X2/1.29
      C
141 GO TO 5
      C
142 SPECIFICATION OF BEAM QUALITY FOR PD = 0
      C
143 (TRUNCATED GAUSSIAN)
      C
144 M1=1.
      C
145 M2=1.4104
      C
146 IF (PROP.EQ.1) GO TO 5
      C
147 (INFINITE GAUSSIAN)
      C
148 M2=M
      C
149 IF (PROP.EQ.3) GO TO 5
      C
150 (PLANE WAVE)
      C
151 M1=0.89
      C
152 M2=1.29*H
      C
153 WRITE (6,15) M1,M2
      C
154 CALL ATM
      C
155 CONTINUE
      C
156 STOP 01
      C
157
158
159
160
161
162
163
164
165
166
167
168
169
170

```

```

175 171 SIC
176 172 SIC
177 173 SIC
178 174 SIC
179 175 SIC
180 176 SIC
181 177 SIC
182 178 SIC
183 179 SIC
184 180 SIC
185 181 SIC
186 182 SIC
187 183 SIC
188 184 SIC
189 185 SIC
190 186 SIC
191 187 SIC
192 188 SIC
193 189 SIC
194 190 SIC
195 191 SIC
196 192 SIC
197 193 SIC
198 194 SIC
199 195 SIC
200 196 SIC
201 197 SIC
202 198 SIC
203 199 SIC
204 200 SIC
205 201 SIC
206 202 SIC
207 203 SIC

```

7 C FORMAT (121)
8 FORMAT (7A10)
9 FORMAT (12.0X.6E10.0)
10 FORMAT (1M.30X.7A10/)
11 FORMAT(//.10X.05.20M OUTPUT FORMAT, WITH.010.//.10X.40M.TARGET RANGE SIC
12 1GE (L) -----.1PE10.3.0 METERS.5A.34MDEVICE POWER SIC
13 2 (PD) -----.E10.3.0 WATTS/.10X.40M.FOCAL DISTANCE (FL) SIC
14 3 -----.E10.3.0 METERS.5A.34M. POWER OUT OF THE TELESCO SIC
15 4PE (PT) ---.1PE10.3.0 WATTS.//)
16 12 FORMAT (//.10X.05.20M OUTPUT FORMAT, WITH.010.//.10X.40M.DESIRED I SIC
17 INTENSITY (DI) -----.1PE9.2.0 WATTS/M.3M.22X.34MDEVICE SIC
18 2 POWER (PO) -----.E10.3.0 WATTS.//.10X.40M.FOCAL DISTANCE SIC
19 3E (FL) -----.0PF4.0.0 METERS.6A.34M. POWER OUT OF TM SIC
20 4E TELESCOPE (PT) ---.1PE10.3.0 WATTS.//)
21 13 FORMAT (10A.40M.GROUND LEVEL (GL) -----.0PF5.0.0 SIC
22 1 METERS.6A.34M.WAVELENGTH (LAMBDA) -----.1PE9.2.0 METERS SIC
23 2.//10A.40M DEVICE ALTITUDE (HIGH) -----.E9.2.0 METERS. SIC
24 35A. INPUT JITTER (HIGH FREQUENCY) ---.1PE9.2.//.50M.1PE9.2.0 FE SIC
25 4E10.21A. * (LOW FREQUENCY) ---.1PE9.2.//.10X.40M.TARGET ALTITUDE SIC
26 5DE (MIN) -----.E9.2.0 METERS.6A.34M.HACKING RATE (CM SIC
27 6GE (A) -----.0PF5.2.0 RADIAN/SEC.//.53A.1PE9.2.0 FEET.6A SIC
28 8 OPTICS RADIUS (RO) -----.0PF6.2.0 METERS//.10X.0.VEHETICA SIC
29 7L ANGLE (PM) -----.0PF7.3 SIC
30 8 * RADIANS. NA. (ASCURATION RADIUS (RI) -----.0.F6.2. SIC
31 9 METERS.//)
32 14 FORMAT (10A.0 AZIMUTH ANGLE (CM) -----.0.F7.3. SIC
33 2. RADIANS.6A.0.FEAM TYPE (PHYS) -----.0. A10.//.10X. SIC
34 3. PLAZIFON VELOCITY (VP) -----.0.F7.0.0M (METERS/SEC.5A. SIC
35 4. TYPE OF PROPAGATION (BEAM) -----.0. A10.//.10X.0.SPECIFIED CROSS SIC
36 5. WIND (VARI) -----.0.F6.2.19A.0. BEAM QUALITY (M) -----.0. SIC
37 6.6B.15A.0.F6.2.//.10X.0.SEVERITY OF TURBULENCE (MTR) -----.0. SIC
38 61P.//.10X.0. NUMBER OF BEAMPATH INCREMENTS -----.0.F4.2.//) SIC
39 7. RELATIVE HUMIDITY (RH) -----.0.F5.3.5A.0.02 * 0. SIC
40 15 FORMAT (10A.0. RESULTANT BEAM QUALITY.5A.0M) * 0.0.F5.3.5A.0.02 * 0. SIC
41 1F5.3) SIC
42 END SIC

```

SUBROUTINE OPTRAIN
C
C OPTRAIN CALCULATES THE POWER LOSSES, BEAM QUALITY DEGRADATIONS, AND
C JITTER INDUCED BY THE OPTICAL TRAIN EXTERNAL TO THE DEVICE.
C
S REAL IOPS, LC, LMIR, LBE, LEA, LI, MI, MZ
REAL LM, MAG
C
C COMMON /OPTIN/ OPA, PI, WL, EPSI, OVAL, DT, RI, TMI, DIOVI, CL1, DELTA, RREF
C 1, LC, OC, N, REFL, SFAS, ITYPE, LMIR, MAG, DIR, ITYPE, LEA, BE, TA, ASAS, ITYPEA
C 2, TFM, TMB, TMA, TMS, DT, DELT, C, ITYP
C COMMON /OPTOUT/ DE, P, MI, MZ, TH
C
C DIMENSION M(2), M(2), MEA(2), MAM(2)
C
C DATA M4/MON-AA, / SMOFF-ASIS/
C DATA M4/MCOOLED, / SMOCCOOL/
C DATA M4/MPI-074, / MOPEN/
C DATA M4/M7-FOCUSED, / SMOFOCUS/
C DATA M4/M /
C
C OREQDA
C ZP=0.0
C QREQ=1.0
C RI=1.E70
C WRITE (6,19) OPA, PI, WL, EPSI, OVAL, DT, RI, TMI, DIOVI
C WRITE (6,20) DLI, MAM(ITYP), DELTA, RREF, LC, OC, N, REFL, SFAS, MI, ITYPE
C AM
C WRITE (6,21) LMP, MAG, DIR, M(ITYPE), MEA(ITYPE), LEA, BETA, DELT, ASAS
C WRITE (6,22) TMR, TMS, TMA
C PRINT BEAM CALCULATIONS
C IOPS=4.*PI*DIOVI/(10.*BdJDDI*DBI)
C SIPS,
C IF (OVAL.GT.1.0) SIPSQTI=-LOG(11.-EPI-4.*J340/OVAL/OVAL)**.992808
C I21)
C
C AEPDOP/MIC MI*DD4
C SASE1=4522E-5*DBI*DELTA/RREF/ML
C IF (ITYPE.EQ.1) SASE=0.0
C
C BEAM CLIPPER
C FMSCH3=OMI/(4.*WL*LC)
C A=3.14/50MIFM)
C OAO=O4I/11.-A)
C DBISE=MI*(EPSI-A)
C IF (OPI.LT.0.) DBIN=0.
C C=1.0
C DBI=DO
C IF (DBI.LE.OCI) GO TO 1
C C=OC/OAO**2
C D=1*CC
C CONTINUE
C
C RELAY MICRONS
C TMA=SMICSI04
C MADD=FI*0.04

```

2 OPT
3 OPT
4 OPT
5 OPT
6 OPT
7 OPT
8 OPT
9 OPT
10 OPT
11 OPT
12 TCP
13 OPT
14 OPT
15 TCP
16 OPT
17 OPT
18 OPT
19 OPT
20 TCP
21 OPT
22 OPT
23 OPT
24 OPT
25 OPT
26 OPT
27 OPT
28 OPT
29 OPT
30 OPT
31 OPT
32 OPT
33 OPT
34 OPT
35 OPT
36 OPT
37 OPT
38 OPT
39 TCP
40 OPT
41 OPT
42 TCP
43 OPT
44 OPT
45 OPT
46 OPT
47 OPT
48 OPT
49 OPT
50 OPT
51 OPT
52 OPT
53 OPT
54 OPT
55 OPT


```

64      SPAP=6.2A31900.546E-6*WAB/WL
        GO TO (2.3), ITYPE
      C
      C      COOLED MIRRORS
      C      COM=5.E-14*6.2A319/WL
      C      SMCON=(1.0-REFL)*IRMS
      C      FINV=0.0
      C      GO TO 4
65
      C      UNCOOLED MIRRORS
      C      AMO=2.205E6
      C      CP=0.02
      C      CONO=0.0138E2
      C      ALFA=3.E-6
      C      TMS=10
      C      F1=1.E70
      C      IF (REFL.LT.1.0) F=7070*TK X(1-DI)*SORT(CP*AMO*CONO/DI)/(2.2*CP)*
      C      ALFA*(1.-REFL)
      C      S41=4.03.14159*(1.0-REFL)*ALFA*DI*IRMS/(WL*CP*AMO)
      C      FINV=1.0/F
      C      S45=SPAP*(S4P**2)*((M-1)*SMI*SMI/MAG/MAG)**2
      C      S45=SMI*(S45Q)
      C      LM=2.
      C      IF (S45Q.GT.0.) LM=DLIM*SMI*SMI/MAG/MAG
      C      A=1.0
      C      P=LMIR
      C      C=FITV
      C      D=LM*FINV*1.0
      C      DC 5 X*2*N
      C      A=ALMIR*0
      C      B=PLMIR*0
      C      C=C*FINV*A
      C      D=O*FINV*B
      C      CO=TIME
      C      P2=(A*B/M)/(C*D/M)
      C
      C      REAM EXPANDER
      C      R2=420*P2
      C      DO=DI/M/MAG
      C      OI=DI/M/MAG
      C      C=DI**2-D*DI**2
      C      GO TO (4.10), ITYPE
      C
      C      ON=DI*IS
      C      IF (OI.ME.DI) GO TO 6
      C      IF (OI.ME.OI) GO TO 7
      C      TIME=(O**2-D*DI**2)/C
      C      EXD=DI/O
      C      EXM=MAG*O
      C      GO TO 12
      C      TME=(O**2-DI**2)/C
      C      E=DI/O
      C      O=MAG*O
      C      GO TO 12
      C      IF (OI.ME.OI) GO TO 9
      C      TME=1.0
      C      EXM=M/O

```

```

115 09=MAG*DH1
      GO TO 12
      YAE=(DH1**2-01**2)/C
      EXD1/041
      DH=MAG*DH1
      GO TO 12

120 C OFF-AXIS
      C IF (DH1.LE.00) GO TO 11
      C THE=(CO/DH1)**2
      EXD=14/20
      DH=MAG*00
      GO TO 12
      YAE=1.0
      EXD=14/041
      DH=MAG*DH1

125 C COMPUTE QUALITY LOSS DUE TO CENTRAL OBSCURATION
      C SAE=0.0
      C LME=0.0
      C IF (E.LF.0) GO TO 13
      A=.6541114891-.1884071484*E-.632167832*E*E-2-.34243636*E*E*E
      B=.27342657-3.115550116*E-36.78787879*E*E-26.75986676*E*E*E
      SEESURT(A*4-.433111257)
      LPE=(A*B*E-.196218053)/(158E*5HE)

130 C EXIT APPERTYPE
      C SST=SORI(ASAM)
      C GO TO (14,15), ITYPE

135 C SOLID WINDOW
      C TEA=EXP(-METAPLEA)*(1.0-ASAM)
      C SEAE=E-12*DT*PETA*LEA*IRMS*6.28319/ML
      C TME=0.
      C GO TO 14
      C OPEY PORT
      C TEA=1.0-ASAM
      C SEAE=0.5
      C TME=2.14E-7*(11LEA**3)*(DELTA**6)/(ML*09*08)**.2)
      C CONTINUE

140 C COMPUTE TOTAL DISTORTION
      C SDE=.3312*S1**2+SAM**2+SMS*SMC**2+SEAE**2+SST**2
      C SFS=RT(SO)
      C LTR=(1.4*Z1d*DLI*((H-1)*SHI)*SHI/MAG/MAG)**2)+LSE*SMC*SMC*DLI*SEAE
      C X SEAY/50
      C A=EXP(1-SO)
      C H=1.2/(L1*LT)
      C P1X=.85*50*A*(1.-A)*(1.-EXP(-2./A))
      C P2X=.87*65*50*A*(1.-A)*(1.-EXP(-6./A))
      C XZ=.
      C Y=Z1/42
      C TIEAP(-2./A)
      C T2=1.-T1
      C T3=EXP(-6./A)
      C T=2.1-T3
      C T5=(-2.*T1+76.A*0T3+T2)/(X*X*Y+0T4+0T6)

```

OPT 113 OPT 114 OPT 115 OPT 116 OPT 117 OPT 118 OPT 119 OPT 120 OPT 121 OPT 122 OPT 123 OPT 124 OPT 125 OPT 126 OPT 127 OPT 128 OPT 129 OPT 130 OPT 131 OPT 132 OPT 133 OPT 134 OPT 135 OPT 136 OPT 137 OPT 138 OPT 139 OPT 140 OPT 141 OPT 142 OPT 143 OPT 144 OPT 145 TCP 14 TCP 146 OPT 147 OPT 148 OPT 149 TCP 15 TCP 16 OPT 150 OPT 151 OPT 152 OPT 153 OPT 154 TCP 17 TCP 18 OPT 156 OPT 157 OPT 158 OPT 159 OPT 160 OPT 161 OPT 162 OPT 163 OPT 164 OPT 165 OPT 166

```

167 OPT
168 OPT
169 OPT
170 OPT
171 OPT
172 OPT
173 OPT
174 OPT
175 OPT
176 OPT
177 OPT
179 OPT
180 OPT
181 OPT
182 OPT
183 OPT
184 OPT
185 OPT
186 OPT
187 OPT
188 OPT
189 OPT
190 OPT
191 OPT
192 OPT
193 OPT
194 OPT
195 OPT
196 OPT
197 OPT
198 OPT
199 OPT
200 OPT
201 TCP
202 OPT
203 OPT
204 OPT
205 OPT
206 OPT
207 OPT
208 OPT
209 OPT
210 OPT
211 OPT
212 OPT
213 OPT
214 OPT
215 OPT
216 OPT
217 OPT
218 OPT
219 OPT
220 OPT

T6=(T2/T4-Y)/T5
X=X-T6
IF (ABS(T6).GT.1.E-5) GO TO 17
M2=SQRT(X)
M1=P1/T2

TRANSMISSION
T=TC*TM*TB*TEA
P=T*PI

JITTER
TH=SQRT((THTR**2+THSV**2+THBS**2+THE**2+(THI**2+THAA**2)/(MAG**2)))
WRITE (6,23)
WRITE (6,24)
WRITE (6,25) ALK,ONE,SI,ZR,BLK,ONE,SAW,ZR,BLK,TC,ZR,ZR,HH(ITYPEM),
1TH,SH,LN,HH(ITYPER),TRE,SBE,LBE,HEA(ITYPEA),TEA,SEA,DLI,BLK,T,S,LT
WR=1.*(J+1+159*DB*DB/(4.*WL*R2))**2
WR=SQRT(WR)
XM2=M2
M2=WR*M2
WRITE (6,26) DB,P,M1,XM2,WR,M2
WRITE (6,27) TH,R2
RETURN

FORMAT(10X,30(IH*).*INPUT TO OPTICAL TRAIN*,30(1H*))
FORMAT(20X,*LASER BEAM DIAMETER * , G12.4,* METERS*/
1 20X,*LASER POWER * , OP612.4,* WATTS * /
2 20X,*WAVELENGTH * , E12.4,* METERS*/
3 20X,*OBSCURATION * , OP612.4,* * /
4 20X,*BEAM QUALITY * , G12.4,* * /
5 20X,*PULSE LENGTH * , G12.4,* SECONDS * /
6 20X,*PHASE FRONT CURVATURE * , G12.4,* METERS*/
7 20X,*JITTER * , OP612.4,* RADIANS * /
8 20X,*INTENSITY FLUCTUATIONS * , G12.4,* PEAK-TO-PEAK* * /
FORMAT(20X,*SCALE SIZE OF FLUCTUATIONS * , G12.4,* L/W * /
X 20X,*TYPE OF AEROWINDOW * , A9/ * /
1 20X,*AEROWINDOW DELTA RHO/RHO * , G12.4,* * /
2 20X,*RHO/RHO REF * , G12.4,* * /
3 20X,*DISTANCE TO CLIPPER * , G12.4,* METERS*/
4 20X,*CLIPPER DIAMETER * , G12.4,* METERS*/
5 20X,*NUMBER OF MIRRORS * , I2,* * /
6 20X,*REFLECTIVITY * , OP612.4,* * /
7 20X,*FARRICTION ERROR * , G12.4,* VIS. LAMBDA*/
8 20X,*TYPE OF MIRRORS * , A8) * /
FORMAT(20X,*DISTANCE BETWEEN MIRRORS * , G12.4,* METERS*/
1 20X,*TELESCOPE MAGNIFICATION * , OP612.4,* * /
3 20X,*TELESCOPE DIAMETER * , G12.4,* METERS*/
4 20X,*TELESCOPE TYPE * , AB,* * /
2 20X,*TYPE OF EXIT APERTURE * , AB,* * /
5 20X,*EXIT APERTURE LENGTH * , G12.4,* METERS * /
6 20X,*ABSORPTION COEFFICIENT * , OP612.4,* METERS-1 * /
X 20X,*TEMPERATURE FLUCTUATION * , G12.4,* DEG K * /
7 20X,*STIPUT AREA/ BEAM AREA * , G12.4,* * /
FORMAT(20X,*TRACKER JITTER * , G12.4,* RADIANS * /
1 20X,*SCRE-SIGHT JITTER * , G12.4,* RADIANS * /
2 20X,*SERVO JITTER * , G12.4,* RADIANS * /
3 20X,*STYLOJITTER JITTER * , G12.4,* RADIANS * /

```

```

230 23  FORMAT(1H1,10X,30(1H*),OPTICAL TRAIN OUTPUT*,30(1H*))//
24 24  FORMAT(20X,SOURCE * ,8X,TRANSMISSION SIGMA * ) OPT
25 25  FORMAT(20X,INPUT BEAM * ,8X,TRANSMISSION SIGMA * ) OPT
1 20X,AERODYNAMIC WINDOW * ,8X,2X,FB,4,2X,2F8.4/ OPT
2 20X,BEAM CLIPPER * ,8X,2X,FB,4,2X,2F8.4/ OPT
3 20X,MIRRORS * ,8X,2X,FB,4,2X,2F8.4/ OPT
4 20X,BEAM EXPANDER * ,8X,2X,FB,4,2X,2F8.4/ OPT
5 20X,EXIT APERTURE * ,8X,2X,FB,4,2X,2F8.4/ OPT
6 20X,TOTALS * ,8X,2X,FB,4,2X,2F8.4/ OPT
26 26  FORMAT(20X,TRANSMITTED BEAM DIAMETER*,FR,4,* METERS*/ OPT
1 20X,TRANSMITTED POWER*,G12.4,* WATTS*/ OPT
2 20X,BEAM QUALITY BEFORE ACCOUNTING FOR DIVERGENCE*/ OPT
3 31X,M1 =*,FB,4,4X,M2 =*,FR,4/ OPT
4 20X,EFFECT OF BEAM DIVERGENCE ON WAIST*,G12.4/ OPT
X 20X,FINAL BEAM SPREAD PARAMETER, M2*,G12.4) OPT
27 27  FORMAT(20X,TOTAL BEAM JITTER*,G12.4,* RADIANS*/ OPT
X 20X,PHASE FRONT CURVATURE*, G12.4,* METERS*,//) OPT
231 231  OPT
232 232  OPT
233 233  OPT
234 234  OPT
235 235  OPT
236 236  OPT
237 237  OPT
238 238  OPT

```

```

SUBROUTINE ATM
  C
  C ATM SETS UP THE VARIABLES FOR THE FOUR MAIN PROPAGATION SUBROUTINE
  C IT CALCULATES THE INITIAL STEP OF ALL TYPES OF PROPAGATION AND
  C REFINES THE ESTIMATES FOR THE REVERSE CALCULATIONS UNTIL THEY ARE
  C WITHIN THE SPECIFIED RANGE.
  C
  LOGICAL CPHI,EQUAL,EHR,PRINT
  INTEGER TYPED(4),TYPEE(4)
  INTEGER REAR,DEHUG,FINAL,OUT,PO,PROP,TYPE,WTHR
  REAL I,IBD,IOLD,KAS,KOL,KIP,L,LAMDA,LT2,LT2SO,MSO,NBAR,NU
  REAL KI,IP,M2,M1

  COMMON /ERROR/ ERR
  COMMON /ATM/ M,OI,PROP,SIGLF,SIGNF,WTHR,M1,M2
  COMMON /MESH/ XPKAS,ZPREV,XN,AREA
  COMMON /ALFDTA/ DUMMY(4),PLINE(3),ABL,ARE,SCL,SCE
  COMMON /ATMS/ REAR,FL,GL,HTM,IBD,L,LAMDA,NSTEP,PHI
  COMMON /IN/ COEFP,MOM,PI
  COMMON /IRS/ DEHUG,I,TYPE,OUT,PT,R0
  COMMON /INT/ PD
  COMMON /SAIM/ COEF1,COEF2,COEF3,COSPHI,EQUA,,FINAL,FIVE3,FIVE9,62,
103,G4,G5,HIF,I,IFLAG,KAS,KIP,LT2,LT2SO,MSO,VSML,PI,PO,PRINT,R0SO,R
210,SIGASO,SIGHSO,SIGMAT,SIGSO,HOLD
  COMMON /ALFA/ LAM,RH
  COMMON /CNRW/ IW
  COMMON /X/ CHI,OMEGA,VP,VPSC,VXB

  EXTERNAL ALFAEX,CNSU
  NAMELIST /USPEC/ PLINE,ABL,ABE,SCL,SCE

  DATA PI/3.14159/
  DATA TYPED/SHAHOVE,SHBELOW,SHABOVE,SHBELOW/
  DATA TYPEE/SHAHOVE,SHRELOW,SHBELOW,SHABOVE/

  SELECT LAMS
  LAM=1
  PLINE(1)=-.338
  PLINE(2)=-.32
  PLINE(3)=-.342
  ABL=ABE=SCL=SCE=0.
  IF (LAMDA.GT.0.) GO TO 2
  READ (5,USPEC)
  IF (ABL.NE.0.) LAM=4
  LAMDA=AMS(LAMDA)
  TEMP=1./((PLINE(1)+PLINE(2)+PLINE(3)))
  DO I III=1,3
  PLINE(III)=PLINE(III)+TEMP
  WRITE (6,44) PLINE(1),PLINE(2),PLINE(3),ABL,ABE,SCL,SCE
  IF (LAM.EQ.4) GO TO 3
  IF (LAMDA.EQ.3.HE-6) LAM=2
  IF (LAMDA.EQ.5E-6) LAM=3
  COLLIMATED OR FOCUSED BEAM
  (FOCUSED)
  G4=0.
  G5=1.

```

```

59 ATM
60 ATM
61 ATM
62 ATM
63 ATM
64 ATM
65 ATM
66 ATM
67 ATM
68 ATM
69 ATM
70 ATM
71 ATM
72 ATM
73 ATM
74 ATM
75 ATM
76 ATM
77 ATM
78 ATM
79 ATM
80 ATM
81 ATM
82 ATM
83 ATM
84 ATM
85 ATM
86 ATM
87 ATM
88 ATM
89 ATM
90 ATM
91 ATM
92 ATM
93 ATM
94 ATM
95 ATM
96 ATM
97 ATM
98 ATM
99 ATM
100 ATM
101 ATM
102 ATM
103 ATM
104 ATM
105 ATM
106 ATM
107 ATM
108 ATM
109 ATM
110 ATM
111 ATM
112 ATM
113 ATM
114 ATM
115 ATM

IF (REAR.EQ.1) GO TO 4
(COLLIMATED)
G5=0.
G4=1.

SET CONSTANTS AND VARIABLES
G3=1.-.R65*H1
COFF2=PT/PI
COEF3=.R65*H1*PT
EKPKAS=1.
FINAL=2
FIVE3=5./3.
FIVE9=5./9.
HOM=HOM+GL
HTM=HTM+GL
IFLAG=1
IW=WT*H*2
KAS=0.
KOUNT=0
LCOUNT=0
M=M2
MSQ=M*4
OIM=1.05*O1
OIL=.95*O1
PO=1
R0SQ=R0*R0
R1G=R0*10.
SIGSO=SIGLF**2+SIGMF**2
ZPHEV=0.
SIGMAH=0.3183*M2*LAMDA/(R0**2.)
SIGMAR=SIGMAR+SIGMAR
SIGMA=SQRT(SIGRSO+SIGSO)
SIGASU=SIGMA*SIGMA
SIGMAT=0.
Z=0.
IF (ITYPE.NE.5) GO TO 5

CALCULATE L FOR REVERSE PROPAGATION--O1 AND PT KNOWN
FL=L
IF (L.GY.0.) GO TO 5
NU=.865*PT*M1-PI*G4*R0SQ*O1
L=SQRT(NU/(4.*PI*O1*SIGASO))
IF (DEHUG.EQ.2) WRITE (6,33) NU*L
IF (L.LT.R10) L=100.
FL=L

CALCULATE PHI OR HTM
CPHI=.FALSE.
IF (PHI.LT.0.) GO TO 6
COSPHI=COS(PHI)
HTM=HOM*L*COSPHI
GO TO 7
CPHI=.TRUE.
HD=HTM-HCM
HDP=ABS(HD)
NKD=1
IF (HDP.NE.HD) NKD=-1

```

```

115 IF (L.LT.HDP) MD=L*NMND
    COSPHI=MD/L
    PHI=ACOS(COSPHI)
    VPSG=VP*((SIN(PHI)*SIN(CHI))**2+COSPHI**2)
120 IF (DENUMG.EQ.2) WRITE (6,J6) MOM,HTM,PHI
    HTF=3.281*HTM
    LI2=L*2.
    LI2SO=LI2*LI2
125 IF (MOM.GT.1.E5.AND.HTM.GT.1.E5) NSTEP=1
    NSM1=NSTEP-1
    C
    C
    GAUSSIAN OR PLANE WAVE
    G2=6.54
    IF (PROP.EQ.2) G2=3.58
    IF (PROP.EQ.3) G2=5.9
    IF (OUT.EQ.2) WRITE (6,49)
    C
    C
    DECIDE WHICH TYPE OF CALCULATIONS TO DO
    IF (MOM.LT.1.E5) GO TO 9
    IF (HTM.LT.1.E5) GO TO 8
    TYPE=1
    GO TO 11
    8 TYPE=3
    GO TO 11
    9 IF (HTM.LT.1.E5) GO TO 10
    TYPE=4
    GO TO 11
    10 TYPE=2
    11 WRITE (6,35) TYPED(TYPE),TYPEE(TYPE)
    C
    C
    PROPAGATION OR REVERSE PROPAGATION
    IF (ITYPE.NE.5) GO TO 12
    C
    C
    REVERSE PROPAGATION--OI AND PT KNOWN
    FINAL=1
    150 REGULAR PROPAGATION
    C
    C
    COMPUTE STARTING VALUES OF AREA AND INTENSITY
    AREA=PI*R0SQ
    I=PT/AREA
    IP=2.312*I
    155 EXPKAS=I.
    KAS=0.
    SIGMAT=0.
    PRINT=.FALSE.
    160 IF (OUT.EQ.2.AND.(FINAL.EQ.2.OR.DERUG.EQ.2)) PRINT=.TRUE.
    IF (PRINT) WRITE (6,36) Z,MOM,SIGMAT,SIGTST,EXPKAS,AREA,I,IP
    C
    GO TO (13,14,15,16), TYPE
    165 CALL AA (MOM)
    GO TO 4A
    14 CALL HM (MOM)
    GO TO 4B
    15 CALL AH (MOM)
    GO TO 4B
    170 CALL MA (MOM)
    171

```

```

175      C      IF (ERR) RETURN
176      C      IF (XN.LT.1.E-8) RETURN
177      C      IF (TYPE.EQ.1) RETURN
178      C      IF (ITYPE.EQ.5) GO TO 22
179
180      C      COMPUTE AND PRINT DISPLACEMENT, ECCENTRICITY AND ISO-INTENSITY
181      C      CONTOUR DATA.
182      AF=.70710678*ROLD
183      PTOTAL=PT*XP/KAS*(1.-G3)
184      ETA=ROLD/MO
185      ANOM=3.1415926*AF*AF/KIP
186      ECC=0.3*0.7*KIP
187      DISP=(1.-0.692)*SORT(0.478864-2.6666667*ALOG(KIP))
188      DISP=AF*(ETA*(-.29))*DISP
189      IF (PD.EQ. 0.) WRITE (6,49)
190      WRITE (6,42) DISP,ECC
191      GAMMA=1.0
192      DGAM=0.1
193      DO 17 KGAM=1,9
194      GAM=ASGAMMA-DGAM
195      AREA=(1.-ANOM)*ALOG(GAMMA)
196      POWER=PTOTAL*(1.-GAMMA)
197      AVGI=POWER/AREA
198      WRITE (6,43) GAMMA,AREA,POWER,AVGI
199      CONTINUE
200
201      BREAKDOWN POWER AND OPTIMUM POWER CALCULATIONS
202
203      IF (PD.NE. 0.)WRITE (6,49)
204      PRD = PRD + PT * KIP / (2.312 * I)
205      PRINT 45, PRD,PD
206      PMAK=PT*5.54/XN
207      XI=1.205/(XN*KIP)
208      IF (PMAK.LE.PRD) GO TO 18
209      PMAK=PRD
210      XI=IMD
211      PRINT 32, XI,PMAK
212
213      EFFECT OF POWER VARIATIONS
214
215      DP=PT*0.1
216      DN=AN*0.1
217      PP=0.
218      YN=0.
219      PTOT=I/(KIP*PT)
220      DO 20 III=1,20
221      PP=PP+DP
222      IF (PP.GT.PRD) GO TO 21
223      YN=YN+DN
224      ZZ=KI*(HEAM,YN)
225      ZN=I*ZZ*YI/(XN*KIP)
226      ZAXX=ZN*2.312
227      FACTOR=ZI/ZXXX
228      IF ((FACTOR.LT.1).AND.(FACTOR.GT.0.1)) GO TO 19

```



```

230 PUSE=0.
    AUSE=0.
    GO TO 20
19 PUSE=PI*OTOPP*(1.-FACTOR)
    AUSE=-0.5*AREA*ALOG(FACTOR)/ZZ
20 PRINT 46, PP,ZN,PUSE,AUSE
21 PRINT 47, OI
    RETURN
C REFINEMENT LOOP FOR ITYPE 5
C
22 LCOUNT=LCOUNT+1
    IF (LCOUNT.GT.20) GO TO 31
    IF (FINAL.EQ.2) RETURN
C SELECTION OF NEXT FOCAL LENGTH
C
23 XK=0.7
    RATE=1/OI
    IF (RAT.LT.0.45.OR.RAT.GT.2.22) GO TO 26
    IF (RAT.LT.0.62.OR.RAT.GT.1.6) GO TO 25
    IF (RAT.LT.0.8.OR.RAT.GT.1.25) GO TO 24
    IF (RAT.LT.0.91.OR.RAT.GT.1.1) GO TO 23
    XK=1.0
    GO TO 26
23 XK=0.95
    GO TO 26
24 XK=0.9
    GO TO 26
25 XK=0.8
    FL=FL*XK*SORT(RAT)
    IF (FL.GE.R10) GO TO 27
    KOUNT=KOUNT+1
    IF (KOUNT.GT.2) GO TO 30
    FL=100.
    L=FL
    LT2=L*2
    LT250=LT2*LT2
C RECALCULATE PHI OR MTM
C
26 IF (CPHI) GO TO 28
    MTM=HGM*L*COSPHI
    HTM=HTM*GL
    GO TO 29
28 MD=MTM-HGM
    MDP=MD*(MD)
    MHD=1
    IF (MHP.NE.MD) MHD=-1
    IF (L.LT.MDP) MD=L*MHD
    COSPHI=MD/L
    PHI=ACOS(COSPHI)
    IF (DEHUG.EQ.2) WRITE (6,37) FL,MTM,PHI
    IF (L.LT.OIL.OR.I.GI.OIH) GO TO 12
    WRITE (6,38) L
    FINAL=2
    GO TO 12
C RANGE TOO SMALL
C
29

```

```

30 WRITE (6,39)
   ERR=.TRUE.
   RETURN
C
C
31 TOO MANY TIMES THROUGH THE LOOP
   WRITE (5,40) LCOUNT,FL,I,OI
   ERR=.TRUE.
   RETURN
C
C
32 FORMAT (30X,'MAXIMUM INTENSITY ON TARGET =',1PE10.2,10X,'ACHIEVED
   1 AT TELESCOPE POWER =',E10.2,'/',56X,'POWER RANGE AVAILABLE',/,/,
   2 '110.
   3TS)='70',*(WATTS/M**2),770,'(WATTS)',7110,6H(M**2))
   FORMAT (//10X,'FOR ITYPE 5. NU =',1PE12.5,'. L =',E12.5)
   FORMAT (//10X,6HMM =',E12.5,8H, MFM =',E12.5,8H, PHF =',E12.5)
   FORMAT (//10X,24HCALCULATIONS FOR ORIGIN AS,19H 100 KM AND TARGET
   1 AS,8M 100 KM.)
   FORMAT (//7X,'DISTANCE',8X,'HEIGHT',7X,'SIGNAL-LT',6X,'SIGNAL-ST',
   18X,'EAPKAS', 10X,'AREA',8X,'INTENSITY',8X,'IPEAK',/,'8X,'METERS',
   2,9X,'METERS',8X,'RADIANS',8X,'RADIAN',23X,' METERS',3M**2,5X,
   3 'WATTS',/,'3M**2, 5X,'WATTS/M**2',/,'1X,1PHE15.4)
   FCPMAT (//10X,13HREFINED FL =',E12.5,8H, HTX =',E12.5,8H, PHF =',E
   112.5)
   FCPMAT (10X,19H'TARGET RANGE (L) --',1PE10.3,7H METERS/)
   FORMAT (//10X,23H'REFINED RANGE TOO SMALL)
   FCPMAT (//10X,11TYPE 5 HAS NOT CONVERGED AFTER,13,
   11M I
   1TERATIONS/10X,5HFL =',E12.5,6H, I =',E12.5,7H, OI =',E12.5)
   FCPMAT(10X,5H'DISPLACEMENT =',F6.3,' METERS',10X,'ECCENTRICITY =',
   1,F6.3,'/',37X,'I/IPEAK',10X, 'AREA',8X,'CUMULATIVE',7X, 'AVERAG
   1E',/,'37X, 'CONTOUR',7X,'(METER',4M**2),7X, 'POWER',9X,'INTENSIT
   2Y',/)
   FCPMAT (35X,F6.1,4X,1P3E15.3)
   FCPMAT(10X,5H'PLINE (1) =',1PE10.2,3X,'PLINE (2) =',E10.2,3X,
   1'PLINE (3) =',E10.2,'/',10X,'ARL =',E10.2,99,'PBE =',E10.2,5X,
   2'SCL =',E10.2,9X,'SCE =',E10.2,/)
   FCPMAT(//30X,4H'BREAKDOWN INTENSITY
   1ED AT TELESCOPE POWER =',E10.2)
   FCPMAT (110,1PE10.3,140,E10.3,170,E10.3,110,C,E10.3)
   FCPMAT (/,10X, 'USEFUL INTENSITY =',1PE10.3,'WATTS/M**2)
   FCPMAT (1M)
   END

```

2	AA	SUBROUTINE AA (HOM)
3	AA	
4	AA	
5	AA	
6	AA	
7	AA	
8	AA	
9	AA	
10	AA	CALCULATIONS FOR ORIGIN AND TARGET ABOVE 100 KM
11	AA	LOGICAL EQUAL=EMP.PRINT
12	AA	INTEGER PEAN=DEHUG.FINAL.OUT.PO
13	AA	REAL I=IRD.KAS.KIP.L.LAMDA.LT2.LI250.MSO
14	AA	
15	AA	COMMON /MESH/ XTRA(3).AREA
16	AA	COMMON /EPORR/ ERR
17	AA	COMMON /ATMS/ BEAM.FL.GL.MTM.IRD.L.LAMDA.NSTEP.PMI
18	AA	COMMON /INS/ DEHUG.ITYPE.OUT.PI.PO
19	AA	COMMON /SAFM/ COEF1.COE2.COE3.CUSPMI.EQUAL.FINAL.FIVE3.FIVE9.G2.
20	AA	IC3.G4.G5.MTF.I.IFLAG.KAS.KIP.LT2.LI250.MSO.NSM1.PI.PO.PRINT.H650.R
21	AA	210.SIG450.SIG450.SIGHAT.SIG50.HOLD
22	AA	
23	AA	220.SIG450.SIG450.SIGHAT.SIG50.HOLD
24	AA	
25	AA	CALCULATE RADIUS. AREA. AND INTENSITY
26	AA	RSO=L1250*SIG450
27	AA	RSORT(RSO)
28	AA	AREA=PI*RSO
29	AA	I=COEF3/AREA
30	AA	IF (FINAL.NE.2.AND.DERUG.EQ.1) RETURN
31	AA	
32	AA	WRITE RESULTS
33	AA	ROLD=8
34	AA	IF (OUT.EQ.1) GO TO 1
35	AA	WRITE (6,2) L.HOW,I.AREA,R
36	AA	RETURN
37	AA	
38	AA	WRITE (6,3) MTM,MTF,L,R.AREA,I
39	AA	RETURN
40	AA	
41	AA	FORMAT (10X,12HTARGET ABOVE 100 KM/1X,1P2E15.4,5X,2M0.8X,3E15.4,5X,10M).AA
42	AA	1000E-0C//)
43	AA	FORMAT (/10X,23HTARGET ALTITUDE (MTM) =.1PE10.3,9M METERS (.E16.3 AA
	AA	1,6M FEET)/10X,42HTARGET RANGE (L)
	AA	2M METERS,12X,29RADIUS WITHOUT BLOOMING (R) =.CP7.2,7M METERS/10X AA
	AA	3,4ZAREA WITHOUT BLOOMING (AREA)
	AA	4,2,8A,29HTARGET PLANE INTENSITY (I) =.E11.4,11M WATTS/M**2//)
	AA	END

```

SUBROUTINE AB (NOM)
C
C
C
CALCULATIONS FOR ORIGIN ABOVE 100 KM AND TARGET BELOW 100 KM
REAL I,L,L1,L2
REAL IP
LOGICAL PRINT
COMMON /ATM5/ HEAV,FL,GL,HTM,IPD,L,LAND,NSTEP,PHI
COMMON /INS/ DEHUG,ITYPE,OUT,PI,R0
COMMON /SATM/ COEF1,COEF2,COEF3,COSPHI,EQUAL,FINAL,FIVE3,FIVE9,G2,
IG3,G4,G5,HTF,I,IFLAG,KAS,KIP,L12,L250,MSO,NSMI,PI,PO,PRINT,R050,R
210,SIGASO,SIGBSO,SIGMAT,SIGSO,HOLD
COMMON /MESM/ EXPKES,L1,NI,AREA
L1=(IES-HOM)/COSPHI
L2=L-L1
C
C
C
ABOVE 100 KM
C
C
C
R0=R050
IF (HEAV.EQ.1) R0=(R0*L2/L)**2
R0=R0*4.*L1*L1*SIGASO
R=SQRT(R0)
AREA=PI*R*H50
L1=(IES-H0)/COSPHI
L2=L-L1
C
C
C
ABOVE 100 KM
R0=R050
IF (HEAV.EQ.1) R0=(R0*L2/L)**2
R0=R0*4.*L1*L1*SIGASO
R=SQRT(R0)
AREA=PI*R*H50
IP=1+2.*R12
IF (PRINT) WRITE (6,1) L1,AREA,I,IP
HOLD1=FL
HOLD2=R050
HOLD3=L
FL=L2
R050=R50
C
C
C
CALL BR (1.E5)
FL=HOLD1
R050=HOLD2
L=HOLD3
RETURN
C
C
C
FORMAT (4I,0,PAROVE 100 KM,/,1X,1PE15.4,5X,0.1,0000E-05,0.5X,0.0,0.13X
100.0,13X,0.1,0000E-09,3E15.4,/)
END

```

```

SUBROUTINE 9A (HQM)
C
C
C
5     COMMON /AY/ SIGST
COMMON /MESM/ EXPKAS,ZOPEV,MI,AREA
INTEGER DEBUG,FINAL,OUT
REAL I,KIP,L,LT2,L1,L2
REAL IP
10    COMMON /AIMS/ BEAR,FL,GM,MTM,SD,C,L,LANDA,NSSTEP,PHI
COMMON /IMS/ OFBIG,STY,OUT,PT,P0
COMMON /SAT/ COEF1,COEF2,COEF3,COSPHI,EQUAL,FINAL,FIVE3,FIVE9,62,
13    103,C4,C5,MI,IP,FL,CO,ES,KIP,LT2,LT2SC,MSD,MS1,PI,PO,PRINT,ROSCOR
14    210,SIGASD,SIGAS,SIGMAT,SIGSO,ROLD
15    LI=(1E5-HQM)/COSPHI
16    LP=L-LI
17    C
18    C
19    C
20    BELOW 100 KM
21    C
22    C
23    C
24    HOLD1=L
25    HOLD2=MTM
26    L=LI
27    MTM=1.ES
28    WRITE (5,3)
29    C
30    CALL 9B (HQM)
31    L=HOLD1
32    C
33    C
34    C
35    ABOVE 100 KM
36    C
37    C
38    C
39    RELTSSORT(SIGASD-SIGTSD)
40    AREA=PI*OR
41    HLEP=AREA/KIP
42    I=COEF3*EXPKAS*KIP/AREA
43    IF (FINAL.EQ.2.AND.DEBUG.EQ.1) RETURN
44    IP=12.312
45    WRITE (5,4)
46    IF (OUT.EQ.1) GO TO 1
47    WRITE (10,2) L,MTM,SIGMAT,SIGST,EXPKAS,DLAREA,I,IP
48    RETURN
49    C
50    C
51    C
52    C
53    C
54    C
55    C
56    C
57    C
58    C
59    C
60    C
61    C
62    C
63    C
64    C
65    C
66    C
67    C
68    C
69    C
70    C
71    C
72    C
73    C
74    C
75    C
76    C
77    C
78    C
79    C
80    C
81    C
82    C
83    C
84    C
85    C
86    C
87    C
88    C
89    C
90    C
91    C
92    C
93    C
94    C
95    C
96    C
97    C
98    C
99    C
100   C
101   C
102   C
103   C
104   C
105   C
106   C
107   C
108   C
109   C
110   C
111   C
112   C
113   C
114   C
115   C
116   C
117   C
118   C
119   C
120   C
121   C
122   C
123   C
124   C
125   C
126   C
127   C
128   C
129   C
130   C
131   C
132   C
133   C
134   C
135   C
136   C
137   C
138   C
139   C
140   C
141   C
142   C
143   C
144   C
145   C
146   C
147   C
148   C
149   C
150   C
151   C
152   C
153   C
154   C
155   C
156   C
157   C
158   C
159   C
160   C
161   C
162   C
163   C
164   C
165   C
166   C
167   C
168   C
169   C
170   C
171   C
172   C
173   C
174   C
175   C
176   C
177   C
178   C
179   C
180   C
181   C
182   C
183   C
184   C
185   C
186   C
187   C
188   C
189   C
190   C
191   C
192   C
193   C
194   C
195   C
196   C
197   C
198   C
199   C
200   C
201   C
202   C
203   C
204   C
205   C
206   C
207   C
208   C
209   C
210   C
211   C
212   C
213   C
214   C
215   C
216   C
217   C
218   C
219   C
220   C
221   C
222   C
223   C
224   C
225   C
226   C
227   C
228   C
229   C
230   C
231   C
232   C
233   C
234   C
235   C
236   C
237   C
238   C
239   C
240   C
241   C
242   C
243   C
244   C
245   C
246   C
247   C
248   C
249   C
250   C
251   C
252   C
253   C
254   C
255   C
256   C
257   C
258   C
259   C
260   C
261   C
262   C
263   C
264   C
265   C
266   C
267   C
268   C
269   C
270   C
271   C
272   C
273   C
274   C
275   C
276   C
277   C
278   C
279   C
280   C
281   C
282   C
283   C
284   C
285   C
286   C
287   C
288   C
289   C
290   C
291   C
292   C
293   C
294   C
295   C
296   C
297   C
298   C
299   C
300   C
301   C
302   C
303   C
304   C
305   C
306   C
307   C
308   C
309   C
310   C
311   C
312   C
313   C
314   C
315   C
316   C
317   C
318   C
319   C
320   C
321   C
322   C
323   C
324   C
325   C
326   C
327   C
328   C
329   C
330   C
331   C
332   C
333   C
334   C
335   C
336   C
337   C
338   C
339   C
340   C
341   C
342   C
343   C
344   C
345   C
346   C
347   C
348   C
349   C
350   C
351   C
352   C
353   C
354   C
355   C
356   C
357   C
358   C
359   C
360   C
361   C
362   C
363   C
364   C
365   C
366   C
367   C
368   C
369   C
370   C
371   C
372   C
373   C
374   C
375   C
376   C
377   C
378   C
379   C
380   C
381   C
382   C
383   C
384   C
385   C
386   C
387   C
388   C
389   C
390   C
391   C
392   C
393   C
394   C
395   C
396   C
397   C
398   C
399   C
400   C
401   C
402   C
403   C
404   C
405   C
406   C
407   C
408   C
409   C
410   C
411   C
412   C
413   C
414   C
415   C
416   C
417   C
418   C
419   C
420   C
421   C
422   C
423   C
424   C
425   C
426   C
427   C
428   C
429   C
430   C
431   C
432   C
433   C
434   C
435   C
436   C
437   C
438   C
439   C
440   C
441   C
442   C
443   C
444   C
445   C
446   C
447   C
448   C
449   C
450   C
451   C
452   C
453   C
454   C
455   C
456   C
457   C
458   C
459   C
460   C
461   C
462   C
463   C
464   C
465   C
466   C
467   C
468   C
469   C
470   C
471   C
472   C
473   C
474   C
475   C
476   C
477   C
478   C
479   C
480   C
481   C
482   C
483   C
484   C
485   C
486   C
487   C
488   C
489   C
490   C
491   C
492   C
493   C
494   C
495   C
496   C
497   C
498   C
499   C
500   C
501   C
502   C
503   C
504   C
505   C
506   C
507   C
508   C
509   C
510   C
511   C
512   C
513   C
514   C
515   C
516   C
517   C
518   C
519   C
520   C
521   C
522   C
523   C
524   C
525   C
526   C
527   C
528   C
529   C
530   C
531   C
532   C
533   C
534   C
535   C
536   C
537   C
538   C
539   C
540   C
541   C
542   C
543   C
544   C
545   C
546   C
547   C
548   C
549   C
550   C
551   C
552   C
553   C
554   C
555   C
556   C
557   C
558   C
559   C
560   C
561   C
562   C
563   C
564   C
565   C
566   C
567   C
568   C
569   C
570   C
571   C
572   C
573   C
574   C
575   C
576   C
577   C
578   C
579   C
580   C
581   C
582   C
583   C
584   C
585   C
586   C
587   C
588   C
589   C
590   C
591   C
592   C
593   C
594   C
595   C
596   C
597   C
598   C
599   C
600   C
601   C
602   C
603   C
604   C
605   C
606   C
607   C
608   C
609   C
610   C
611   C
612   C
613   C
614   C
615   C
616   C
617   C
618   C
619   C
620   C
621   C
622   C
623   C
624   C
625   C
626   C
627   C
628   C
629   C
630   C
631   C
632   C
633   C
634   C
635   C
636   C
637   C
638   C
639   C
640   C
641   C
642   C
643   C
644   C
645   C
646   C
647   C
648   C
649   C
650   C
651   C
652   C
653   C
654   C
655   C
656   C
657   C
658   C
659   C
660   C
661   C
662   C
663   C
664   C
665   C
666   C
667   C
668   C
669   C
670   C
671   C
672   C
673   C
674   C
675   C
676   C
677   C
678   C
679   C
680   C
681   C
682   C
683   C
684   C
685   C
686   C
687   C
688   C
689   C
690   C
691   C
692   C
693   C
694   C
695   C
696   C
697   C
698   C
699   C
700   C
701   C
702   C
703   C
704   C
705   C
706   C
707   C
708   C
709   C
710   C
711   C
712   C
713   C
714   C
715   C
716   C
717   C
718   C
719   C
720   C
721   C
722   C
723   C
724   C
725   C
726   C
727   C
728   C
729   C
730   C
731   C
732   C
733   C
734   C
735   C
736   C
737   C
738   C
739   C
740   C
741   C
742   C
743   C
744   C
745   C
746   C
747   C
748   C
749   C
750   C
751   C
752   C
753   C
754   C
755   C
756   C
757   C
758   C
759   C
760   C
761   C
762   C
763   C
764   C
765   C
766   C
767   C
768   C
769   C
770   C
771   C
772   C
773   C
774   C
775   C
776   C
777   C
778   C
779   C
780   C
781   C
782   C
783   C
784   C
785   C
786   C
787   C
788   C
789   C
790   C
791   C
792   C
793   C
794   C
795   C
796   C
797   C
798   C
799   C
800   C
801   C
802   C
803   C
804   C
805   C
806   C
807   C
808   C
809   C
810   C
811   C
812   C
813   C
814   C
815   C
816   C
817   C
818   C
819   C
820   C
821   C
822   C
823   C
824   C
825   C
826   C
827   C
828   C
829   C
830   C
831   C
832   C
833   C
834   C
835   C
836   C
837   C
838   C
839   C
840   C
841   C
842   C
843   C
844   C
845   C
846   C
847   C
848   C
849   C
850   C
851   C
852   C
853   C
854   C
855   C
856   C
857   C
858   C
859   C
860   C
861   C
862   C
863   C
864   C
865   C
866   C
867   C
868   C
869   C
870   C
871   C
872   C
873   C
874   C
875   C
876   C
877   C
878   C
879   C
880   C
881   C
882   C
883   C
884   C
885   C
886   C
887   C
888   C
889   C
890   C
891   C
892   C
893   C
894   C
895   C
896   C
897   C
898   C
899   C
900   C
901   C
902   C
903   C
904   C
905   C
906   C
907   C
908   C
909   C
910   C
911   C
912   C
913   C
914   C
915   C
916   C
917   C
918   C
919   C
920   C
921   C
922   C
923   C
924   C
925   C
926   C
927   C
928   C
929   C
930   C
931   C
932   C
933   C
934   C
935   C
936   C
937   C
938   C
939   C
940   C
941   C
942   C
943   C
944   C
945   C
946   C
947   C
948   C
949   C
950   C
951   C
952   C
953   C
954   C
955   C
956   C
957   C
958   C
959   C
960   C
961   C
962   C
963   C
964   C
965   C
966   C
967   C
968   C
969   C
970   C
971   C
972   C
973   C
974   C
975   C
976   C
977   C
978   C
979   C
980   C
981   C
982   C
983   C
984   C
985   C
986   C
987   C
988   C
989   C
990   C
991   C
992   C
993   C
994   C
995   C
996   C
997   C
998   C
999   C
1000  C

```

```

40 RADIANSE./10X*LINEAR EFFECTS ON TRANSMISSION (EXPAS) ** BA
50PF6.3.19X*PADIHS MIT-OUT BLOWING (R) ** F7.3. BA
50 METERSE./104. **NON-LINEAR EFFECTS BA
60 JON TRANSMISSION (KIP) **F6.3.19X* AVERAGE INTENSITY (I) BA
60 **1PE11.4.0 WATTS/10X*2/10X*AREA WITHOUT BLOWING (AREA) BA
5 **E10.3.0 METERSE./3M*2.5X*PEAK INTENSITY (IP) BA
6 **E11.4.0 WATTS/10X*2/10X*AREA WITH BLOWING (BLAREA) BA
7 **E10.3.0 METERSE./3M*2.0/ BA

```

END

59
60
61
62
63
64
65
66
67

```

SUBROUTINE 88 (MOM)
C
C CALCULATIONS FOR ORIGIN AND TARGET BELOW 100 KM
C
S LOGICAL CNV-GEOMED,UNIFRM
LOGICAL EQUAL,ERR,LESS,PRINT
C
C INTERP HEAD,DEG,FINAL,OUT,PO,ST
REAL I,IMU,KAS,NI,KIP,L,LAMDA,LT2,LT250,MSO,N,NAJ,NI,IP,M1,M2,M
C
C COMMON /MESM/ FAP,KAS,ZPHEV,NI,AREA
COMMON /EMOM/ EPM
COMMON /ATMS/ HEAD,FL,GL,MTM,IMD,L,LAMDA,NSICP,PME
COMMON /IMS/ DEMO,TYPE,OUT,PI,EO
COMMON /SMT/ COEF1,COEF2,COEF3,COSPHI,EQUAL,FINAL,FIVES,FIVE9,62,
1G,64,95,MTF,I,IFLAG,KAS,KIP,LT2,LT250,MSO,MSI,M1,PI,PC,PRINT,ROSO,R
210,SIGASO,SIGAS,SIGMA1,SIGSO,HOLD
COMMON /ATM1/ M,NI,PROP,SIGL,SIGM,F,MTM,M1,M2
COMMON /AT/ SIGST
C
C LOGICAL OK
C
C DIMENSION UG10(15), OG10(15)
C DIMENSION SVS10(50)
C
C DATA UG10/.699533,.4325317,.3397068,.2166777,.07443717/
DATA OG10/.9333567,.07472567,.1095432,.1346334,.16773717/
DELTAZ=L/NSSTEP
C
C COMPARE STARTING Z WITH R0=10
C DO I=1,NSM1
KJJK
Z=DELTAZ*IK
IF (Z.GE.P10) GO TO 2
CONTINUE
WRITE (K,22) Z,R10
ERR=.TRUE.
RETURN
C
C LESS=.FALSE.
C IF (INT(LT.MOM) LESS=.TRUE.
Y50.
R=OINT=0.
OK=.TRUE.
CALL ALFSET (NLAN,LAM)
DZ=DELTAZ*O.I
DMS=DZCOSPHI
MMS=O9-DMOJ.5
TEMP2=1./FLOAT(NSSTEP)
TEMPAS6.695/LAMDA*O.O.4
TEMP7=1.439*(LAMDA/6.20319)*O.1.2
C
C LINEAR LOOP
C
C DO M=JK,J+NSTEP
NAJ=FLOAT(NSSTEP-J)*TEMP2
TEMP1=NAJ*O.5*TEMP

```

```

59 Z=DELTAZ*J
60 Z1=DELTAZ*(J-1)
61 IF (LESS) GO TO 3
62
63 SHOOTING UP
64 MLZ1=COSPHI*HOM
65 MUZ1=COSPHI*HOM
66 POS=MJ
67 GO TO 4
68
69 SHOOTING DOWN
70 MLZ=COSPHI*HOM
71 MUZ=COSPHI*HOM
72 POS=ML
73
74
75
76
77
78
79
80
81
82
83
84
85
86
87
88
89
90
91
92
93
94
95
96
97
98
99
100
101
102
103
104
105
106
107
108
109
110
111
112
113
114
115

```

TURBULENCE CALCULATIONS

```

ZJL=Z/L
CG10A=0.5*(ML*HJ)-GL
CG10B=ML*HJ
DO 5 I=CG10A,1.5
TEMP3=CG10B*(CG10A)
CG10C=TEMP3*CG10A
TEMP3=TEMP3*TEMP3
TEMP4=CG10A*(CG10B)*DELTAZ
TEMP4=CG10B*(CG10A)*DELTAZ
TEMP5=CG10C*(CG10A)*DELTAZ
TEMP5=CG10C*(CG10A)*DELTAZ
YAT=TEMP4*(TEMP1-TEMP3)+TEMP5*(TEMP1-TEMP3)+TEMP5*(TEMP1-TEMP3)
R=GT1*(1.7*YAT)**.5
FAC1=0.3*(TEMP4*HJ)/(H0*H0)**.5
SIGTU=TEMP4*YAT*.2
SVT50(J)=SIGTU*(FAC*FAC)**.2
SIGT51=SVT50*(SVT50(J))**.5
IF (MINV) SIGT51=SVT50*(SIGT50)

```

RC=AS(FL-Z)/FL
RC=SEM*COM*DOSS
Z65=0*(Z*H*E)**.2
P55=M1*(AL*NC5)*G5*RC50*Z65*(SIG550-SIGT50+SIG50)
P55=Z65
DO 6 JJ=1,10
W=AS(MJ)
EAPKAS=ALFKAS*(Z*H*H*OY)
COEF=COEF*(1.0-93*ZJL)
I=COEF*EAPKAS/MSO
I=Z7.312*I
IF (IP.LI.100) GO TO 7

```

105 I GREATER THAN I BREAKDOWN: WRITE AND RETURN
106 WRITE (4,23) Z,IPQ
107 E=AS*THUE.
108 RETURN
109
110 APEL=PI*MSO
111
112 WRITE OUTPUT
113
114
115

```



```

115      IF (PRINT) WRITE (6,24) Z,H0,SIGMAT,SIGTST,EXPKAS,AREA,I,IP
      CONTINUE
      ROLD=R
      FINDID=1./DELTAZ
120      START COMPUTATION OF BLOOMING LOSSES
      ENDED=.FALSE.
      CNVRGD=.FALSE.
      HOM=HOM
      SIGMAT=SQRT(SIGTSQ)
      CALL ALFSET (NLAM,LAM)
      TEMP3=(SIGHF+SIGHF)**2+4.*SIG8SQ
      TEMP4=GA*ROSO
      TEMP5=OS*WOSO
      UNIFORM=.FALSE.
      RSR=TEMP4+TEMP5+TEMP3*ZPREV**2
135      CALCULATIONS FOR Z = R * 10
      DZ=R*10
      HDZ=DZ*0.5
      TFDZ=DZ*0.9+16666666667
      DZFL=DZ/FL
      TEMP1=DZ*COSPHI
      DZSQ=DZ*0Z
      TEMP6=G3*0Z/L
      GPREV=GALTIM(HOM)*ALFFAC(0.,HOM,OK)/(VX(GL,H0,HOM,PHI,0.),RSQ)
      Z=DZ
      L=HOM*TEMP1
      G3TRM=1.-TEMP6
      RC=1.-DZFL
      RSO=TEMP4+TEMP5*PC**2+(TEMP3+SVSTSO(KJ))*(Z-ZPREV)**2
      GCURR=GALTIM(H)*ALFFAC(DZ,H,OK)*G3TRM/(VX(GL,H,HOM,PHI,Z)*RSQ)
      XCURR=DZSQ*(-0.5*GPREV-(GPREV-GCURR)*0.0416665666667)/SQRT(RSQ)
      NI=XCURR
      G=(GCURR*GPREV)*HDZ
      GUESS=GCURR+GCURR-GPREV
155      CALCULATIONS FOR NEXT INTERVAL
      Z=Z+DZ
      IF (Z.GE.L) GO TO 16
      H=H*TEMP1
      G3TRM=G3TRM-TEMP6
      RC=RC-DZFL
      TGINO=Z*FINDID+1.
      INDO=TGINO
      IF (INDO.GE.NSTEP) INDO=NSTEP-1
      SVSTSO=SVSTSO(INDO)
      SVSTSO=SVSTSO+(TGINO-FLOAT(INDO))*(SVSTSO(INDO+1)-SVSTSO)
      RSO=TEMP4+TEMP5*PC**2+(TEMP3+SIGTSQ)*(Z+ZPREV)**2
      GNEW=GALTIM(H)*ALFFAC(DZ,H,OK)*G3TRM/(VX(GL,H,HOM,PHI,Z)*RSQ)
      IF (ABS(GNEW)-1.1.E-4) GO TO 12
      OK=.FALSE.
170
172

```

CHECK ACCURACY OF LINEAR EXTRAPOLATION

DEVIAT=ABS((GNEW-GUESS)/GUESS)
 IF (DEVIAT.GT.0.05) GO TO 15
 OK=.TRUE.

RSOHLD=RSU
 G=G*GNEW*OZ
 XPREV=XCURR

XCURR=DZ*((HOZ*GNEW-G)-(GCURR-GNEW)*TFDZ)/SORT(RSQ)
 NI=NI+XCURR

IF (EMDEN) GO TO 17
 IF (DEVIAT.LT.0.01) GO TO 12

GPREV=GNEW
 GCURR=GNEW

GUESS=GCURR+GCURR-GPREV
 UNIFRM=.TRUE.
 GO TO 9

IF (CNVAGD) GO TO 11

INCREASE SIZE OF INTERVAL

CONTINUE

HOZ=DZ

DZ=DZ*OZ

UNIFRM=.FALSE.

IF ((Z*OZ).GE.L) GO TO 14

TFDZ=TFDZ+TFDZ

OZFL=OZFL*OZFL

TEMP1=TEMP1+TEMP1

TEMP6=TEMP6+TEMP6

GCURR=GNEW

GUESS=GCURR+GCURR-GPREV

GO TO 9

FINAL INTERVAL

CNVAGD=.TRUE.

FRACT=(L-Z)/OZ

IF (FRACT.LT.5.E-4) GO TO 17

DZ=(L-Z)*0.5

HOZ=DZ*0.5

TFDZ=DZ*0.0416666666667

OZFL=OZFL*FRACT

TEMP1=TEMP1*FRACT

TEMP6=TEMP6*FRACT

GUESS=(GNEW-GCURR)*FRACT+GNEW

GPREV=GNEW+GNEW-GUESS

GCURR=GNEW

GO TO 9

TRY EXPONENTIAL EXTRAPOLATION

DEVIAT=ABS(GCURR**2/(GPREV*GNEW)-1.)

IF (DEVIAT.LT.0.05) GO TO 19

IF (OZ.LT.0.01) GO TO 19

CNVAGD=.FALSE.

EMDEN=.FALSE.

BB 173
 BB 174
 BB 175
 BB 176
 BB 177
 BB 178
 BB 179
 BB 180
 BB 181
 BB 182
 BB 183
 BB 184
 BB 185
 BB 186
 BB 187
 BB 188
 BB 189
 BB 190
 BB 191
 BB 192
 BB 193
 BB 194
 BB 195
 BB 196
 BB 197
 BB 198
 BB 199
 BB 200
 BB 201
 BB 202
 BB 203
 BB 204
 BB 205
 BB 206
 BB 207
 BB 208
 BB 209
 BB 210
 BB 211
 BB 212
 BB 213
 BB 214
 BB 215
 BB 216
 BB 217
 BB 218
 BB 219
 BB 220
 BB 221
 BB 222
 BB 223
 BB 224
 BB 225
 BB 226
 BB 227
 BB 228
 BB 229

```

230          C          C          C
231          C          C          C
232          C          C          C
233          C          C          C
234          C          C          C
235          C          C          C
236          C          C          C
237          C          C          C
238          C          C          C
239          C          C          C
240          C          C          C
241          C          C          C
242          C          C          C
243          C          C          C
244          C          C          C
245          C          C          C
246          C          C          C
247          C          C          C
248          C          C          C
249          C          C          C
250          C          C          C
251          C          C          C
252          C          C          C
253          C          C          C
254          C          C          C
255          C          C          C
256          C          C          C
257          C          C          C
258          C          C          C
259          C          C          C
260          C          C          C
261          C          C          C
262          C          C          C
263          C          C          C
264          C          C          C
265          C          C          C
266          C          C          C
267          C          C          C
268          C          C          C
269          C          C          C
270          C          C          C
271          C          C          C
272          C          C          C
273          C          C          C
274          C          C          C
275          C          C          C
276          C          C          C
277          C          C          C
278          C          C          C
279          C          C          C
280          C          C          C
281          C          C          C
282          C          C          C
283          C          C          C
284          C          C          C
285          C          C          C
286          C          C          C

INTERVAL MUST BE REDUCED
M=H-TEMP1
GTRM=GTRM+TEMP6
RC=RC+DZFL
Z=Z-DZ
DZ=HDZ
HDZ=HDZ*0.5
TFDZ=HDZ*0.0416666666667
DZFL=DZFL*0.5
TEMP1=TEMP1*0.5
TEMP6=TEMP6*0.5
GPREV=(GCURR+GPREV)*0.5
GUESS=GCURR+GCURR-GPREV
GO TO 9

FRAC=(L-Z+DZ)/DZ
IF (FRAC.LT.1.E-3) GO TO 17
IF (ABS(FRAC-1.) .LE. 1.E-3) GO TO 10
UNIFRM=.FALSE.
DZ=L-Z+DZ
HDZ=HDZ*0.5
TFDZ=HDZ*0.0416666666667
DZFL=DZFL*FRAC
TEMP1=TEMP1*FRAC
TEMP6=TEMP6*FRAC
GUESS=(GCURR-GPREV)*FRAC+GCURR
GPREV=GCOMP+GCURR-GUESS
FMODE=.TRUE.
CNVPGD=.TRUE.
Z=L
GO TO 10
IF (UNIFRM) NI=NI*0.5*XCURR-(XCURR-XPREV)*0.041666666667
NI=R2*COEF2*ARS(NI)
NI=NI*(17.6+5.44E-13/LAMDA**2)/(17.6+5.84E-13/1.1236E-10)
SIGT50=SIGMAT**2

CALCULATION OF INTENSITY WITH BLOOMING
KIP=KI*REAM,ABS(NI)
I=I+KIP
IP=2.312*I
HOLD50=HOLD*ROLD
BLAREA=PI*HOLD50/KIP
IF (FINAL.NE.2.AND.DERUG.EQ.1) RETURN
IF (OUT.EQ.1) GO TO 18
WRITE (A,25) NI,KIP,ALAREA,I,IP
RETURN

WRITE (6,26) HIM,HTF,SIGMAT,L,SIGTST,EXPXAS,R,KIP,I,AREA,IP,BLAREA
RETURN
UNIFRM=.FALSE.
OK=.TRUE.
GOLD=G/SORT(RSQHLD)
RSQ=LC/RSQ
G=G*(GNEW-GCURR)*DZ/ALOG(GNEW/GCURR)
TEMP=G/SORT(RSQ)

```

```

290      XPREV=XCURR
      XCURR=D7*(GOLD-TEMP)/ALOG(TEMP/GOLD)
      NI=NI+XCURR
      IF (ENDED) GO TO 17
      IF (DEVIAT.LT.0.01) GO TO 21
      GPREV=GCURR
      GCURR=GNEW
      GUESS=GCURR+GCURR-GPREV
      GO TO 9
295      IF (CNVRGD) GO TO 20
      GO TO 13
      C
      C
      C
300      FORMAT (59H THE LENGTH OF THE BEAM PATH IS LESS THAN 10 TIMES R0,
      IZ = 1PE10.3,7H R10 = E10.3)
      FORMAT (/10X*INTENSITY HAS REACHED BREAKDOWN, Z(J) = *,1PE10.3,* 18 89
      10 = *,E10.3)
      C
      C
305      FORMAT (1X,1PRE15.4)
      FORMAT (//,* NI = *,1PE12.5,8X,*KIP = *,E12.5,8X,*SLAREA = *,
      IE12.5,8X,*IAVL = *,E12.5,8X,*IPEAK = *,E12.5,/)
      C
310      FORMAT (//,10X,*TARGET ALTITUDE (HTM) =*,1PE10.3,* METERS (*,
      IE10.3,* FEET)*,10X,*LONG-TERM TURBULENCE (SIGMAT) =*,E10.3,
      2* RADIANS*,/,10X,*TARGET RANGE (L)
      3E9.2,* METERS*,10X,*SHORT-TERM TURBULENCE (SIGST) =*, E10.3,
      4* RADIANS*,/,10X,*LINEAR EFFECTS ON TRANSMISSION (EXPKAS) =*, 88
      50PF6.3,19X,*RADIUS WITHOUT BLOOMING (R) =*, F7.3,
      5* METERS*,/,10X,
      3 ON TRANSMISSION (KIP) =*,F6.3,19X,*AVERAGE INTENSITY (I)
      4 =*,1PE11.4,* WATTS/*,3H*2/10X,*AREA WITHOUT BLOOMING (AREA)
      5 =*,E10.3,* METERS*,3H*2,5X,*PEAK INTENSITY (IP)
      6 =*,E11.4,* WATTS/*,3H*2/10X,*AREA WITH BLOOMING (BLAREA)
      7 =*,E10.3,* METERS*,3H*2,/)
      END

```

```

89      287
88      288
88      289
88      290
88      291
88      292
88      293
88      294
88      295
88      296
88      297
88      298
88      299
88      300
88      301
88      302
88      303
88      304
88      305
88      306
88      307
88      308
88      309
88      310
88      311
88      312
88      313
88      314
88      315
88      316
88      317
88      318
88      319
88      320

```

```

5      C      SUBROUTINE ALFSET (NL,IL)
        C      POWER RATIOS FOR MULTILINE PROPAGATION
        C      COMMON /ALFDIA/ P(3),RHOFAC,PLINE(3)
        C      COMMON /ALFA/ LAM,RH
        C      IF (LAM.EQ.2) GO TO 1
        C      P(1)=1.
        C      RETURN
10     DO 2 I=1,3
        C      P(I)=PLINE(I)
        C      IF (RM.EQ.0.) PH=1.E-6
        C      RHOFAC=0.9446*RH-1.
        C      RETURN
15     END
        SET 2
        SET 3
        SET 4
        SET 5
        SET 6
        SET 7
        SET 8
        SET 9
        SET 10
        SET 11
        SET 12
        SET 13
        SET 14
        SET 15
        SET 16
        SET 17

```

```

5          C          FUNCTION ALFFAC (OZ,H,OK)
          C          MULTI-LINE POWER LOSSES
          C          LOGICAL OK
          C          COMMON /ALFDIA/ P(3),RMOFAC
          C          COMMON /ALFA/ LAM,RH
          C          DIMENSION POLD(3)
          C          IF (LAM.EQ.2) GO TO 3
          C          IF (OK) GO TO 1
          C          P(1)=POLD(1)
          C          GO TO 2
          C          POLD(1)=P(1)
          C          TEMP=P(1)*EXP(-ALFAEX(H)*OZ)
          C          P(1)=TEMP
          C          ALFFAC=ALFAAB(H)*TEMP
          C          RETURN
          C          IF (OK) GO TO 5
          C          DO 4 I=1,3
          C          P(I)=POLD(I)
          C          GO TO 7
          C          DO 6 I=1,3
          C          POLD(I)=P(I)
          C          ASSIGN 17 TO J1
          C          ASSIGN 20 TO J2
          C          ASSIGN 23 TO J3
          C          ASSIGN 12 TO J4
          C          SUM=0.
          C          IF (H.GT.13500.) GO TO 11
          C          IF (H.GT.9500.) GO TO 10
          C          IF (H.GT.5000.) GO TO 9
          C          ALFAS=3.6E-8*EXP(4.1056*RH-H*0.6333333333333E-3)
          C          GO TO 14
          C          ALFAS=9.3998E-6*EXP(4.1056*RH-H*1.031E-3)
          C          GO TO 16
          C          ALFAS=4.32E-10*EXP(4.1056*RH)
          C          GO TO 15
          C          CALCULATIONS FOR H GREATER THAN 13500 METERS
          C          XTRA=EXP(-ALFAEX(H)*OZ)
          C          GO TO J4(12,14)
          C          AS=ALFAAB(H)
          C          DO 13 I=1,3
          C          TEMP=P(I)*XTRA
          C          P(I)=TEMP
          C          SUM=SUM+TEMP*AS
          C          ALFFAC=SUM
          C          RETURN
          C          DO 15 I=1,3
          C          TEMP=P(I)*XTRA
          C          P(I)=TEMP
          C          SUM=SUM+TEMP
    
```

```

60          ALFFAC=SUM
          RETURN
          C
16  RMOSTR=1.0*RMOFAC*EXP(-H*(6.738E-5+9.61E-9*H))
    AS=RMOSTR*EXP(-10.047*H*(-6.38HE-4+H*2.25E-8))
    IF (H.GT. 8000) AS = EXP(-((RM*.9471)* 10.37917)+((4.6303E-4)-(RM
1*1.6251E-4))*H))
65  A#3 = AS
    AS3 = ALFAS
    TEMP=P(1)*EXP(-(AS+ALFAS)*DZ)
    P(1)=TEMP
          C
70  GO TO J1(17,1F)
    SUM=SUM+AS*TEMP
    GO TO 19
18  SUM=SUM+TEMP
19  AS=RMOSTR*EXP(-10.082*H*(-6.952E-4+H*1.55E-8))
    IF (H.GT. 8000) AS = EXP(-((RM*.9474)*12.6721)+((2.9317E-4)-(RM*
11.6251E-4))*H))
    A#4 = AS
    AS4 = ALFAS
    TEMP=P(2)*EXP(-(AS+ALFAS)*DZ)
    P(2)=TEMP
          C
80  GO TO J2(20,2I)
    SUM=SUM+AS*TEMP
    GO TO 22
21  SUM=SUM+TEMP
22  AS=EXP(-9.948*H*(-2.199E-4+H*1.96E-9))
    IF (H.GT. 8000) AS=EXP(-((RM*1.813)*4.8547)+((8.7225E-4)-(R
17E-4))*H))
    A#2 = AS
    AS2 = ALFAS
    TEMP=P(3)*EXP(-(AS+ALFAS)*DZ)
    P(3)=TEMP
          C
90  GO TO J3(23,24)
    ALFFAC=SUM+AS*TEMP
    RETURN
24  ALFFAC=SUM+TEMP
    RETURN
100  ENTRY ALFKAS
          C
    IF (LAM.EQ.2) GO TO 25
    TEMP=P(1)*EXP(-ALFAEX(H)*DZ)
    P(1)=TEMP
    ALFFAC=TEMP
    RETURN
105  ASSIGN 18 TO J1
    ASSIGN 21 TO J2
    ASSIGN 24 TO J3
    ASSIGN 14 TO J4
    GO TO 8
          C
110  FIN
59  FAC
60  FAC
61  FAC
62  FAC
63  FAC
32  TCP
33  TCP
34  TCP
35  TCP
64  FAC
65  FAC
66  FAC
67  FAC
68  FAC
69  FAC
70  FAC
71  FAC
36  TCP
37  TCP
38  TCP
39  TCP
72  FAC
73  FAC
74  FAC
75  FAC
76  FAC
77  FAC
78  FAC
79  FAC
40  TCP
41  TCP
42  TCP
43  TCP
60  FAC
81  FAC
82  FAC
83  FAC
84  FAC
85  FAC
86  FAC
87  FAC
88  FAC
90  FAC
91  FAC
92  FAC
93  FAC
94  FAC
95  FAC
96  FAC
97  FAC
98  FAC
99  FAC
100  FAC
101  FAC
102  FAC
103  FAC

```

C 5 FUNCTION ALFAAB (H)
 C SINGLE LINE ABSORPTION COEFFICIENTS IN 1/M
 COMMON /ALFA/ LAM,RH
 COMMON /ALFCO2/ DUM4Y(7),ARL,ARE
 MF=3.2R1*H
 CALL MEGAIR (MF,TR,PMP,MSF)
 P=0.359*PMP/0.4765025*MSF
 T=19*5.0/4.0
 PW=6.0724E-10*RH*P*EXP(0.05*6*P)
 GO TO (1.5*8+11), LAM
 C LAMDA IS 10.6
 C
 C
 C 1 IF (M.GT.16000.0) GO TO 3
 ALFCO2=7.94577416E-5-2.18262795E-9*M-3.57576007E-12*M*M+1.07366914
 1E-15*M**3-1.69645494E-19*M**4+1.50366450F-23*M**5-7.16578722E-28*M
 20 20*4+.61586924E-32*M**7-1.13662124E-37*M**8
 GO TO 4
 C
 C 2 IF (M.GT.55000.0) GO TO 3
 ALFCO2=7.67462668E-5-1.89713935E-7*M-1.98650379E-11*M*M-1.14976017
 1E-15*M**3+4.04716134E-20*M**4-R.90401506E-25*M**5+1.19826061E-29*M
 20 20*6-9.03345045E-35*M**7+2.92529072E-40*M**8
 GO TO 4
 C
 C 3 ALFCO2=1.0E-7*EXP(-1.74E-4*M+12.18)
 C
 C 4 ALFH20=4.32E-9*PW*(P+193.0*PW)
 ALFAAB=ALFCO2+ALFH20
 RETURN
 C LAMDA IS 3.6
 C
 C 5 ALFH20=5.4E-6*PW
 IF (P1.GE.0.2) ALFH20=-5.923E-7+8.3633E-6*PW+3.1184E-8*PW*PW
 C
 C 40 IF (M.GT.7500.0) GO TO 6
 ALFCO2=1.84E-6*EXP(-2.272E-4*M)
 GO TO 7
 C
 C 6 ALFCO2=4.25E-6*EXP(-3.36E-4*M)
 C
 C 7 ALFAAB=ALFH20+ALFCO2
 RETURN
 C LAMDA IS 5.0
 C
 C 8 IF (PW.GT.4.5E-4) GO TO 9
 AAA=1.9222
 BBB=1.4032
 GO TO 10
 AAA=1.14256
 BBB=4.6052
 C
 C 9 ALFAAB=(1.E-3)*EXP(AAA*ALOG(PW)+BBB)
 C
 C 10

60
C
C
C
11

RETURN
INSERT EQUATIONS FOR OTHER WAVELENGTHS HERE
ALFAAB=ABL*EXP(-ABE*H)
RETURN
END

AA8
AA9
AA2
AA4
AA4
AA4
AA4
AA4

59
60
61
62
63
64
65

```

2 AEX
3 AEX
4 AEX
5 AEX
6 AEX
7 AEX
8 AEX
9 AEX
10 AEX
11 AEX
12 AEX
13 AEX
14 AEX
15 AEX
16 AEX
17 AEX
18 AEX
19 AEX
20 AEX
21 AEX
22 AEX
23 AEX
24 AEX
25 AEX
26 AEX
27 AEX
28 AEX
29 AEX
30 AEX
31 AEX
32 AEX
33 AEX
34 AEX
35 AEX
36 AEX
37 AEX
38 AEX
39 AEX
40 AEX
41 AEX
42 AEX
43 AEX
44 AEX
45 AEX
46 AEX
47 AEX
48 AEX
49 AEX
50 AEX
51 AEX
52 AEX
53 AEX

FUNCTION ALFAEX (M)
THIS ROUTINE CALCULATES THE EXTINCTION COEFFICIENT IN 1/M
COMMON /ALFAEX/ DUMMY(17),ABL,ABE,SCL,SCE
GO TO (1+3*10), LAM
LAMDA IS 10.6
ALFAS0=1.0E-5*EXP(4.75*RM)
GO TO 4
LAMDA IS 3.8
ALFAS0=3.6E-6*EXP(4.1056*RM)
GO TO 4
INSERT EQUATIONS FOR OTHER WAVELENGTHS HERE
LAMDA IS 5.0
ALFAS0=3.E-6*EXP(4.2*RM)
THE REST OF THE FUNCTION IS INDEPENDENT OF LAMDA
IF (M.GT.1350.0) GO TO 7
IF (M.GT.9500.0) GO TO 6
IF (M.GT.5000.0) GO TO 5
ALFAS=ALFAS0*EXP(-M/1.2E+3)
GO TO 9
ALFAS=ALFAS0*2.586*EXP(-M*1.031E-3)
GO TO 9
ALFAS=ALFAS0*1.2E-4
GO TO 9
IF (M.GT.25000.0) GO TO 8
ALFAS=ALFAS0*(-3.251E-3+3.730E-7*M-9.6557E-12*M*M)
GO TO 9
ALFAS=ALFAS0*1.8E-3*EXP(-1.535E-6*(M-25000.))
ALFAS = ALFAS/9.7725
ALFAEX=ALFAS*ALFAEX(M)
RETURN
USER SPECIFIED COMPUTATION
ALFAEX=ABL*EXP(-ABE*M)+SCL*EXP(-SCE*M)
RETURN
END

```

2	CMP	
3	CMP	
4	CMP	
5	CMP	
6	CMP	
7	CMP	
8	CMP	
9	CMP	
10	CMP	
11	CMP	
12	CMP	
13	CMP	
14	CMP	
15	CMP	
16	CMP	
17	CMP	
18	CMP	
19	CMP	
20	CMP	
21	CMP	
22	CMP	
23	CMP	
24	CMP	
25	CMP	
26	CMP	
27	CMP	
28	CMP	
29	CMP	
30	CMP	
31	CMP	
32	CMP	
33	CMP	
34	CMP	
35	CMP	
36	CMP	
37	CMP	
38	CMP	
39	CMP	
40	CMP	
41	CMP	
42	CMP	
43	CMP	
44	CMP	
45	CMP	
46	CMP	
47	CMP	
48	CMP	
49	CMP	
50	CMP	
51	CMP	
52	CMP	
53	CMP	
54	CMP	
55	CMP	
56	CMP	
57	CMP	
58	CMP	

```

FUNCTION CNSO (M)
ATMOSPHERIC STRUCTURE CONSTANT IN M**2(2/3)
COMMON /CNWD/ IW
IF (M.GE.1.0) GO TO 4
SET CNSO FOR ALTITUDES LESS THAN 1 METER
GO TO (1,2,3), IW
BAD WEATHER CONDITIONS
CNSO=2.55E-13
RETURN
NOMINAL WEATHER CONDITIONS
CNSO=1.0E-13
RETURN
GOOD WEATHER CONDITIONS
CNSO=.5E-15
RETURN
CALCULATE CNSO FOR ALTITUDES AT OR ABOVE 1 METER
GO TO (5,9,10), IW
BAD WEATHER CONDITIONS
IF (M.GT.100.0) GO TO 7
IF (M.GT.10.0) GO TO 6
CNSO=2.9E-13*M**2(-0.6993)
RETURN
CNSO=.696E-13*M**(-1.216)
RETURN
IF (M.GT.1.0E4) GO TO 8
CNSO=2.55E-12*M**(-1.4386)
RETURN
IF (M.GT.1.5E4) GO TO 9
CNSO=2.0E-15
RETURN
NOMINAL WEATHER CONDITIONS
CNSO=2.0E-16
IF (M.LE.1000.0) OR (M.GE.12000.0) CNSO=1E-13*M**(-1.07535)
RETURN
GOOD WEATHER CONDITIONS
IF (M.GT.2.5E3) GO TO 12
IF (M.GT.20.0) GO TO 11
CNSO=.55E-15*M**(-0.6664)
RETURN
CNSO=1.51E-13*M**(-1.396)
    
```

A

FUNCTION CNSO 73/74 OPT=0 TRACE FTN 6.0.P357 03/05/75 18.12.15. PAGE 2

	59
	60
	61
	62
	63
	64

```

RETURN
IF 14.GY.1.5241 GO TO 4
CNSO=3.08-12
RETURN
END

```

69
C
12

5	C	REAL FUNCTION(I(REAL,X))	KI	2
	C	COMPUTES THE INTENSITY RATIO	KI	3
	C	IF (A.GT.0.1) GO TO 1	KI	4
		KI=1.0	KI	5
		RETURN	KI	6
	C	X2=AX	KI	7
10	I	IF (REAL.EQ.0) GO TO 5	KI	8
	C	FOCUSED BEAM	KI	9
	C	X32=X**1.5	KI	10
	C	X15=X**0.2	KI	11
15	C	IF (A.GT.1.0) GO TO 2	KI	12
	C	X1=X**0.164/X15**0.733*EXP(-X2)	KI	13
	C	RETURN	KI	14
20	C	IF (A.GT.2.0) GO TO 3	KI	15
	C	X1=X**0.176/X**0.793	KI	16
	C	RETURN	KI	17
25	C	IF (A.GT.100.0) GO TO 4	KI	18
	C	X3=X**0.7	KI	19
	C	X36=X**0.7	KI	20
	C	X12=1.57/X5*6.3/X32*2.42/X34-12.9/(X2*1)-1.71*ALOG(X)/X	KI	21
	C	RETURN	KI	22
30	C	X1=X**2-2.445*ALOG(X)+5.378	KI	23
	C	RETURN	KI	24
35	C	COLLIMATED BEAM	KI	25
	C	X4=X2*12	KI	26
	C	IF (A.GE.5.0) GO TO 6	KI	27
	C	X12=X**0.5	KI	28
	C	X13=X**0.1/3.1	KI	29
	C	X24=X**0.75	KI	30
40	C	X1=X-4.14E-4*X4-2.99E-5/X4+599*X13-0.384/X12+0.6/X34	KI	31
	C	RETURN	KI	32
45	C	X1=X**(-2.183*ALOG(X)+3.145)	KI	33
	C	RETURN	KI	34
	C	END	KI	35
	C		KI	36
	C		KI	37
	C		KI	38
	C		KI	39
	C		KI	40
	C		KI	41
	C		KI	42
	C		KI	43
	C		KI	44
	C		KI	45
	C		KI	46

```
FUNCTION GALTIN (M)
C
C ALTITUDE DEPENDENT PARAMETERS FOR THE BLOOMING CALCULATION--CHANGE
C IN REFRACTIVE INDEX FOR A GIVEN TEMPERATURE CHANGE DIVIDED BY THE
C REFRACTIVE INDEX * DENSITY AND SPECIFIC HEAT.
C
DIMENSION FAC(101)
DATA FAC/-.772409, -.753677, -.952073, -.912121, -.1043965, -.1044595, -.1.
101245, -.525778, -.525664, -.525664, -.1.044612, -.1.044612, -.1.044624, -.1.044624, -.1.044633,
20 3, -.1.044637, -.1.039937, -.1.034473, -.1.030055, -.1.025163, -.1.020354, -.1.01
4573, -.1.010434, -.1.006136, -.1.001845, -.997474, -.993049, -.988675, -.984306, -.979974,
5 62, -.975685, -.971435, -.967247, -.963048, -.958856, -.954656, -.950456, -.946256, -.942056,
15 7, R25A51, -.876666, -.865553, -.854541, -.843529, -.832517, -.821505, -.810493, -.799481,
82564, -.788428, -.777216, -.766004, -.754792, -.743580, -.732368, -.721156, -.709944,
93, -.698732, -.687520, -.676308, -.665096, -.653884, -.642672, -.631460, -.620248,
17 18 19 20 21 22 23 24 25 26 27 28 29 30 31 32 33 34 35 36
1.027424, -.1.044114, -.1.069470, -.1.093583, -.1.112527, -.1.135273, -.1.154,
5966, -.1.183577, -.1.209224, -.1.235951, -.1.263569, -.1.293569, -.1.263569, -.1.263569, -.1.263569,
3.243569, -.1.263569, -.1.263569, -.1.263569, -.1.263569, -.1.263569, -.1.263569, -.1.263569,
59 -1.263569, -.1.262521, -.1.221822, -.1.202361, -.1.135508, -.1.105236, -.1.1
3-7517, -.1.130327, -.1.113643, -.1.097463, -.1.081117

IF IMAGE=1.E5I GO TO 1
IM=01.E-3
DM=(M-FLOAT(IM))*1.E-3
I=I+1
IF (IM.LE.1) I=2
GALTIN=(FAC(IM)*(FAC(101))-FAC(IM)*DM)*1.E-9
RETURN
C
C GALTIN=FAC(101)*1.E-9
RETURN
C
END
```



```

115      G=50*(RO/(PO+H))**2
      RETURN
C
C
120      PERFORM CALCULATIONS FOR H GREATER THAN 30000 FEET.
C
C      SINCE MOLECULAR WEIGHT IS NO LONGER CONSTANT, MOLECULAR SCALE
C      TEMPERATURE IS NO LONGER EQUAL TO KINETIC TEMPERATURE.
C      THREE INDEX EQUATIONS ARE REQUIRED IN THE REGION ABOVE 30000 FEET
C      MAKE AN INDEX APPROXIMATION FOR VALUES OF H GREATER THAN 30000
C      FEET BUT LESS THAN 492126 FEET.
C
C      IF (H.GT.492126.) GO TO 7
C      I=.000257344*H*1.88
C      IF (I.GT.12) I=12
C      IF (H.GE.DELTAH(I)) GO TO 6
C      IF (H.GE.DELTAH(I-1)) I=I-1
C
C      ESTABLISH BASE VALUES OF TEMPERATURE, PRESSURE, AND GRADIENT.
C      H=DELTAH(I)
C      TH=DELTAH(I)
C      PR=DELTAH(I)
C      L=DELTAH(I)
C
C      CALCULATE MOLECULAR WEIGHTS FROM EMPIRICAL, GRAPHICALLY DERIVED,
C      EQUATIONS.
C      MW=COEFF1(I)-COEFF2(I)*H+COEFF3(I)*H*H
C      HP=HA/(1.+H/RO)
C
C      CALCULATE MOLECULAR SCALE TEMPERATURE AND CONVERT TO KINETIC
C      TEMPERATURE.
C      TH=((TH*L*(H-HB))**4)/MWO
C
C      PRESSURE (P), IN LB/FT**2.
C      X=RO*H*TB/L
C      Y=1./((X*(RO+H))-1./((X*(RO+H)))+(1./((X*X)))*4LOG(((H-HB)*TB/L)*(RO+H)
C      1)*LI/((RO+H)*TH))
C      B=(50*MWO*RO*RO)/(L*P)
C      P=EXP(PH-B*Y)
C      PMR=P*X*H
C
C      DENSITY
C      D=(M*P*GO)/(R*TH)
C
C      GRAVITATIONAL ACCELERATION
C      G=GO*(RO/(RO+H))**2
      RETURN
C
C      MAKE AN INDEX APPROXIMATION FOR VALUES OF H GREATER THAN 492126
C      FEET BUT LESS THAN 984252 FEET.
C
C      IF (H.GT.984252.) GO TO A
C      Z=(H-740000.)/50000.
C      I=17.5+.50*Z-.04348*Z*Z
C      IF (H.GE.DELTAH(I)) GO TO 6
C      IF (H.GE.DELTAH(I-1)) I=I-1
C      GO TO 6
C
170      MEG
171      MEG
172      MEG
116      MEG
117      MEG
118      MEG
119      MEG
120      MEG
121      MEG
122      MEG
123      MEG
124      MEG
125      MEG
126      MEG
127      MEG
128      MEG
129      MEG
130      MEG
131      MEG
132      MEG
133      MEG
134      MEG
135      MEG
136      MEG
137      MEG
138      MEG
139      MEG
140      MEG
141      MEG
142      MEG
143      MEG
144      MEG
145      MEG
146      MEG
147      MEG
148      MEG
149      MEG
150      MEG
151      MEG
152      MEG
153      MEG
154      MEG
155      MEG
156      MEG
157      MEG
158      MEG
159      MEG
160      MEG
161      MEG
162      MEG
163      MEG
164      MEG
165      MEG
166      MEG
167      MEG
168      MEG
169      MEG
170      MEG
171      MEG
172      MEG

```

C MAKE AN INDEX APPROXIMATION FOR VALUES OF H GREATER THAN 984252
C FEET.

175 C 8 IF (H.GT.2320000.) GO TO 9
I=.000093048*H+15.
IF (H.GE.DELTA(I)) GO TO 6
IF (H.GE.DELTA(I-1)) I=I-1
GO TO 6

180 C 9 WRITE (6,10) H
RETURN

185 C 10 FORMAT (1H ,20X,22H**ERROR FROM MEGAIR2**,.5H H = ,E12.5)
END

MEG 173
MEG 174
MEG 175
MEG 176
MEG 177
MEG 178
MEG 179
MEG 180
MEG 181
MEG 182
MEG 183
MEG 184
MEG 185
MEG 186
MEG 187
MEG 188

```

FUNCTION VX (GL,H,HOM,PHI,ZJ)
CROSS WIND VELOCITY PLUS SLEW VELOCITY IN METERS/SECOND
COMMON /MESH/ XTRA,ZPREV
COMMON /CNVM/ IN
COMMON /X/ CHI,OMEGA,VP,VPSC,VXB
VX=VXB
IF (VXR,NE.0.) RETURN
VS=OMEGA*(ZJ-ZPREV)
VX=13.6
IF (H.GE.5.E4) GO TO 6
IF (H.GE.2.44E4) GO TO 2
IF (H.GE.1.22E4) GO TO 1
VX=3.42E-3*H+.75
GO TO 3
VX=R2.4-2.53E-3*H
GO TO 3
VX=27.2-2.72E-4*H
IF (1A-2) 4,5,6
VX=VX*.27
GO TO 6
VX=VX*.5
IF ((H0-X-GL).GT.10.) VX=VX*.2
IF (VPSC.GE.VX) VX=VPSC
VX=VX+VS
RETURN
END

```

VX 2
VX 3
VX 4
VX 5
VX 6
VX 7
VX 8
VX 9
VX 10
VX 11
VX 12
VX 13
VX 14
VX 15
VX 16
VX 17
VX 18
VX 19
VX 20
VX 21
VX 22
VX 23
VX 24
VX 25
VX 26
VX 27
VX 28
VX 29
VX 30
VX 31

5

10

15

20

25

30

CASE 1 BELOW-BELOW.PD

SHORT OUTPUT FORMAT, WITHOUT CEBUG

TARGET RANGE (L) ----- 1.000E+03 METERS
 FOCAL DISTANCE (FL) ----- 1.000E+03 METERS

DEVICE POWER (PD) ----- 1.000E+06 WATTS
 POWER OUT OF THE TELESCOPE (PT) ----- 0.

GROUND LEVEL (GL) ----- 0. METERS
 DEVICE ALTITUDE (HOM) ----- 1.00E+02 METERS
 3.28E+02 FEET
 TARGET ALTITUDE (HTM) ----- 0. METERS
 0. FEET
 VERTICAL ANGLE (PHI) ----- -.000 RADIAN

WAVELENGTH (LAM, A) ----- 3.00E-06 METERS
 INPUT JITTER (HIGH FREQ) ----- 5.00E-06
 (LOW FREQ) ----- 5.00E-06
 TRACKING RATE (CMER) ----- 0.00 RADIAN/SEC
 OPTICS RADIUS (RO) ----- .35 METERS
 OBSCURATION RADIUS ----- .00 METERS

AZIMUTH ANGLE (CHI) ----- .520 RADIAN
 PLATFORM VELOCITY (VP) ----- 0. METERS/SEC
 SPECIFIED CROSS WIND (VIS) ----- 10.00
 SEVERITY OF TURBULENCE (WTHR) ----- NORMAL
 RELATIVE HUMIDITY (RH) ----- .50

BEAM TYPE (PROP) ----- GAUSSIAN
 TYPE OF PROPAGATION (BEAM) ----- FOCUSED
 BEAM QUALITY (M) ----- 1.50
 NUMBER OF BEAMPATH INCREMENTS ----- 30

*****INPUT TO OPTICAL TRAIN*****

LASER BEAM DIAMETER .1600 METERS
 LASER POWER .1000E+07 WATTS
 WAVELENGTH .3000E-05 METERS
 OSCURATION .3600
 BEAM QUALITY 1.500
 PULSE LENGTH 2.000 SECONDS
 PHASE FRONT CURVATURE .1000E+71 METERS
 JITTER .7071E-05 RADIAN
 INTENSITY FLUCTUATIONS .5000 PEAK-TO-PEAK
 SCALF SIZE OF FLUCTUATIONS .1000 L/λ
 TYPE OF AEROKINOW FOCUSED
 AEROKINOW DELTA KHC/RHO .1000
 RHO/RHO REF 2.500
 DISTANCE TO CLIPPER 50.00 METERS
 CLIPPER DIAMETER .1600 METERS
 NUMBER OF MIRRORS 7
 REFLECTIVITY .9160
 FABRICATION ERROR .1250 VIS. LAMBDA
 TYPE OF MIRRORS COOLED METERS
 DISTANCE BETWEEN MIRRORS .1500 METERS
 TELESCOPE MAGNIFICATION 4.375
 TELESCOPE DIAMETER .7000 METERS
 TELESCOPE TYPE ON-AXIS
 TYPE OF EXIT APERTURE WINDOW
 EXIT APERTURE LENGTH .5000E-01 METERS
 ABSORPTION COEFFICIENT .1000E-01 METERS-1
 TEMPERATURE FLUCTUATION 1.000 DEG K
 SERJUT AREA/ BEAM AREA .5000E-01
 TRACKER JITTER .5000E-05 RADIAN
 BORE-SIGHT JITTER .5000E-05 RADIAN
 SERVO JITTER .5000E-05 RADIAN
 AUTOALIGNMENT JITTER .5000E-05 RADIAN

*****OPTICAL TRAIN OUTPUT*****

SOURCE
 INPUT BEAM
 AERODYNAMIC WINDOW
 BEAM CLIPPER
 MIRRORS
 COOLED
 BEAM EXPANDER
 ON-AXIS
 WINDOW
 EXIT APERTURE
 TOTALS
 TRANSMITTED BEAM DIAMETER .7000 METERS
 TRANSMITTED POWER .5233E+05 WATTS
 BEAM QUALITY BEFORE ACCOUNTING FOR DIVERGENCE
 M1 = .4987 M2 = 1.1130
 EFFECT OF BEAM DIVERGENCE ON WAIST 1.090
 FINAL BEAM SPREAD PARAMETER M2 1.113
 TOTAL BEAM JITTER .4884E-05 RADIANS
 PHASE FRONT CURVATURE .4375E+71 METERS

RESULTANT BEAM QUALITY M1 = .560 M2 = 1.215

CALCULATIONS FOR ORIGIN BELOW 100 KM AND TARGET BELOW 100 KM.

TARGET ALTITUDE (HTM) = 0. METERS (0. FEET)
 TARGET RANGE (L) = 1.00E+03 METERS
 LINEAR EFFECTS ON TRANSMISSION (EAPKAS) = .946
 NON-LINEAR EFFECTS ON TRANSMISSION (KIP) = .500
 AREA WITHOUT BLOOMING (AREA) = 1.069E-03 METERS**2
 AREA WITH BLOOMING (BLAREA) = 2.131E-03 METERS**2

DISPLACEMENT = .025 METERS ECCENTRICITY = .650

I/PEAK CONTOUR	AREA (METER**2)	CUMULATIVE POWER	AVERAGE INTENSITY
.9	1.122E-04	3.774E-04	3.265E+08
.8	2.377E-04	7.547E-04	3.175E+08
.7	3.800E-04	1.112E-03	2.979E+08
.6	5.442E-04	1.519E-03	2.774E+08
.5	7.384E-04	1.817E-03	2.555E+08
.4	9.761E-04	2.264E-03	2.326E+08
.3	1.263E-03	2.642E-03	2.060E+08
.2	1.715E-03	3.015E-03	1.761E+08
.1	2.450E-03	3.390E-03	1.395E+08

LONG-TERM TURBULENCE (SIGMAT) = 1.159E-06 RADIANS
 SHORT-TERM TURBULENCE (SIGMIST) = 8.633E-07 RADIANS
 RADIUS WITHOUT BLOOMING (R) = .010 METERS
 AVERAGE INTENSITY (I) = 1.7712E+08 WATTS/M**2
 PEAK INTENSITY (IP) = 4.0950E+08 WATTS/M**2

BREAKDOWN INTENSITY ON TARGET = 1.00E+12
 MAXIMUM INTENSITY ON TARGET = 2.56E+18

ACHIEVED AT TELESCOPE POWER = 1.01E+09
 ACHIEVED AT TELESCOPE POWER = 2.74E+06

POWER RANGE AVAILABLE

TELESCOPE POWER (WATTS)	INTENSITY (WATTS/M**2)	USEFUL POWER (WATTS)	OVER AREA (M**2)
8.233E+04	3.426E+07	3.542E+07	1.139E-02
1.647E+05	6.783E+07	7.085E+07	1.307E-02
2.470E+05	8.602E+07	1.063E+08	1.469E-02
3.293E+05	1.063E+08	1.417E+08	1.652E-02
4.116E+05	1.194E+08	1.771E+08	1.853E-02
4.949E+05	1.311E+08	2.125E+08	2.051E-02
5.763E+05	1.454E+08	2.479E+08	2.175E-02
6.585E+05	1.573E+08	2.834E+08	2.307E-02
7.409E+05	1.687E+08	3.189E+08	2.450E-02
8.233E+05	1.771E+08	3.544E+08	2.605E-02
9.056E+05	1.834E+08	3.897E+08	2.777E-02
9.879E+05	1.874E+08	4.251E+08	2.967E-02
1.070E+06	1.936E+08	4.605E+08	3.126E-02
1.153E+06	1.998E+08	4.960E+08	3.270E-02
1.235E+06	2.062E+08	5.314E+08	3.405E-02
1.317E+06	2.128E+08	5.668E+08	3.534E-02
1.400E+06	2.184E+08	6.022E+08	3.662E-02
1.492E+06	2.239E+08	6.377E+08	3.791E-02
1.564E+06	2.290E+08	6.731E+08	3.922E-02
1.647E+06	2.335E+08	7.085E+08	4.055E-02

USEFUL INTENSITY = 1.000E+06 WATTS/M**2

REFERENCES

1. P.R. Carlson, R.T. Liner, and L. Peckham, Propagation Modeling and Analysis for High Energy Lasers - First Interim Report, SAI-74-587-WA, Science Applications, Inc., October 1974.
2. R.T. Liner, P.R. Carlson, and L.N. Peckham, Propagation Modeling and Analysis for High Energy Lasers - Second Interim Report, SAI-74-622-WA, Science Applications, Inc., 31 January 1975.
3. E.A. Sziklas, et al. System Optical Quality Study, Phase I - Problem Definition, AFWL-TR-73-231, Air Force Weapons Laboratory, Kirtland AFB, New Mexico 87117, June 1974.
4. K.R. Vogelsang and S.H. Brewer, System Optical Quality Study, Phase I - Final Report, Report No. P73-401, Hughes Aircraft Company, Culver City, California, October 1973.
5. D.A. Holmes and P.V. Avizonis, "An Approximate Optical System Model," Laser Digest, Spring 1974, AFWL-TR-74-100, Air Force Weapons Laboratory, Kirtland Air Force Base, New Mexico, 1974.
6. C.B. Hogge, R.R. Butts, and M. Burlakoff, "Characteristics of Phase-Aberrated Nondiffraction-Limited Laser Beams," Appl. Optics, Vol. 13, No. 5, p. 1065, May 1974.
7. B.D. O'Neil, Laser Digest, Fall 1974, p.54, AFWL-TR-74-344, Air Force Weapons Laboratory, Kirtland Air Force Base, N.M. 87117.
8. B. Skehan, et al., NPT/Chemical Laser Compatibility Study (U), Report No. P74-29, Hughes Aircraft Company, Culver City, California, January 1974 (Confidential).
9. SAI Memorandum, "Cooled/Uncooled Mirrors in the NPT," R.E. Hodder and R.A. Greenberg to J. Bachkosky, 4 June 1974.
10. A.E. Siegman, An Introduction to Lasers and Masers, McGraw-Hill Book Company, 1971.

11. L.N. Peckham and R.W. David, A Simplified Propagation Model for Laser System Studies, AFWL-TR-72-95, Revised, Air Force Weapons Laboratory, Kirtland AFB, New Mexico, April 1973.
12. L.N. Peckham and R.W. Davis, High Power Gas Laser Technology Forecast (U), AFWL-TR-72-154, Air Force Weapons Laboratory, Kirtland AFB, New Mexico, November 1972 (SECRET).
13. F.G. Gebhardt, and D.C. Smith, Investigation of Self-Induced Thermal Effects of CO₂ Laser Radiation Propagation in Absorbing Gases, United Aircraft Research Laboratories, Report L-921004-8, April 1972.
14. R.W. Davis, et al., "Comparative Analysis of HEL Simplified Propagation Codes (U)," First DOD Conference on High Energy Laser Technology, San Diego, California, October 1974. (This paper is included as an appendix in Reference 1) (SECRET)
15. L.N. Peckham, Laser Analysis Codes Review and Recommendations for the Naval Ordnance Laboratory, SAI-74-5.1-WA, January 1974.
16. H.T. Yura, "Short-Term Average Optical-Beam Spread in a Turbulent Medium," J. Opt. Soc. Am., 63, No. 5 pp. 567-572, May 1973.
17. D.L. Fried, "Limiting Resolution Looking Down through the Atmosphere," J. Opt. Soc. Am., Vol 56, No. 10, pp.1360-1389, October 1966.
18. W.P. Brown and J.E. Pearson, "Multidither Coat Compensation for Thermal Blooming and Turbulence," First DOD Conference on High Energy Laser Technology, San Diego, California, October 1974.
19. R.W. Davis and L.N. Peckham, A Simplified Propagation Model for Laser System Studies, Supplement, AFWL-TR-72-95 Supplement, Air Force Weapons Laboratory, Kirtland AFB, New Mexico, November 1974.
20. F.G. Gebhardt, and D.C. Smith, Investigation of Self-Induced Thermal Effects of CO₂ Laser Radiation Propagation in Absorbing Gases, United Aircraft Research Laboratories, Report K-921004-4, April 1971.

- A-1. R. A. McClatchey and J. E. A. Selby, Atmospheric Attenuation of HF and DF Laser Radiation, AFCRL-72-0312, 23 May 1972.
- A-2. D. E. Burch, D. A. Gryvnak and J. D. Pembroke, Investigation of the Absorption of Infrared Radiation by Atmospheric Gases: Water, Nitrogen, Nitros Oxide, AFCRL-71-0124, January 1971.
- A-3. S. L. Valley (ed.), Handbook of Geophysics and Space Environments, AFCRL, 1965.
- A-4. R. E. Meridith, T. W. Tuer and D. R. Woods, Investigation of DF Laser Propagation, SAI-74-001-AA, Science Applications, Inc., Ann Arbor, July 1974.